

---

Electronic Thesis and Dissertation Repository

---

8-24-2017 12:00 AM

## Triple Positive Microparticles as a “Liquid Biopsy” for Risk Stratification of Prostate Cancer

Harmenjit Singh Brar, *The University of Western Ontario*

Supervisor: Pautler, Dr. Stephen, *The University of Western Ontario*

Co-Supervisor: Power, Dr. Nicholas, *The University of Western Ontario*

Co-Supervisor: Leong, Dr. Hon, *The University of Western Ontario*

A thesis submitted in partial fulfillment of the requirements for the Master of Science degree in Surgery

© Harmenjit Singh Brar 2017

Follow this and additional works at: <https://ir.lib.uwo.ca/etd>



Part of the [Surgery Commons](#), and the [Urology Commons](#)

---

### Recommended Citation

Brar, Harmenjit Singh, "Triple Positive Microparticles as a “Liquid Biopsy” for Risk Stratification of Prostate Cancer" (2017). *Electronic Thesis and Dissertation Repository*. 4933.

<https://ir.lib.uwo.ca/etd/4933>

This Dissertation/Thesis is brought to you for free and open access by Scholarship@Western. It has been accepted for inclusion in Electronic Thesis and Dissertation Repository by an authorized administrator of Scholarship@Western. For more information, please contact [wlsadmin@uwo.ca](mailto:wlsadmin@uwo.ca).

## **Abstract**

Prostate cancer remains a substantial contributor to cancer-related mortality worldwide. Current screening methods include obtaining a PSA blood test. However, controversy surrounds its use as it is neither sensitive nor specific.

Nanoscale flow cytometry is a type of microfluidics-based technology that allows enumeration of submicron tumor fragments known as microparticles (MPs). In this study, prostate specific microparticles in patient plasma were targeted using fluorophore-conjugated antibodies. Targeted cell surface antigens or biomarkers include: prostate specific membrane antigen (PSMA), six-transmembrane epithelial antigen of the prostate-1 (STEAP1), ghrelin receptor (GHSR1a) and CD151.

A statistically significant difference in the level of MP levels was measured with PSMA+STEAP1+GHSR1a and PSMA+STEAP1+CD151 triple-expressing MPs when comparing Gleason score (GS) 6 to GS3+4, GS4+3 and  $GS \geq 8$  cohorts. In this pilot and exploratory study, I show that MPs have the potential of becoming a “liquid biopsy” that can assist in risk stratification prior to a prostate needle biopsy.

## **Keywords**

Prostate Cancer, Prostate Neoplasm, Microparticles, Oncosomes, Prostatosomes, Extracellular Vesicles, Nanoscale Flow Cytometry, Prostate Specific Membrane Antigen, Six-transmembrane Epithelial Antigen of the Prostate-1, Ghrelin Receptor, GHSR1a, CD151

## **Co-Authorship Statement**

**Dr. Stephen Pautler:** Interpreted data with clinical correlations and structure of written thesis.

**Dr. Nicholas Power:** Interpreted data with clinical correlations and structure of written thesis.

**Dr. Hon Leong:** Designed study and supervised day to day activities regarding the technical aspects of the project.

**Dr. Fabrice Lucien:** Also provided supervision over day to day activities regarding the technical aspects of the project and data analysis.

## Acknowledgments

I would like to express my deepest appreciation to a key number of people who helped immensely in the completion of this thesis. Firstly, a special thanks to my graduate committee. **Dr. Stephen Pautler**, you have been such an integral component in my development as a scientist and surgical resident. I cherish all the mentorship I've received over the course of the year and will continue to build on the lessons you have taught. All your feedback has been vital in my growth and I appreciate all the challenges you have put forth to enhance my development. **Dr. Nicholas Power**, I cannot thank you enough for your constant support through this entire process. Your words of encouragement and advice were key to the success of this manuscript. Your continuous, timely feedback meant a great deal and I thank you for the willingness to mentor me with your busy schedule. **Dr. Hon Leong**, thank you for everything that you have done in developing me as a scientist. With your support, I was able to achieve new reaches that I only once dreamt about. You were always available when most needed and I appreciate you made sure I got the help I need.

Through this whole process, I have one member of the lab that was instrumental in the completion of this manuscript. **Dr. Fabrice Lucien**, thank you so much for the day to day feedback and help with troubleshooting throughout this process. Your support and assistance with data analysis meant a great deal.

Finally, I want to thank my family. Your constant support and love were integral in me achieving my goals. Especially to **my mother**, words cannot express enough gratitude for all your sacrifices and prayers that helped me become that man I am today. To **my late father**, although our time together was cut short you remain a major role model and help drive me to become something more. I want to thank **my brother and sister** for always being there for me no matter what. Your words of encouragement and casual conversations on the phone help bridge the gap of being away from home while I get to do what I love.

Thank you to all who've helped me achieve my goals.

# Table of Contents

<b>Abstract</b> .....	ii
<b>Co-Authorship Statement</b> .....	iii
<b>Acknowledgments</b> .....	iv
<b>Table of Contents</b> .....	v
<b>List of Abbreviations</b> .....	viii
<b>List of Tables</b> .....	x
<b>List of Figures</b> .....	xi
<b>List of Appendices</b> .....	xiv
<b>Chapter 1</b> .....	1
1 Introduction .....	1
1.1 Epidemiology .....	1
1.2 Prostate Anatomy.....	2
1.3 Prostate Cancer and Risk Factors .....	4
1.4 Digital Rectal Exam .....	6
1.5 Prostate Specific Antigen (PSA).....	6
1.6 Effect of Prostate Specific Antigen (PSA) on Clinical Practice .....	7
1.7 Prostate Specific Antigen (PSA) Permutations That Improve Detection of Prostate Cancer .....	8
1.8 Transrectal Ultrasound Guided (TRUS) Biopsy and Gleason Score .....	10
1.9 Gleason Score: Current Gold Standard of Prognosis.....	13
1.10 Staging of Prostate Cancer .....	14
1.11 Controversy Surrounding PSA Based-Screening.....	17
1.12 Biomarkers .....	18
1.13 Microparticles (MPs) .....	20
1.14 Nanoscale Flow Cytometry.....	23

1.15 Prostate Cancer Surface Markers .....	26
1.16 Prostate Specific Membrane Antigen (PSMA) .....	27
1.17 Six-transmembrane Epithelial Antigen of the Prostate-1 (STEAP1).....	28
1.18 Ghrelin Ligand and its Receptor (GHSR1a) .....	29
1.19 CD151 .....	30
1.20 Hypothesis.....	31
1.21 Research Objectives.....	31
<b>Chapter 2</b> .....	<b>33</b>
2 Materials and Methods .....	33
2.1 Patient Sample Preparation, Blinding and Ethics .....	33
2.2 Antibody and Reagents .....	33
2.3 Immunolabeling of Prostate Cancer-derived Microparticles .....	34
2.4 Acquisition settings for nanoscale flow cytometry.....	34
2.5 Data analysis and Statistics.....	37
<b>Chapter 3</b> .....	<b>39</b>
3 Results .....	39
3.1 Study Cohort .....	39
3.2 Optimization of Antibodies used in Detection of Prostate-derived Microparticles .....	41
3.3 Gating of Cytograms.....	44
3.4 Scatterplot data.....	54
3.5 Assessment of Performance Characteristics .....	65
<b>Chapter 4</b> .....	<b>71</b>
4 Discussion .....	71
4.1 General Discussion .....	71
4.2 Potential Role of PCMP Assay in the Diagnosis of Prostate Cancer .....	72

4.3 Measurement of Microparticles .....	73
4.4 Calculated Area Under the Curve (AUC) for Biomarkers.....	77
4.5 Limitations .....	79
<b>Chapter 5</b> .....	<b>81</b>
5 Conclusion .....	81
5.1 Conclusion .....	81
5.2 Future Directions .....	82
<b>Bibliography</b> .....	<b>83</b>
<b>Appendices</b> .....	<b>97</b>
<b>Curriculum Vitae</b> .....	<b>97</b>

## List of Abbreviations

AJCC	American Joint Committee on Cancer
AS	Active Surveillance
AUC	Area Under the Curve
BPH	Benign Prostatic Hypertrophy
CD	Cluster of Differentiation
CM	Confocal Microscopy
CSS	Cancer-specific Survival
DRE	Digital Rectal Exam
EM	Electron Microscopy
EPIC	European Prospective Investigation into Cancer and Nutrition
ERSPC	European Randomized Trial of Prostate Cancer Screening
EV	Extracellular Vesicle
FDA	Food and Drug Administration
fPSA	Free PSA
GHSR1a	Ghrelin receptor or type 1a growth hormone secretagogue receptor
HG PIN	High Grade Prostatic Intraepithelial Neoplasia
IGF-1	Insulin-like Growth Factor-1
LAPC-4	Los Angeles Prostate Cancer
LNCaP	Lymph Node Carcinoma of the Prostate
MMP	Metalloproteinases
MP	Microparticles
MRI	Magnetic Resonance Imaging
NK	Natural Killer Cell
PAP	Prostatic Acid Phosphatase



PBS	Phosphate Buffered Saline
PC3	Prostate Cancer Cell Line-3
PCA3	Prostate Cancer Antigen-3
PCIe	Peripheral Component Interconnect Express
PCMPs	Prostate Cancer Microparticles
PLA	Proximity Ligation Assay
PLCO	Prostate, Lung, Colon, and Ovary Trial
PMP	Platelet Microparticles
PPV	Positive Predictive Value
PSA	Prostate Specific Antigen
PSAD	Prostate Specific Antigen Density
PSA DT	PSA Doubling Time
PSMA	Prostate Specific Membrane Antigen
ROC	Receiver Operating Curve
ROI	Region of Interest
SELECT	The Selenium and Vitamin E Cancer Prevention Trial
STEAP1	Six-transmembrane Epithelial Antigen of the Prostate-1
TCGA	The Cancer Genome Atlas
TMA	Tissue Microarray
TNM	Tumor, Nodes, Metastasis Classification System
TRUS	Transrectal Ultrasound Guided
TURP	Transurethral Resection of the Prostate
USPSTF	United States Preventive Services Task Force

## List of Tables

Table 1. Prostate cancer stages according to AJCC, 2016.....	16
Table 2. Clinical and pathological features of the patient cohort. Pathologic stage of six patients is unknown.....	40
Table 3. Distribution of the positive microparticles for each individual biomarker displayed as events/ $\mu$ L. GS6 (n=15), GS3+4 (n=14), GS4+3 (n=15), and GS $\geq$ 8 (n=15).....	56
Table 4. Distribution of microparticles that are dual positive displayed in events/ $\mu$ L. GS6 (n=15), GS3+4 (n=14), GS4+3 (n=15), and GS $\geq$ 8 (n=15). ....	61
Table 5. Distribution of microparticles that are triple positive displayed in events/ $\mu$ L. GS6 (n=15), GS3+4 (n=14), GS4+3 (n=15), and GS $\geq$ 8 (n=15). ....	64
Table 6. AUC results for the all combinations of microparticles comparing GS6 to GS3+4.	70
Table 7. AUC results for the all combinations of microparticles comparing GS6 to GS4+3.	70
Table 8. AUC results for the all combinations of microparticles comparing GS6 to GS $\geq$ 8...	70

## List of Figures

- Figure 1. Anatomy of the zones of the prostate. Image obtained from: Verze, P., Cai, T. & Lorenzetti, S. (2016). The role of the prostate in male fertility, health and disease. *Nature Reviews Urology*. 13, 379–386. .... 3
- Figure 2. Portrayal of a routine TRUS biopsy. Image obtained from website: <https://perthurologyclinic.com.au/what-we-do/procedures/337-2/> (Accessed January 2017).11
- Figure 3. Apogee, A-50M nanoscale flow cytometer (Apogee FlowSystems Inc., UK). ..... 24
- Figure 4. Depiction of light scatter detectors and the three fluorescent channels in the Apogee A-50M nanoscale flow cytometer. Image obtained from website: <https://flowcytometry.med.ualberta.ca> (Accessed January 2017). ..... 25
- Figure 5. An example of histograms portraying PSMA-PE isotype (A) and PSMA-PE antibody (B). The x-axis represents sizing as long angle light scatter (LALS) and y-axis represents degree of fluorescence represented by a log scale. Each dot represents one positive event within the gate (displayed in red). ..... 36
- Figure 6. Example of a triple positive histogram (A, MPs that are positive for PSMA, STEAP1 and GHSR1a). MPs within blue rectangle gate are recorded and represented as events/ $\mu$ L. The x-axis represents sizing as long angle light scatter (LALS) and y-axis represents degree of fluorescence represented by a log scale. This gate was created by superimposing dual positive MPs (B, PSMA+STEAP1) with single positive MP gate (C, GHSR1a). Each dot represents one positive event within the gate (displayed in red). ..... 38
- Figure 7. Titration curve for each antibody and their respective isotype using metastatic prostate cancer patient plasma. For Prostate Specific Membrane Antigen clone 3E/7 conjugated with PE (PSMA 3E/7), 0.75  $\mu$ g was selected as optimal mass for study (A). For Six Transmembrane Antigen of Prostate-1 conjugated with Alexa Fluor 647 (STEAP1), 0.40  $\mu$ g was selected as optimal mass for study (B). For Ghrelin receptor conjugated with FITC (GHSR1a), 0.80  $\mu$ g was selected as optimal mass for study (C). For CD151 conjugated with FITC, 0.68  $\mu$ g was selected as optimal mass for study (D). X-axis indicates mass of isotype

or antibody used in micrograms and y-axis indicates percentage of positive events within the region of interest (i.e. within the gate)..... 43

Figure 8. Cytograms displaying single positive microparticles within their respected gates: isotype-matched controls (A) and antibodies (B) for STEAP1-Alexa647, isotype-matched controls (C) and antibodies (D) for PSMA-PE, isotype-matched controls (E) and antibodies (F) for GHSR1a-FITC, and isotype-matched controls (G) and antibodies (H) CD151-FITC. The x-axis represents sizing as long angle light scatter (LALS) and y-axis represents degree of fluorescence represented by a log scale. Each dot represents one positive event within the gate (displayed in red)..... 47

Figure 9. Cytograms displaying dual positive microparticles with their respected gates: isotype-matched controls (A) and antibodies (B) for PSMA-PE+STEAP1-Alexa647, isotype-matched controls (C) and antibodies (D) for PSMA-PE+GHSR1a-FITC, isotype-matched controls (E) and antibodies (F) for STEAP1-Alexa647+GHSR1a-FITC, isotype-matched controls (G) and antibodies (H) for PSMA-PE+CD151-FITC, and isotype-matched controls (I) and antibodies (J) for STEAP1-Alexa647+CD151-FITC. The x-axis represents sizing as long angle light scatter (LALS) and y-axis represents degree of fluorescence represented by a log scale. Each dot represents one positive event within the gate (displayed in red). ..... 51

Figure 10. Cytograms displaying triple positive microparticles with their respected gates: isotype-matched controls (A) and antibodies (B) for PSMA-PE+STEAP1-Alexa647+GHSR1a-FITC and isotype-matched controls (C) and antibodies (D) for PSMA-PE+STEAP1-Alexa647+CD151-FITC. The x-axis represents sizing as long angle light scatter (LALS) and y-axis represents degree of fluorescence represented by a log scale. Each dot represents one positive event within the gate (displayed in red). ..... 53

Figure 11. Scatterplots showing levels of PSMA (A), STEAP1 (B), GHSR1a (C), and CD151 (D) expressing MPs in patient plasmas for GS6 (n=15), GS3+4 (n=14), GS4+3 (n=15), and GS $\geq$ 8 (n=15). Bars represent the mean in events/ $\mu$ L and +/- s.e.m. (\* p <0.05, \*\* p<0.01 in one-way ANOVA test). ..... 55

Figure 12. Scatterplots showing levels of PSMA+STEAP1 (A), PSMA+GHSR1a (B), STEAP1+GHSR1a (C), PSMA+CD151 (D), STEAP1+CD151 (E) co-expressing

microparticles (MP) in patient plasmas for GS6 (n=15), GS3+4 (n=14), GS4+3 (n=15), and GS $\geq$ 8 (n=15). Bars represent the mean in events/ $\mu$ L and +/- s.e.m. (\* p <0.05, \*\* p<0.01, \*\*\* p<0.001 in one-way ANOVA test). ..... 59

Figure 13. Scatterplots showing levels of PSMA+STEAP1+GHSR1a (A) and PSMA+STEAP1+CD151 (B) triple-expressing MP in patient plasmas for GS6 (n=15), GS 3+4 (n=14), GS4+3 (n=15), and GS $\geq$ 8 (n=15). Bars represent the mean in events/ $\mu$ L and +/- s.e.m. (\* p <0.05, \*\* p<0.01, \*\*\* p<0.001 in one-way ANOVA test). ..... 63

Figure 14. ROC curves comparing GS6 to GS3+4 for various combinations of microparticles. .... 66

Figure 15. ROC curves comparing GS6 to GS4+3 for various combinations of microparticles. .... 67

Figure 16. ROC curve comparing GS6 to GS $\geq$ 8 for various combinations of microparticles. .... 68

## **List of Appendices**

Appendix 1. REB approval letter.....	97
--------------------------------------	----

# Chapter 1

## 1 Introduction

### 1.1 Epidemiology

Prostate cancer continues to be the most common non-cutaneous neoplasm affecting North American men (Howlander et al., 2017). In 2016, it is estimated that 21% percent of all new diagnosed cancers in males will be from the prostate, making it the number one diagnosed neoplasm in Canadian men (Canadian Cancer Society, 2017). It will account for approximately 10% of all cancer deaths in Canadian males, ranking third, after lung cancer and colorectal cancer (Canadian Cancer Society, 2017). Men over the age of 60 have the greatest risk of developing prostate cancer. The incidence rate in Canada peaked in 1993 and 2001, with a decline in the following years. These peaks were believed to be attributed to intensified screening with the use of PSA (Canadian Cancer Society, 2017). Since 2001, incidence rates have been declining roughly at 1.5% rate per year and mortality rates have been declining at a rate of 3.3% per year. This decline in mortality is likely attributed to improvements of treatment in radiation and use of hormonal therapy especially in the setting of metastatic castrate resistant prostate cancer (Cooperberg et al., 2003; Kupelian et al., 2003; Joelle et al., 2013).

In the United States, it is estimated that in 2016, 180,890 men will be diagnosed with prostate cancer and 26,120 will die from the disease (Howlander et al., 2017). Similar to Canada, 1 in 8 American men will develop prostate cancer in their lifetime. (Howlander et al., 2017). The median age of diagnosis and death in 2016 are 66 and 80, respectively.

In 2012, estimated global incidence makes prostate cancer the second most common cancer in men with over a million cases resulting in 307,000 deaths. Prostate cancer incidence varies more than 25-fold worldwide (Globocan, 2012). High-income countries who adopted PSA screening had the largest decline in mortality, such as, United States (-3.5%), Canada (3.1%), England (-2.6%), and Australia (-1.7%) (Canadian Cancer Society, 2016; Collin et al., 2008; Feletto et al., 2015). Mortality rates are the highest in

Sub-Saharan Africa (Globocan, 2012).

## 1.2 Prostate Anatomy

The prostate is part of the male reproductive system that works in tandem with the seminal vesicles to produce and store seminal fluid that nurtures, protects, and facilitates sperm transport for reproduction (Aumüller, 1979). Embryologically, the prostate is distinct from the seminal vesicles as it arises from the urogenital sinus under the hormonal influences of dihydrotestosterone, while the seminal vesicles develop from the Wolffian ducts through testosterone stimulation. It is comprised of 70% glandular tissue and 30% fibromuscular stroma. (Aumüller, 1979; Wein et al., 2016).

The prostate gland is divided into 4 zones: peripheral, central, transition and anterior fibromuscular stroma zone (**Figure 1**). The peripheral zone is a sub-capsular region of small round acini lined by simple columnar epithelium with clear cytoplasm and basal nuclei (McNeal, 1969). Approximately, 70% of prostate cancers are contained in this zone (Prostate Cancer Information, 2010). The central zone arises close to the ejaculatory duct orifices and follows these ducts proximally, branching laterally near the prostate base. Its lateral border fuses with the proximal peripheral zone border (McNeal, 1981). Central zone accounts for 2.5% of prostate cancers (Cohen et al., 2008). The transition zone surrounds the proximal urethra and is the site for benign prostatic hyperplasia (McNeal, 1981). It also accounts for 10-20% of prostate cancers (Prostate Cancer Information, 2010). The anterior fibromuscular stroma forms the entire anterior surface of the prostate which is thick, nonglandular and typically not involved with prostate cancer (McNeal, 1981).



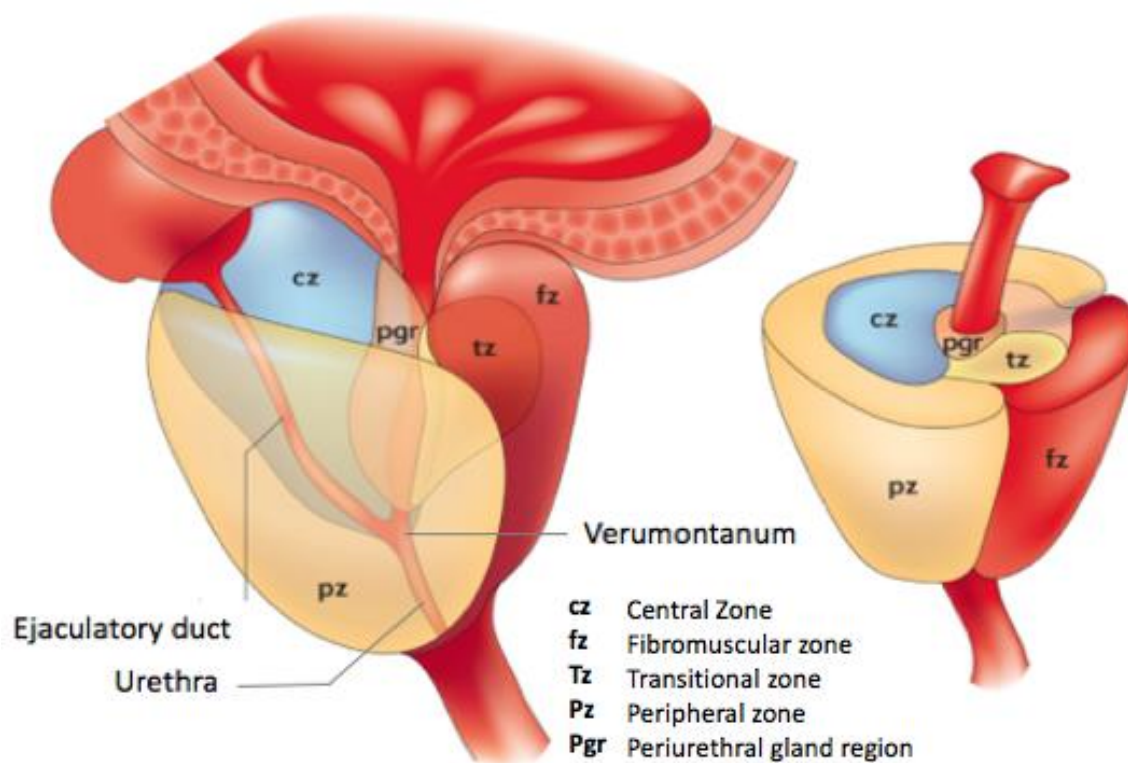


**Figure 1. Anatomy of the zones of the prostate.** Image obtained from: Verze, P., Cai, T. & Lorenzetti, S. (2016). The role of the prostate in male fertility, health and disease. *Nature Reviews Urology*. 13, 379–386.

### 1.3 Prostate Cancer and Risk Factors

The most common form of prostate cancer is adenocarcinoma which arises from the prostate's abundant secretory epithelial cells (Miller et al., 2003). In the post-PSA era, average age for diagnosis and death is 65 and 77 years of age respectively. Prostate cancer in its early stages often does not produce symptoms. However, advanced cases of prostate cancer may give rise to: hematuria, urinary obstruction, sexual dysfunction impacting erectile function, local invasion of surrounding structures, bony pain and spinal compression (Miller et al., 2003). These advanced stages of disease are more commonly seen in men with high preoperative PSA and high histological grade cancers (Miller et al., 2003). Localized extra-capsular extension is most common in the posterolateral prostate near the neurovascular bundle but can also involve the urethra, bladder and rectum in advanced cases (Prostate cancer statistics, 2017). Common metastatic sites include pelvic lymph nodes and bone while lung, liver, and brain are rare metastatic sites (Prostate cancer statistics, 2017). Prostate cancer is incidentally reported in up to 10% of men undergoing transurethral resection of the prostate (TURP) (Otto et al., 2014) and in 14-50% in men undergoing cystoprostatectomy for bladder cancer (Kaelberer et al., 2016). Complete prostate gland analysis from cystoprostatectomy specimens have shown the presence of clinically significant prostate cancer (Filter et al., 2017).

Risk factors strongly associated with prostate cancer include family history, genetic variability, ethnicity and age. Epidemiology studies have shown that relative risk of developing prostate cancer increases with number of affected family members, their degree of relatedness, and the age at which they were diagnosed. A meta-analysis by Zeegers et al., 2003, reported a relative risk (RR) of 2.17 if the father was affected, RR 3.37 if brother was affected, RR 3.34 if first degree relative was <65 years old at time of diagnosis, and RR 5.08 if >2 first-degree relatives were affected. Over 100 alleles have been identified that may increase one's risk of prostate cancer (Amin et al., 2015). Tumor suppressor genes, BRCA 1 and BRCA 2, have been linked to early on-set of prostate cancer with evidence suggesting more aggressive prostate cancer in those with BRCA2 mutation (Amin et al., 2015; Siegel et al., 2016). Patients with hereditary prostate cancer may develop cancer 6 to 7 years earlier when compared to spontaneous cases (European

Association of Urology, 2016).

Ethnicity also impacts both incidence and mortality of prostate cancer. African Americans and Jamaicans of African descent have the greatest risk. African Americans are estimated to have mortality rates that are 2.4 times higher when compared to Caucasians (Siegel et al., 2016). Hispanics are considered at intermediate risk as they have similar incidence and mortality from prostate cancer as their Caucasian counterparts. Finally, Asians are considered low risk as they have the lowest incidence and mortality rates (Siegel et al., 2016; Globocan, 2012).

Age appears to be the most significant risk factor for developing prostate cancer. It is estimated that men aged 45 to 54 years will comprise of <10% of the newly diagnosed cases in 2016. On the other hand, men aged 55 to 64 years and men aged 65-74 years will comprise of 32.9% and 37.6% of all newly diagnosed cases, respectively (Siegel et al., 2016). The incidence of prostate cancer declines in men over 75 years of age which is linked to decreased screening in this population, however, mortality rates continue to rise with advancing age (Siegel et al., 2016).

Other risk factors that have been explored but have shown limited or conflicting data include diet and environmental factors. The western diet is believed to be linked to an increased risk of prostate cancer. There is evidence suggesting high intake of red meat such as beef or pork, especially when it is cooked at a high temperature, may increase the risk of developing prostate cancer (John et al., 2011). European Prospective Investigation into Cancer and Nutrition (EPIC) showed a weak correlation between Insulin-like Growth Factor-1 (IGF-1) levels and high intake of protein from dairy products as a risk of prostate cancer (Key, 2014). Metabolic syndrome may have a small role in the development of prostate cancer. A meta-analysis by Esposito et al., 2013, found that metabolic syndrome increased risk by 12%, however the results were not statistically significant. When examining factors individually, hypertension and waist circumference >102 cm were associated with 15% ( $p=0.035$ ) and 56% ( $p=0.007$ ) increased risk of prostate cancer, respectively (Esposito et al., 2013). Migration studies of first-generation Chinese and Japanese immigrants show increased incidence of prostate cancer when they

settle in the United States, but further prospective studies failed to show a dietary link (Muir et al., 1991; Wu et al., 2006). Nonetheless, diet may be a risk factor in developing prostate cancer but significant limitations impact our understanding due to the nutritional variability of the western diet as well as patient genetic variability.

## 1.4 Digital Rectal Exam

In order to screen and diagnose prostate cancer, Urologists rely on history, physical exam, PSA blood tests and tissue biopsies. As mentioned previously, family history is a vital component of the history taking process. An individual's risk significantly increases with greater number of first-degree family members diagnosed, especially if at a younger age. Physical exam incorporates the digital rectal exam (DRE) to help detect palpable tumors in the prostate's peripheral zone. The prostate lies about 4 cm from the anus (Wein et al., 2016). DRE notes the size of the prostate, tender areas, irregularities within the anal canal and any firm prostatic nodules. The examination is simple to complete. Therefore, DRE is routinely performed regardless of PSA level. The positive predictive value (PPV) of the DRE increases when used with prostate specific antigen (PSA) (Schröder et al., 1998). PPV of a suspicious DRE for PSA ranges between 0 to 1.0 ng/mL have been quoted at 5%, PSA 1.1 to 2.5 ng/mL PPV is 14%, PSA 2.6 to 4.0 ng/mL PPV is 30%, and PSA level is 3.0 to 9.9 ng/mL the PPV is 33-83% (Schröder et al., 1998; Carvalhal et al., 1999). Abnormal DRE is associated with an increased risk of higher Gleason score and is an indication for prostate biopsy.

## 1.5 Prostate Specific Antigen (PSA)

Prostatic specific antigen (PSA) was first identified in the 1979 and introduced for clinical use a decade later (Rao et al., 2008). PSA is part of the kallikrein gene family, also referred as the human kallikrein peptidase 3 (hK3) (Wein et al., 2016). It is secreted primarily by the luminal epithelial cells within the prostate (Warade, 2014). This protease's function is to liquefy semen after ejaculation, aiding in freeing up sperm for insemination.

PSA is an organ-specific serine protease that is widely accepted as a prostate cancer

tumor marker, however, it is not cancer specific as numerous causes can alter PSA serum levels. PSA increases with factors such as age, introduction of androgens after puberty, post-ejaculation, African ethnicity, urinary retention and urinary tract infection (Warade, 2014; Klein and Lowe, 1997). It also increases in prostate diseases such as benign prostatic hyperplasia, prostatitis or prostate cancer and from transurethral prostatic surgeries or prostatic biopsy (Warade, 2014; Klein and Lowe, 1997). PSA levels drop with increasing BMI, men suffering from hypogonadism, use of 5-alpha reductase inhibitors, post radical prostatectomy, post radiation therapy and hormonal medications for prostate cancer (Warade, 2014; Baillargeon et al., 2005). PSA is highly concentrated in semen and not present in the blood in healthy individuals. However, when prostate specific diseases are present such as prostate cancer, it disrupts the prostate gland architecture leading to greater release of PSA in the blood (Warade, 2014).

Unfortunately, PSA varies on a day to day basis. Therefore, serial tests are required in order to interpret the results (Roehrborn et al., 1996). There is no agreed upon PSA threshold level that would trigger prostate biopsy for prostate cancer (Semjonow et al., 1996). PSA is a continuous parameter, with higher levels indicating a greater likelihood of prostate cancer and advanced disease. Men may also harbour cancer despite having low serum PSA (Thompson et al., 2004). Traditionally, a PSA level of 4.0 ng/mL was defined as the upper limit of normal (Catalona et al., 1994). However, in a subgroup analysis of the Prostate Cancer Prevention Trial (PCPT), 2950 men who had PSA levels <4.0ng/mL and benign DRE underwent an end of study prostate biopsy. PCPT showed that 449 of these men (15.2%) had prostate cancer of which 67 (14.9%) had Gleason score (GS) 7 or greater (Thompson et al., 2004). This unexpected finding of higher risk disease unfortunately indicates that there is no safe cut off for PSA.

## 1.6 Effect of Prostate Specific Antigen (PSA) on Clinical Practice

Since the introduction of PSA testing, prostate cancer mortality has decreased nearly 45% along with a 75% reduction in the proportion of advanced-stage disease at diagnosis (Etzioni et al., 2008). Furthermore, 81% of newly diagnosed men have localized disease,

and rates of metastases have declined from 20 to 40% in 1980s to less than 4% today (National Cancer Institute, 2015; Newcomer et al., 1997). Therefore, evidence does reveal that PSA serves an important marker in decreasing the mortality rates of prostate cancer patients. However, widespread use of PSA screening and the long natural history of prostate cancer has led to a stage migration to clinically localized disease (T1c) (O'Donnell and Parker, 2008). In a study conducted by Cooperberg et al, 2004, 8,000 patients diagnosed with prostate cancer between 1989-2001 were examined. The findings concluded that the proportion of cases with low-risk disease increased from 28% between 1989–1992 to 45.3% between 1999–2001. The proportion of T1c tumors (diagnosis made from tissue biopsy for elevated PSA) increased from 15.2% to 61.7%, while the proportion of T1a and T1b tumors fell (diagnosis made from TURP surgery). Additionally, PSA can also be used to monitor prostate cancer treatment response (Klein and Lowe, 1997). It is generally understood the fall of PSA post treatment to near zero levels is prognostic for good overall survival outcomes. This is especially the case in patients who have prostatic glands but receive radiation therapy or are on androgen deprivation therapy.

## 1.7 Prostate Specific Antigen (PSA) Permutations That Improve Detection of Prostate Cancer

Various manipulations of PSA have been explored to improve its use as a screening tool in clinical practice. One thought was to increase the PSA threshold in order to improve the specificity of clinically significant cancers. Increasing the PSA threshold increases the PPV of detecting cancer but also increases the likelihood that these cancers will be diagnosed in more advanced stages while missing those with clinically relevant cancer. PSA lacks specificity at low PSA levels (Brawer, 1999). In order to improve the PPV of the PSA test, many dynamic PSA tests have been studied. One such test is PSA velocity. Carter et al, 1992, noted that if a man's PSA rose at a rate greater than 0.75 ng/ml per year, he was at increased risk of being diagnosed with prostate cancer (Carter et al. 1992). Another dynamic test is PSA doubling time (PSA DT). Klotz et al, 2015, found that a PSA DT of <3 years had a 7.8-fold greater risk of PSA progression after definitive

therapy when compared to those on active surveillance who had a PSA DT >3 years. This supported PSA DT of <3 years is a good indicator for aggressive disease (Klotz et al., 2015).

PSA density (PSAD) has been tested in hopes of improving PPV of PSA. PSAD is calculated by dividing the PSA level with prostate volume. Each gram of prostate tissue contributes to the PSA but cancer is believed to cause a higher PSA level and therefore higher PSAD. Although there is conflicting data on the utility of PSAD (Brawer et al., 1993), a PSAD >0.15 in men with PSA 4-10ng/mL has been recommended to undergo a biopsy to assess for cancer (Bazinet et al., 1994). PSAD has been shown to have utility in men with low risk prostate cancer on active surveillance (Bul et al., 2013).

Age-specific PSA levels have also been examined. Since PSA levels increase with age, having a single PSA cut off value is not in the best interest of the patient. According to Oesterling et al, a man <50 years of age should have a PSA <2.5 ng/ml. This is in contrast to a man in his seventies who is capable of having a normal PSA between 0 and 6.5 ng/ml. They stated that:

“these age-specific reference ranges have the potential to make serum PSA a more discriminating tumor marker for detecting clinically significant cancers in older men (increasing specificity) and to find more potentially curable cancers in younger men (increasing sensitivity) (Oesterling et al., 1993).”

Thus, physicians should place PSA levels in context according to the patient's age.

Furthermore, in systemic circulation, PSA is present in both free form (fPSA) or complexed states with protease inhibitors (Brawer, 1999). Alpha-1 antichymotrypsin and alpha-2 macroglobulin are the most prevalent complexes present in serum. Unlike alpha-2 macroglobulin complex, PSA that is complexed with alpha-1 antichymotrypsin has two epitopes that can be detected with immunoassays. As a result, men with PSA levels between 4-10 ng/mL who have a free to total (fPSA/PSA x 100%) percentage of <20% are at increased risk of harbouring prostate cancer.

Thus, PSA has revolutionized the management of prostate cancer in both early detection and following patient's post-treatment. Using the cut off value of 4 ng/mL, the sensitivity and specificity for detecting any prostate cancer is 21% and 91% respectively (Aubry et al., 2013). The sensitivity of detecting high risk disease (Gleason score >8) is 51%. Unfortunately, PSA is not without its flaws and as of now there is no perfect model when it comes to screening men for prostate cancer. The controversies of PSA based screening will be explored in chapter 1.11.

## 1.8 Transrectal Ultrasound Guided (TRUS) Biopsy and Gleason Score

In order to identify and formally make the diagnosis for prostate cancer, a transrectal ultrasound guided (TRUS) tissue biopsy is required. The procedure requires an ultrasound probe to be inserted into the rectum and multiple core biopsies are taken using a needle biopsy gun. It is common practice to acquire 12 core biopsies in a systematic fashion which are then microscopically examined by a pathologist. A Gleason score (GS) which reflects tumor cell differentiation is assigned if cancer is detected (Gleason, 1966). An overall increase in cancer detection rates was seen when 10 to 12 core biopsy protocols were used instead of the standard sextant biopsy protocol (Bjurlin et al., 2013). Saturation biopsies, which consist of 20 cores or more, can also be considered in patients who are undergoing a repeat biopsy after an initial biopsy was negative (Walz et al., 2006). It is currently estimated that 1.3 million prostate biopsies are performed annually in the United States (Aubry et al., 2013). Portrayal of a routine TRUS biopsy is seen in **Figure 2**.



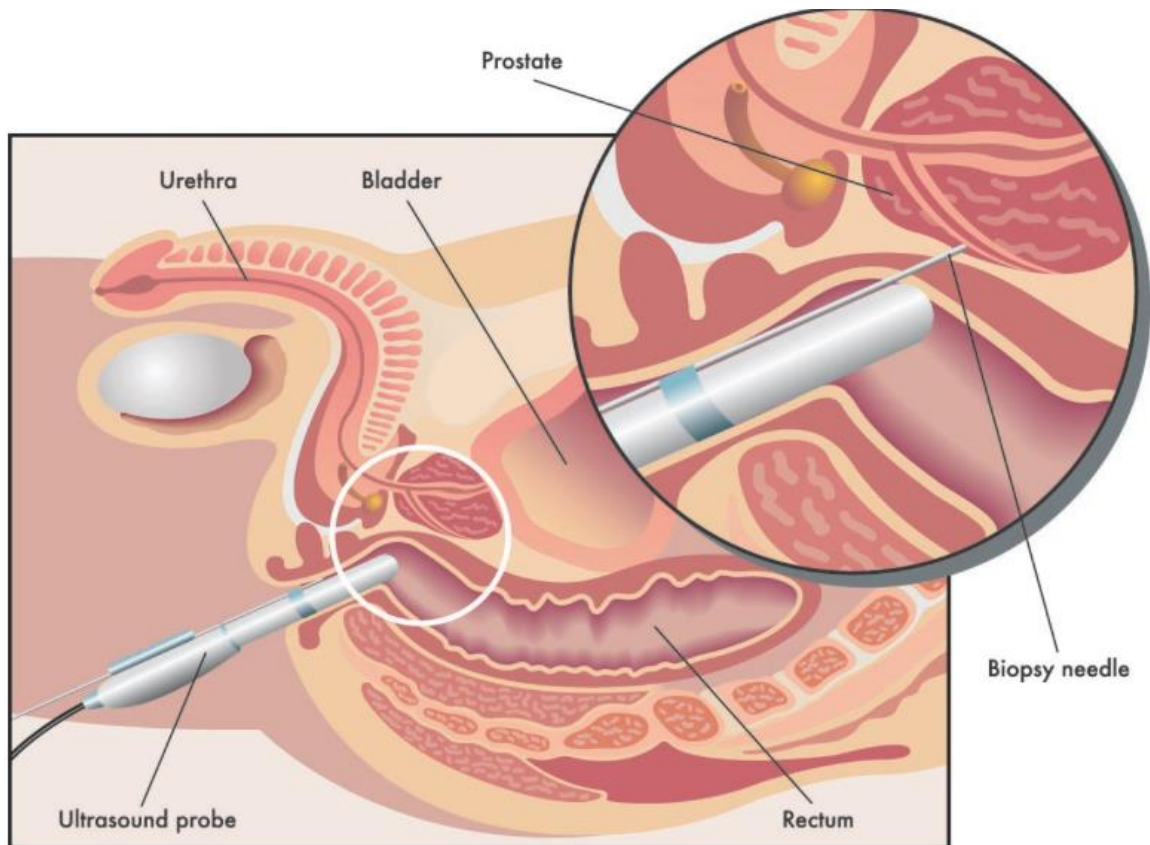


**Figure 2. Portrayal of a routine TRUS biopsy. Image obtained from website: <https://perthurologyclinic.com.au/what-we-do/procedures/337-2/> (Accessed January 2017).**

TRUS biopsy is an invasive procedure and 30% of clinically significant prostate cancer cases continue to be missed (Bouye et al., 2009). Moreover, patient's will incur side effects such as post procedure pain, acute urinary retention, hematuria, hematospermia, blood per rectum, transient fever, epididymitis, prostatitis, and a 4% risk of life threatening sepsis (Hara et al. 2008; Nam et al., 2010). To minimize the risk of infection, it is highly recommended that patients begin antibiotic prophylaxis 24 hours prior to biopsy and continue for a total of 3 days (Wolf et al., 2012). Other modalities using MRI and advancements in ultrasound are currently being investigated in order to improve TRUS biopsy results (Stoianovici, 2012).

The Gleason score (GS) is a numerical grading system that was first developed by Dr. Donald Gleason in the 1960s (Gleason and Mellinger, 1974). Traditionally, a Gleason grade from a scale of 1 to 5 is assigned to each tissue core. Gleason grade of 1 represents well differentiated tissue while a Gleason grade of 5 is the least differentiated and often the most invasive. (Gleason, 1966). Biopsy cores are assigned to the two most common GS patterns giving an accumulated score of 2 to 10. In 2005, the International Society of Urological Pathology updated the original Gleason grading system to incorporate the new changes to prostate cancer management with the advent of screening (Epstein et al., 2005). Gleason grade scale now is graded from 3 to 5. Therefore, new scores now range from 6 through 10 with 6 being classified as low risk cancer (also known as GS 3+3), GS 3+4=7 and GS 4+3=7 as intermediate risk cancer, and GS 8 to 10 (GS 4+4, 3+5, 5+3, 4+5, 5+4, 5+5) as high-risk cancer (Ghani et al., 2005). Higher GS is associated with poor prognosis due to the propensity of the cancer to grow and metastasize (Canadian Cancer Society, 2016). Other biopsy findings such as number of cores involved, percentage of cores involved and potentially perineural invasion can provide prognostic information (Bismar et al., 2003). Therefore, at this point in time, tissue is required to risk stratify newly diagnosed cancer patients or those who have been previously diagnosed and are currently on active surveillance.

## 1.9 Gleason Score: Current Gold Standard of Prognosis

Histological grade of prostatic carcinoma is a dominant predictor of clinical outcome. Alberston et al, 1998 published a retrospective study designed to estimate long-term survival based on age and GS at time of diagnosis in men with a life expectancy greater than 10 years who did not receive treatment (i.e. surgery, external beam radiation, or brachytherapy). 767 men aged 55 to 74 with clinically localized prostate cancer were selected for the study (Alberston et al., 1998). Results showed that men with progressing GS (6 versus 7 versus 8-10) had increasing rates of prostate cancer related death within 15 years of diagnosis independent of age at diagnosis. GS 8 to 10 was significantly associated with poor prognosis with 60% to 87% of patients dying of prostate cancer.

Recent evidence has now revealed that GS6 (low risk) prostate cancer may no longer need to be aggressively treated. In a large prospective cohort on patients with low and intermediate risk disease while on active surveillance, outcomes for low-risk patients were excellent: a metastasis-free survival rate of 97.2% and a 15-year cancer-specific survival (CSS) rate of 94.3%. Only 28 men developed metastatic disease except two patients who had GS 7 on biopsy (these two patients lacked surgical grading). Of note, cancer specific survival did not differ between those younger or older than 70 years of age. Furthermore, 25% of the patients in this study satisfied the D'Amico criteria for intermediate risk (Klotz et al., 2015). With a high CSS rate, this study showed active surveillance can be a viable option in those patients who have favorable intermediate risk disease (GS 7).

Many older studies have grouped GS 7 as a single score without distinguishing 3+4 versus 4+3. However, there is significant evidence indicating prognostic differences between these two scores. GS 4+3 at time of radical prostatectomy was associated with increased risk of progression to metastasis independent of stage or margin status (Chan et al., 2000). Sunnybrook Hospital in Toronto recently published an active surveillance study comparing GS 6 to GS 7. They did a sub-group analysis comparing GS 3+4 to GS 6 and GS 4+3 to GS 6. Despite close monitoring and intervention for evidence of risk progression, the hazard ratio for 15-year prostate cancer metastasis rate was 3.14 in the intermediate risk group. The hazard ratio for 15-year prostate cancer mortality for GS

3+4 versus GS 6 was 4.0 and Gleason 4+3 versus GS 6 was 10.5 (Musunuru et al., 2016; Yamamoto et al., 2016). Overall, evidence supports that as GS progresses so does adverse clinical outcomes. Tissue pathology is needed for diagnosis and prognosis of prostate cancer, with any newly developed non-invasive biomarker to work in conjunction with the Gleason Score.

## 1.10 Staging of Prostate Cancer

After the diagnosis of prostate cancer is made using TRUS biopsy, it must be appropriately staged. The most common system currently used is the Tumor, Nodes, Metastasis (TNM) classification system by the American Joint Committee on Cancer (AJCC) (American Cancer Society, 2016). It looks at the extent of the tumor (T), whether or not there is lymph node involvement (N), and if there is evidence of metastatic disease (M). The new staging system also incorporates PSA at time of diagnosis as well as the Gleason score (American Cancer Society, 2016). Staging ranges from I to IV with stage I having the best prognosis and stage IV having the worst prognosis (**Table 1**). In order to complete the routine staging work up, urologists obtain computerized tomography (CT) scans or magnetic resonance imaging (MRI) of the abdomen and pelvis to assess for lymph node metastasis and bone scans to assess for bony metastasis (Hovels et al., 2008; Langsteger et al., 2012). Definitive treatment with surgery or radiation with the intent to cure is only possible when there is no evidence of metastatic disease.

Stage	Stage Grouping	Stage Description
<b>I</b>	<b>T1, N0, M0 GS 6 PSA &lt;10</b>	Nonpalpable tumor. No evidence of lymph node involvement (N0) or distant metastasis (M0). GS is 6 and PSA is less than 10.
	<b>OR</b>	
	<b>T2a, N0, M0 GS 6 PSA &lt;10</b>	Tumor palpable and only present in less than half of one lobe. No evidence of lymph node involvement or distant metastasis. GS is 6 and PSA is less than 10.
<b>IIA</b>	<b>T1, N0, M0 GS 7 PSA &lt;20</b>	Nonpalpable tumor. No evidence of lymph node involvement or distant metastasis. GS is 7 and PSA is less than 20
	<b>OR</b>	
	<b>T1, N0, M0 GS 6 PSA 10-20</b>	Nonpalpable tumor. No evidence of lymph node involvement or distant metastasis. GS of 6. PSA between 10 and 20.
	<b>OR</b>	
	<b>T2a or T2b, N0, M0 GS ≤7 PSA &lt;20</b>	Tumor palpable and only present in less than half of one lobe (T2a) or tumor palpable and present in more than half of one lobe (T2b). No evidence of lymph node involvement or distant metastasis. GS can be 6 or 7 and PSA is less than 20.
<b>IIB</b>	<b>T2c, N0, M0 Any GS Any PSA</b>	Tumor palpable and present in up to both lobes (T2c). No evidence of lymph node involvement or distant metastasis. Tumor can have any GS and PSA can be any value.
	<b>T1, T2a or T2b, N0, M0 Any GS Any &gt;20</b>	Nonpalpable tumor (T1), tumor palpable and only present in less than half of one lobe (T2a) or tumor palpable and present in more than half of one lobe (T2b). No evidence of lymph node involvement or distant metastasis. Tumor can have any GS and PSA is above than 20.

	<b>OR</b>	
	<b>T1, T2a or T2b, N0, M0 Any <math>\geq</math> 8 Any PSA</b>	Nonpalpable tumor (T1), tumor palpable and only present in less than half of one lobe (T2a) or tumor palpable and present in more than half of one lobe (T2b). No evidence of lymph node involvement or distant metastasis. Tumor can have any GS 8 or higher and PSA can be any value.
<b>III</b>	<b>T3a or T3b Any GS Any PSA</b>	Extracapsular extension of tumor (unilateral or bilateral) (T3a) or tumor invades seminal vesicles (T3b). No evidence of lymph node involvement or distant metastasis. Tumor can have any GS and PSA can be any value.
<b>IV</b>	<b>T4, N0, M0 Any GS Any PSA</b>	Tumor has invaded in nearby structures such as rectum, levator muscles, urethral sphincter, bladder, or pelvic side wall (T4). No evidence of lymph node involvement or distant metastasis. Tumor can have any GS and PSA can be any value.
	<b>OR</b>	
	<b>Any T, N1, M0 Any GS Any PSA</b>	Tumor may or may have not grown outside prostate. Regional lymph nodes are involved (N1). No evidence of distant metastasis. Tumor can have any GS and PSA can be any value.
	<b>OR</b>	
	<b>Any T, any N, M1 Any GS Any PSA</b>	Tumor may or may have not grown outside prostate. Regional lymph nodes may or may not be involved. Evidence of distant metastasis (M1). It can be non-regional lymph nodes (M1a), bones (M1b), or other sites with or without bone involvement (M1c).

**Table 1. Prostate cancer stages according to AJCC, 2016**

## 1.11 Controversy Surrounding PSA Based-Screening

As mentioned earlier, PSA is an organ specific marker that is highly sensitive and specific in the post-treatment setting. However, it lacks sensitivity and specificity in the screening of prostate cancer. The American Cancer Society systematically reviewed the literature regarding PSA's performance test characteristics. They estimated sensitivity and specificity of a PSA cut-off of 4.0 ng/mL for detecting any prostate cancer was 21% and 91%, respectively (Wolf et al., 2010). In 2012, the U.S. Preventive Services Task Force (USPSTF) published a recommendation against the routine use of PSA screening at any age (U.S. Preventive Services Task Force, 2012). This recommendation was dialed back in 2017, stating that clinicians should only offer PSA screening after patients have been informed about its risks and benefits. They still recommended against PSA-based screening in men 70 years or older. (U.S. Preventive Services Task Force, 2017). In 2014, the Canadian Task Force on Preventive Health Care also published guidelines no longer recommending PSA-based screening for prostate cancer (Canadian Task Force on Preventive Health Care, 2014). These recommendations were mainly based on two large prospective studies looking at the role of PSA as a screening tool. The studies were the European Randomized Trial of Prostate Cancer Screening (ERSPC) and the Prostate, Lung, Colon, and Ovary (PLCO) Trial (de Koning et al., 2002; Auvinen et al., 1996). The ERSPC trial is a collection of trials in different countries with different eligibility criteria, randomization schemes, and strategies for screening and follow-up (Barry, 2009). In the ERSPC trial, Schröder et al. reported that PSA screening without digital rectal examination was associated with a 20% relative reduction in prostate cancer death at a median follow-up of 9 years, with an absolute reduction of about 7 prostate cancer deaths per 10,000 men screened. It is estimated that in order to prevent one prostate cancer death, 781 men have to be screened and 27 additional cases of prostate cancer would need to be treated (Schroder et al., 2014; Barry, 2009). Thus, the ERSPC provided the rationale that PSA screening without the use of DRE was not an effective means of reducing cancer related mortality and unnecessarily placed patients at risk of overtreatment.

In the PLCO study based in the United States, cumulative incidence rates for prostate

cancer in the screening arm were 12% higher than control arms (RR = 1.12, 95% CI = 1.07 to 1.17) (Andriole et al., 2012). However, the study concluded that there was no difference in prostate cancer mortality between the screened and control arms at a median follow-up of 13 years. The cumulative mortality rates from prostate cancer in the intervention and control arms were 3.7 and 3.4 deaths per 10,000 person-years, respectively, resulting in a non-statistically significant difference between the two arms (RR = 1.09, 95% CI = 0.87 to 1.36). However, it should be noted that the PLCO study has been criticized for high rates of contamination with more than half the participants in the control arm undergoing PSA testing by year five (Barry, 2009). Overall, these trials describe the potential for over-diagnosis and overtreatment of prostate cancer with PSA-based screening, underscoring the concept that PSA is not an ideal screening marker.

## 1.12 Biomarkers

It is well known that PSA screening and tissue biopsy are prone to underestimating cancer burden. Therefore, in order to meet the challenge of improving prognostication, prostate cancer biomarkers are constantly being developed and studied since the advent of PSA. In addition, a biomarker that could accurately risk stratify prostate cancer may have a role in patients on active surveillance. Ideally, a biomarker that is more sensitive and specific than PSA would improve current methods of risk stratification of prostate cancer, thus, reducing the number of TRUS biopsies and side effects within this patient population. Biomarkers could have a role in monitoring disease response after treatment. The first clinical biomarker for prostate cancer was prostatic acid phosphatase (PAP) described in 1940s (Taira et al., 2007). It went on to be replaced by PSA which performed significantly better and allows clinicians to monitor treatment response. Currently, there are a number of serum and urine base biomarkers being studied. In addition to PSA, there are two FDA approved biomarkers available in clinical practice.

In 2012, the United States Federal Drug Administration (FDA) approved a test called the Prostatic Health Index (PHI). PHI includes three biomarkers: [-2]proPSA, fPSA and PSA. These biomarkers are combined into an equation,  $([-2]proPSA/fPSA) \times PSA^{1/2}$ , that provides the percent value for PHI. fPSA was previously addressed in the PSA Chapter 1



Section 5. [-2]proPSA is a truncated PSA isoform that differentiate prostate cancer from benign prostates. Two prospective studies showed that [-2]proPSA can more accurately diagnose prostate cancer from benign tissue when compared to PSA and fPSA within PSA ranges of 2.5-10ng/ml (Lazzeri et al., 2013; Le et al., 2010). Some evidence suggests potential utility of [-2]proPSA and PHI in active surveillance. In a cohort of 167 men on active surveillance, [-2]proPSA and PHI provided greater predictive accuracy for biopsy reclassification during follow-up than PSA and fPSA alone (Tosoian et al., 2012).

Another FDA approved biomarker available in screening for prostate cancer is known as Prostate Cancer Antigen 3 (PCA3). This biomarker is unique as it is a urine based test. It was first isolated in 1999 by Bussemakers and colleagues using differential display and Northern blot analysis to compare normal and prostate cancer tissue in the same patients (Bussemakers et al., 1999). They identified it as a noncoding RNA located on chromosome 9q21-22 that is a very sensitive and specific prostate cancer biomarker. Although its function is not known, it has been shown to be expressed very highly in cancer tissue in comparison to benign tissue with an area under the curve (AUC) of the receiver operating characteristic (ROC) curve of 0.88 (95% CI 0.78-0.97) (de Kok et al., 2002). Currently there is a standardized transcription mediated RNA amplification assay for urine samples that can reliably measure PCA3 mRNA levels in voided samples with an AUC ~0.70 (Groskopf et al., 2006, Sokoll et al., 2008). In 2012, the FDA approved the use of a commercial assay, ProgenSA PCA3 Test (Hologic), to aid clinicians in decision making for men who have elevated PSAs and initial negative TRUS biopsy result. The assay involves performing a reverse transcription polymerase chain reaction on urine samples collected post-DRE. The mRNA of PCA3 and PSA is measured and a ratio (mRNA PCA3/ mRNA PSA) determines the PCA3 score (Wein et al., 2016). Currently there is no standardized cutoff value, however, a threshold of 25 was used in the FDA approval studies. A comparative effectiveness review by Bradley and colleagues showed that a threshold of 25 results in a sensitivity of 74% and specificity of 57% (false-positive rate of 43%) (Bradley et al., 2013).

It should be noted that there are a number of non-FDA approved biomarker tests that are currently being used in clinical research. They include: TMPRSS2-ERG gene fusion test,

Mi-Prostate score test, Oncotype DX test, ProMark test, ConfirmMDx test, Prolaris test, Prostate Core Mitomic test, 4K score test, Prostarix test and Decipher test. There are biomarkers that are early in their development which include: circulating tumor cells, microRNA and exosomal biomarkers (Saini et al., 2016). This thesis will address developing a “liquid biopsy” from patient plasma that enumerates putative prostate cancer biomarkers on the surface of circulating tumor cell fragments that are known as “prostate cancer microparticles” (PCMPs).

### 1.13 Microparticles (MPs)

Patients with prostate cancer have shown to have higher levels of microparticles compared with control patients (Tavoosidana et al., 2011) MPs are able to affect neighboring cells in various ways, such as inducing intracellular signaling or by transferring different molecules such as proteins, mRNAs, or microRNAs to cells. They have been suggested to contribute to cancer cell survival, invasiveness, and metastases (Al-Nedawi et al., 2009). MPs may provide a novel method to risk stratify prostate cancer, monitor cancer progression and follow treatment response after surgery, radiation or hormonal therapy.

Extracellular vesicle (EV) is an umbrella term used to describe exosomes, microparticles (MP) and apoptotic bodies. They are distinguished by their size, biogenesis and mechanism of release. Exosomes range 20-100 nm in size and are released from the cells through inward budding of endosomal membranes to form large multivesicular bodies. The multivesicular bodies then fuse with the plasma membrane of the cell releasing multiple exosomes from the multivesicular body. Exosomes often contain endocytic markers, such as tetraspanins and heat shock protein 73 (HSP73) (Mathivanan and Simpson, 2010; Chaput et al., 2004).

Microparticles range between 100 nm to 1000 nm and are often released concomitantly making differentiation of microparticles and exosomes difficult (Heijnen et al., 1999). The majority of microparticles express phosphatidylserine (PS) on their surface whereas PS is usually absent on the surface of exosomes (They et al., 2002). Other names for microparticles include: microvesicles, oncosomes, apoptotic bodies, ectosomes, and

prostasomes (Ronquist et al., 2012).

Apoptotic bodies measure 1000-5000 nm (Huang-Doran et al., 2017) and are generated during the programmed cell death mechanism known as apoptosis. These apoptotic bodies are then phagocytosed by neighbouring cells and degraded by phagolysosomes. Microparticles and apoptotic bodies are released via direct outward budding from the surface of cells. Contents within EV range from membrane-bound proteins, lipids, metabolites, DNA, and RNAs (mRNA, miRNA, and other small regulatory RNAs) protected in a lipid bilayer (Huang-Doran et al., 2017). Since EV are products of cells, their cargo is often remnants of parent cells. Major sources of EVs in the blood are from platelets, leukocytes and endothelial cells (Yuana et al., 2013). In this thesis, the focus will be on microparticles and their role in prostate cancer identification.

The discovery of microparticles initially stemmed from the observation in 1946, where Erwin Chargaff and Randolph West discovered that platelet-free plasma exhibited clotting properties. This contradicted the major dogma of preceding times, that platelets served necessarily as the blood coagulation contributor (Chargaff and West, 1946). However, microparticles were not formally described until 1976, when Peter Wolf noted vesicular fragments rich in phospholipids originating from activated platelets, which he termed “platelet dust.” This was subsequently replaced with term microparticle (Wolf, 1971). Platelet microparticles (PMP) are by far the most abundant and account for 70% to 90% of circulating microparticles in the bloodstream (Xu et al., 2011). It is now accepted that PMPs play a significant role in modulating normal physiological processes such as coagulation. Coagulation is expressed by way of multifunctional cellular signaling proteins such as tissue factor (Brett et al., 2015), plasminogen activator inhibitor-1 and vitronectin (Podor et al., 2002). In terms of prostate cancer, PMP firmly adhere to prostate cancer cells and significantly increase their adhesion to endothelial cells (Varon et al., 2012). In vitro studies have shown that PMPs promote tumor cell invasive properties through increases in metalloproteinases (MMP-2) synthesis and secretion (Dashevsky et al., 2009). In vivo mouse studies have also shown that platelet microparticles enhance prostate cancer cell accumulation and yield more neoplastic foci within the lungs of mice (Varon et al., 2012).

MPs associated with the prostate were first discovered in 1977 by Ronquist and Hedstrom (Ronquist and Hedstrom, 1977). These EVs were secreted by acinar cells of the prostate and later termed prostasomes (Brody et al., 1983). Studies on semen have shown that their role in protecting sperm from the female innate immune system is by way of suppressing natural killer cell (NK) activation. This is done through CD48 ligand on the prostasomes interacting with NK-activating receptor CD244 (Tarazona et al., 2011). Compared to exosomes, they are enriched with cholesterol, sphingomyelin,  $Ca^{2+}$ , guanosine diphosphate, and many transmembrane proteins (CD13, CD46, CD55, and CD59) (Duijvesz et al., 2011; Sandvig and Llorente, 2012).

Prostasomes are emerging as rich reservoirs of tumor-specific proteins and biomarkers for cancer detection and progression. They can be isolated from prostatic secretions, seminal fluid, tissue, urine or blood. Structurally, they are distinct in size, membrane composition and specific prostate protein content, potentially providing a novel isolatable source of biomarkers (Drake and Kislinger, 2014; Brett et al., 2015). Tavoosidana et al, developed a proximity ligation assay (PLA) to detect these microparticles in blood plasma from patients with prostate cancer and control subjects. The assay identified microparticles to be significantly higher in men with prostate cancer when compared to the controls and was able to successfully distinguish prostate cancers with low Gleason scores from those with medium and high Gleason scores, reflecting disease severity (GS 8/9 and GS 7 from GS 6) (Tavoosidana et al., 2011).

In addition, PCA3 and TMPRSS2-ERG RNA transcripts have been detected in prostasomes isolated from urine of prostate cancer patients. It was revealed that elevated levels were associated with cancer (Nilsson et al., 2009). Biggs CN, Siddiqui KM et al, have enumerated prostate cancer microparticles of patients with various Gleason grades using prostate specific membrane antigen (PSMA) and nanoscale flow cytometry. Their study highlighted the ability of PCMPs to risk stratify  $GS \geq 8$ , high risk prostate cancer, from healthy volunteer plasma. Plasma containing the MPs was collected prior to and after radical prostatectomy and GS was obtained from final surgical pathology. Interestingly, they were able to show that these microparticles significantly decreased post-surgery due to the absence of prostatic tissue, demonstrating their role to monitor

treatment response during clinical follow-up (Biggs et al., 2016).

Elucidating MP composition and functional activity is hampered by the complexity of the biological fluids where MPs are present and the small size of MPs (van der Pol et al., 2010). Visualization techniques such as electron microscopy (EM) and confocal microscopy (CM) with MPs stained with fluorescent antibodies provides good morphological characterization of microparticles but cannot serve as quantitative assays in a high throughput manner. With enhancements in technology, microparticles are able to be enumerated with greater accuracy allowing new avenues of research to study their clinical utility (Leong et al., 2011). One such advancement is flow cytometry which utilizes both fluorescence probes and light scattering. Quantification by flow cytometry shows good correlation with the relative light scattering intensities determined by dynamic light scattering (Xu et al., 2011). However, conventional flow cytometry light scattering has size limitations and usually not able to detect MP with diameters smaller than 300–400 nm as a separate fraction (van der Pol et al., 2010; Zwicker, 2010; Barteneva et al., 2013). Next generation instruments such as nanoscale flow cytometry are able to readily analyze events 100-1000 nm for analysis of multiple biomarkers on MPs such as those from the prostate in a high-throughput and multi-parametric manner (van der Pol et al. 2014; Biggs et al., 2016).

## 1.14 Nanoscale Flow Cytometry

Our lab utilizes an Apogee A-50Micro nanoscale flow cytometer to enumerate EVs smaller than 1000 nm. This specialized instrument analyzes EVs in a high-throughput, multi-parametric manner. The equipment is manufactured by Apogee FlowSystems Inc., in Hertfordshire, UK (**Figure 3**). This machine has three lasers installed; the laser wavelengths are 405 nm, 488 nm and 635 nm (**Figure 4**). The multiple light scattering and fluorescence detectors help increase the detection limit to 100 nm and increase the resolution to <10 nm. This machine is equipped with Peripheral Component Interconnect Express (PCIe) high-speed computer software used for data acquisition at a speed of up to 100k events per second.



**Figure 3. Apogee, A-50M nanoscale flow cytometer (Apogee FlowSystems Inc., UK).**

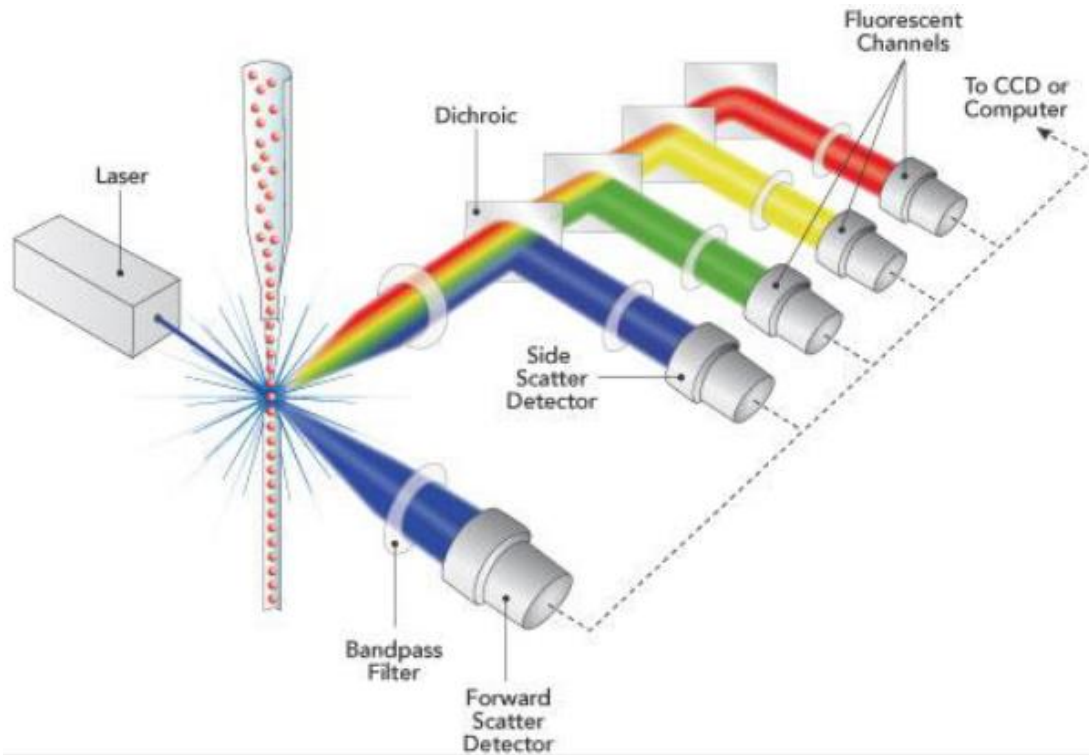


**Figure 4. Depiction of light scatter detectors and the three fluorescent channels in the Apogee A-50M nanoscale flow cytometer. Image obtained from website: <https://flowcytometry.med.ualberta.ca> (Accessed January 2017).**

Conventional flow cytometers on the market today resolve up to 200 nm diameter latex beads by light scatter but will fall close to the instrument's sensitivity limit. Also, latex is far more refractive (refractive index  $\sim 1.59$ ) than biological particles (refractive index  $\sim 1.40$ ). For example, a 400 nm biological particle may scatter about the same as a 200 nm latex bead. Conventional flow cytometers are therefore not suitable for measuring light scattered by biological particles less than about 400 nm diameter. The Apogee A-50M can measure particles which scatter 1000 times less than 200 nm latex beads making it the ideal instrument to accurately enumerating EVs of various sizes (Apogee Flow systems, 2017).

### 1.15 Prostate Cancer Surface Markers

To characterize the cellular origin of MPs in peripheral blood, the most common approach is to stain MPs with fluorescently-labeled antibodies directed against antigens of parental cells. For example, antibodies against CD41, CD61 and platelet activation marker CD62 may be used to identify MPs from platelets, glycophorin for erythrocyte MPs; CD45 for lymphocyte MPs; CD14 for monocyte MPs, and so on (Barteneva et al., 2013). In this study, a combination of three different antibodies targeting distinct antigens will be used to characterize the origins of the MPs from prostate cancer plasma samples from those of control samples. All antibodies were conjugated to a fluorophore that the nanoscale flow cytometer can detect through laser light excitation. Specifically, these antigens are divided into two broad categories, namely prostate tissue specific antigens and cancer specific antigens. The tissue specific antigens include prostate specific membrane antigen (PSMA) and six-transmembrane epithelial antigen of prostate 1 (STEAP1). The prostate cancer specific antigens include ghrelin receptor (GHSR1a), and CD151. The combination of PSMA, STEAP1 and one of the cancer specific antigens will be used to enumerate triple-positive MPs. The hypothesis is these combinations can allow differentiation prostate cancer plasma samples from control group plasma samples (benign prostatic hypertrophy (BPH) or healthy volunteers). A further hypothesis is the Gleason grade for prostate cancer can be accurately determined when analyzed using the triple-positive microparticles.



## 1.16 Prostate Specific Membrane Antigen (PSMA)

PSMA is a type II transmembrane protein. It has a unique 3-part structure: a 19-amino-acid internal portion, a 24-amino-acid transmembrane portion, and a 707-amino-acid external portion (Israeli et al., 1993; Chang, 2004). PSMA has known enzymatic activities and acts as a glutamate-preferring carboxypeptidase. The impact of these enzymatic functions on prostatic tissue remains unclear (Pinto et al., 1996). PSMA does have an internalization signal that allows the surface protein to enter into the cell as an endosome (Rajasekaran et al., 2003).

The original monoclonal antibody developed for PSMA was a mAb 7E11 used on the prostate cancer cell line LNCaP. It binds to a PSMA intracellular or cytoplasmic epitope (Troyer et al., 1997). The US Food and Drug Administration has also approved radiographic testing using mAb 7E11 known as ProstaScint, by linking it to <sup>111</sup>indium-capromab pendetide to produce a radio-diagnostic marker (Petronis et al., 1998; Hinkle et al., 1998). The next-generation of antibodies now bind to the extracellular portion of PSMA and can also be internalized by PSMA expressing cells (Liu et al., 1998). Furthermore, they are now either fully human or humanized as opposed to murine antibodies, thus making them even more likely to be diagnostically and therapeutically effective without possible antimouse reactions (Chang, 2004).

Studies have shown that PSMA is present on all types of prostatic tissue and expression increases in the presence of prostate cancer. Bostwick and colleagues described PSMA immunohistochemical expression in 184 prostate specimens examined. All specimens showed PSMA expression with the degree of expression correlating with the grade of cancer. There was an increase in the percentage of PSMA staining from benign epithelial tissue (69.5%) to HG PIN (77.9%) to malignant cells (80.2%) (Bostwick et al. 1998). Using antibodies compatible with nanoscale flow cytometry, Biggs CN and Siddiqui KM et al, showed that microparticles positive for PSMA could be enumerated in patients with prostate cancer. PSMA 3E7 antibodies can accurately differentiate high-grade prostate cancer (GS 8 or higher) from lower grade prostate cancer and benign prostatic disease (Biggs et al., 2016). While PSMA levels are highest in the prostatic epithelium, it has

been confirmed to be present at four sites in the body albeit at significantly lower levels: prostate (secretory acinar epithelium), kidney (proximal tubules), nervous system glia (astrocytes and schwann cells), and the small bowel (brush border) (Mhaweche-Fauceglia et al., 2007). To establish a “liquid biopsy” specific for prostate cancer, we will also combine PSMA with another putative prostate specific marker, six-transmembrane epithelial antigen of the prostate-1 (STEAP1). When used in combination on the nanoscale flow cytometer, we will be able to specifically enumerate only microparticles that co-express both of these prostate-specific markers, PSMA and STEAP1.

### 1.17 Six-transmembrane Epithelial Antigen of the Prostate-1 (STEAP1)

Six-transmembrane epithelial antigen of the prostate-1 (STEAP1) is a cell surface protein highly expressed in primary prostate cancer, with restricted expression in normal prostate tissues (Challita-Eid et al., 2007). The STEAP1 gene is located on chromosome 7q21.13 and was the first member of the STEAP family to be identified (Gomes et al., 2012). It is a 339-amino acid protein with six potential membrane-spanning regions that was first identified on LAPC-4 (Los Angeles Prostate Cancer) androgen dependent xenografts. LAPC xenografts represent advanced prostate cancer specimens that were derived from bone and lymph node metastases (Hubert et al., 1999). Hubert RS and Vivanco I et al, later went on to identify significant STEAP1 expression in all early and advanced primary prostate cancer specimens, including hormone-refractory samples. Prostate cancer cell lines LNCAP, DU-145, PC3 are also positive for STEAP1, with LNCAP have the highest expression (Challita-Eid et al., 2007; Yamamoto et al., 2013). Furthermore, STEAP1 has been identified on other cancer cell lines such as lung, bladder, testicular cancer, cervical cancer and ovarian cancer. This suggests the potential applicability in cancer research beyond the prostate.

STEAP1 is localized on plasma membranes at cell-cell junctions of secretory epithelium of prostate cells and may function as ion channel/transporter protein for intracellular communication (Challita-Eid et al., 2007). Furthermore, there is supportive evidence of utilizing STEAP1 antigen as targeted immunotherapy in anti-tumor therapy to prevent

growth and metastatic capability in vivo studies (Challita-Eid et al., 2007; Rodeberg et al., 2005; Yamamoto et al., 2013). STEAP1 mRNA has been identified by real-time PCR in serum of patients with cancer indicating possible use as a biomarker (Valenti et al., 2009). In fact, STEAP1 localization on the cell membrane, its overexpression in cancer tissues, and absence in vital organs underscores its potential use as a biomarker of disease and as potential immunotherapeutic targets against prostate cancer (Gomes et al., 2012). Recent studies have looked at imaging STEAP1 using zirconium-89 immunopET to determine who may benefit from immunotherapy in prostate cancer (Doran et al., 2014). There are many commercial STEAP1 antibodies available for nanoscale flow cytometry.

### 1.18 Ghrelin Ligand and its Receptor (GHSR1a)

Ghrelin receptor, also known as type 1a growth hormone secretagogue receptor (GHSR1a), is a G-protein coupled receptor that binds to an endogenous ligand known as ghrelin (Chopin et al., 2012). Ghrelin is a 28-amino acid peptide hormone that has a posttranslational modification of an octanoyl group added to the third amino acid residue, which is serine (Kojima et al., 1999). Ghrelin was first discovered in 1999 from rats and then human stomach (Kojima et al., 1999). Its receptor, GHSR1a, was discovered in 1996, and first noted to be present on the pituitary and hypothalamus (Jeffery et al., 2002). Ghrelin stimulates the release of growth hormone (GH) from the anterior pituitary through the receptor GHSR1a (Howard et al., 1996).

With the discovery of GHSR1a in neuroendocrine tumors in 1997 and in vitro in rat pituitary tumor cells in 1998, it has been suggested that ghrelin and GHSR1a could play a role in autocrine/endocrine pathogenesis of cancer (de Keyzer et al., 1997; Adams et al., 1998). Ghrelin protein is now understood to be expressed on various malignancies involving: the prostate, digestive tract, pancreas, lung, thyroid, breast, ovarian, renal, and adrenocortical tumors (Chopin et al., 2012). Jeffery et al. 2002, was the first to demonstrate functional evidence that ghrelin's autocrine/paracrine role in stimulating prostate cancer cell proliferation. They incubated PC3 cells with ghrelin (5 nanograms) over a 3-day period and noticed a 33% increase in cell growth when compared to the control group (Jeffery et al., 2002). This was again seen in another study using higher

concentrations of ghrelin (1 microgram), however, with less significant growth (Yeh et al., 2005). Researchers at Western University showed that a modified truncated ghrelin molecule conjugated to a fluorophen could be used as a potential novel imaging marker in patients with prostate cancer. The ghrelin signal was significantly higher in prostate cancer tissue specimens when compared to normal tissue and BPH. Although *in vivo* imaging studies are required, this method could be useful in discriminating benign disease and cancer in patients (Lu et al., 2012). GHSR1a clearly has a role in prostate cancer, thus, it may have a role as a surface marker for risk stratification.

## 1.19 CD151

CD151 is a gene located on chromosome 11p15.5 (Hasegawa et al., 1997). CD151 is a tetraspanin that consists of four transmembrane domains with two extracellular (EC1 and EC2) and one intracellular loop (Fitter et al., 1995). Expression has been noted on tissues such as prostate epithelium, endothelial, smooth muscle, cardiac muscle, and lymphocytes, however, to a lower degree than cancer tissues (Geary et al., 2001). The family of tetraspanin proteins are linked to various processes including signal transduction pathways, cellular activation, proliferation, motility, adhesion, tissue differentiation, angiogenesis, tumor progression and metastasis (Detchokul et al., 2014).

CD151 was the first tetraspanin to be associated with metastasis in human cancers (Testa et al., 1999). CD151 forms stable, lateral complexes with laminin-binding integrins, such as,  $\alpha 3\beta 1$ ,  $\alpha 6\beta 1$  and  $\alpha 6\beta 4$  which have been crucial in cancer cell migration and invasion (Longo et al., 2001). Many different cancer cell lines have been transfected to overexpress CD151 to examine its effect on metastasis (Ang et al., 2010). Ang et al. 2010, worked with two prostate cancer cell lines, LNCaP and PC3, to study the effect of CD151 on prostate cancer cells. Through western blot analysis, LNCaP is shown to have a lower expression of CD151 than DU145 and PC3 (Detchokul et al., 2014; Ang et al., 2010). Therefore, LNCaP cells were chosen to be transfected to overexpress CD151 and PC3 cells were transfected with siRNA to knock-down CD151 expression. Overexpression of CD151 was not associated with increased proliferation in LNCaP cell line but showed increased migration and invasion when compared to control ( $p < 0.01$ ).

PC3 knock-down cells showed less migration and invasion when compared to the control siRNA and the no siRNA group ( $p < 0.01$ ) (Ang et al., 2010). These results reiterate findings from previous studies illustrating the role of CD151 in cancer invasion and metastasis.

Ang et al. 2004, also looked at CD151 expression of prostate specimens from patients with prostate cancer vs BPH. Through quantitative immunohistochemistry of pathology specimens, CD151 expression was found to be significantly higher in prostate cancer specimens compared with BPH specimens ( $P < 0.001$ ). Poorly differentiated cancers expressed the strongest staining. The study further concluded CD151 expression was negatively correlated with survival (Ang et al., 2004). Although no definitive conclusion can be drawn from this small retrospective study, it does shed light on CD151 as a potential biomarker in advanced prostate cancers that have a tendency to metastasize.

## 1.20 Hypothesis

In this pilot study, I hypothesize that the level of prostate cancer microparticles in patient plasma that co-express PSMA and STEAP1 in combination with CD151 or GHSR1 represents a “liquid biopsy” that is predictive of the pathologic Gleason Score found in whole gland specimens obtained from radical prostatectomy.

## 1.21 Research Objectives

**Objective #1:** To determine if STEAP1, CD151, and GHSR1 are present on the surface of prostate cancer microparticles in plasma samples from prostate cancer patients using nanoscale flow cytometry. To optimize the flow cytometric assay for enumeration of PSMA, STEAP1, CD151, and GHSR1a expressing microparticles present in prostate cancer patient plasma samples.

**Objective #2:** Using the optimized assay conditions developed in Objective #1, to enumerate every permutation of microparticles expressing tissue biomarkers PSMA and STEAP1 with cancer biomarkers (CD151 or GHSR1a).

**Objective #3:** To assess the diagnostic capability of prostate cancer microparticles (PCMPs) that co-express PSMA and STEAP1 as well as triple positive PCMPs expressing PSMA+STEAP1 and GHSR1a or CD151 for risk stratification in prostate cancer patients. Level of these PCMPs will be compared to final surgical pathology to determine which combination of tissue-specific and cancer-specific biomarkers will result in the best performing “liquid biopsy.”

## Chapter 2

### 2 Materials and Methods

#### 2.1 Patient Sample Preparation, Blinding and Ethics

Research ethics board (REB) approvals were obtained for analyzing retrospectively collected patient blood samples and patient chart information for patients who underwent radical retropubic prostatectomy for prostate adenocarcinoma. This was obtained through Western University under ethics applications (REB#103156). The REB approval was used to obtain plasma samples from two different biorepositories, the GU Biobank at Princess Margaret Hospital (Toronto) and the Ontario Tumor Bank (Ontario Institute for Cancer Research). These samples have been de-identified and experiments were performed blinded. A master list and all clinical information (age, pathologic staging, pre-op PSA levels, Gleason Score from whole mount prostate sections, post-OP PSA levels, and date of surgery) was kept separately in the office of Dr. Hon Leong. All blood samples were collected via venipuncture into 10mL EDTA-K2 vacutainers and plasma was isolated by centrifugation of vacutainers containing whole blood at  $2,000\times g$ 's for 20 minutes at room temperature. The supernatant, platelet poor plasma, was reserved and stored into cryovials (1.5 mL capacity) in 1.0mL aliquots and then stored in liquid nitrogen prior to shipment to Dr. Leong's laboratory. All received plasma samples were then stored in  $-80^{\circ}\text{C}$  freezer until they were analyzed. Samples were thawed slowly in  $4^{\circ}\text{C}$  refrigerators prior to being prepared for analysis.

#### 2.2 Antibody and Reagents

Antibodies used for nanoscale flow cytometry were obtained from commercial sources. The following antibodies were used: mouse IgG<sub>1</sub> anti-CD151 (clone 11G5a) (Abcam #ab33315), mouse IgG<sub>1</sub> anti-GHSR1 (clone #502430) (R&D systems, Inc. #MAB8370), mouse IgG<sub>2b</sub> anti-PSMA 3/E7 (clone J591), and mouse IgG<sub>2b</sub> anti-STEAP1 (clone J2D2) (Novus Biologicals #NBP107094Y).

All primary antibodies were conjugated with fluorescent labels by using commercial antibody labeling kit. Anti-PSMA and mouse IgG<sub>2b</sub> (clone MPC-11) (Abcam #ab18457) isotype-matched control were conjugated to R-PhycoErythrin (R-PE) fluorophore using the Lightning-Link R-PhycoErythrin kit (Innova Biosciences #703-0010) following manufacturer's instructions. Anti-STEAP1 as well as the mouse IgG<sub>2b</sub> isotype-matched control came conjugated by manufacture to Alexa647 fluorophore. Anti-CD151, anti-GHSR and its respective isotype-matched control mouse IgG<sub>1</sub> kappa (clone 11711) (R&D systems, Inc. #MAB002) were conjugated using FITC labeling kit (Thermo Scientific #F6434) Anti-CD151 isotype-matched control mouse IgG<sub>1</sub> kappa (clone MOPC-21) (Abcam #ab106163) came conjugated with FITC from the manufacture.

### 2.3 Immunolabeling of Prostate Cancer-derived Microparticles

10  $\mu$ L of patient plasma was incubated in the dark for 30 minutes at room temperature with 0.8  $\mu$ g of anti-STEAP1-AF 647 [concentration 0.4  $\mu$ g/ $\mu$ L] and 0.75  $\mu$ g of anti-PSMA-PE [concentration 2  $\mu$ g/ $\mu$ L] to label prostate cancer-derived microparticles. 0.68  $\mu$ g of anti-CD151-FITC [concentration 1.0  $\mu$ g/ $\mu$ L] or 0.8  $\mu$ g of anti-GSHR1-FITC [concentration 0.5  $\mu$ g/ $\mu$ L] was also added to the plasma. Phosphate buffered saline (PBS) was added to the plasma samples to achieve a total volume of 300  $\mu$ L (30-fold dilution) and samples were subsequently analyzed via A50-Micro Nanoscale Flow Cytometer (Apogee FlowSystems Inc., UK) for triple-positive EVs between 100-1000 nm in diameter. For each patient, we also incubated plasma samples with isotype-matched control antibodies following the same protocol used for nanoscale flow cytometry analysis as outlined above. Titrations of all antibodies of interest and isotype-matched controls were initially performed in order to determine optimal concentrations.

### 2.4 Acquisition settings for nanoscale flow cytometry

Data was acquired using A50-Micro Nanoscale Flow Cytometer (Apogee FlowSystems Inc., UK) equipped with 50mW 405 nm (violet), 488 nm (blue) and 639 nm (red) lasers. Parameters in the control panel were set to sheath pressure of 150 mbar and number of flush cycles to 2. Sample flow rate of 1.5  $\mu$ L/min was used for all measurements and the

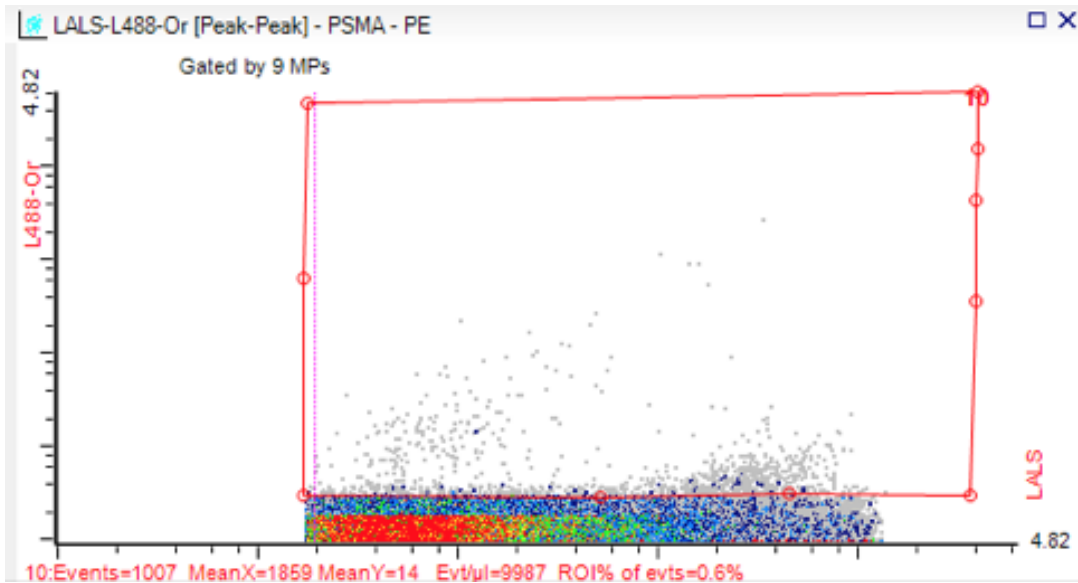


time of acquisition was held constant for all samples at 120 seconds to yield enough events.

Before sample measurements, calibration of flow cytometer was verified using a reference bead mix (*ApogeeMix*, Apogee Flow Systems, #1493) composed of a mixture of plastic spheres with diameters of 180 nm, 240 nm, 300 nm, 590 nm, 880 nm, and 1,300 nm with a refractive index (RI) of 1.42, and 110 nm and 500 nm green fluorescent (excited by blue laser) beads with RI of 1.59 (latex) were used. These beads were used to assess the flow cytometer's (FC) light scattering and fluorescence performance (both sensitivity and resolution). This can easily and quickly inform the user whether the flow cytometer at current settings is capable of quality measurements of EVs. A reference bead mix was used to set the photomultiplier tube (PMT) voltages and the thresholds for light scattering as follows: L488 (320V), L639 (590V), SALS (200V), and LALS (260V). All measurements were performed in log mode. The noise levels in PMT panel were kept below 0.5. Thresholds were set at 5 and 15 (log scale) to eliminate unwanted events (background noise) and avoid loss of particles of interest.

Samples incubated with isotype-matched antibodies were run first in order to determine the nonspecific binding and autofluorescence within the sample. Gates were then designed on the histogram by drawing boundaries that would include the region of interest and exclude nonspecific events. Samples incubated with antibodies of interest were subsequently run and the triple positive microparticle events/ $\mu\text{L}$  were recorded. Each event seen on the histogram is a reflection of a single MP captured as a result of binding to a specific antibody. On the histogram, the x-axis reflects the size of the microparticle while the y-axis reflects the degree of fluorescence (**Figure 5**). The number of triple positive MP events/ $\mu\text{L}$  in the isotype sample were subtracted from the number of triple positive MP events/ $\mu\text{L}$  in the antibody sample to exclude any nonspecific events. PBS washes were included after every respective isotype-control and antibody sample run to exclude carryover of fluorescently positive events (EVs/fluorescent dye) between patient plasma samples.

A



B

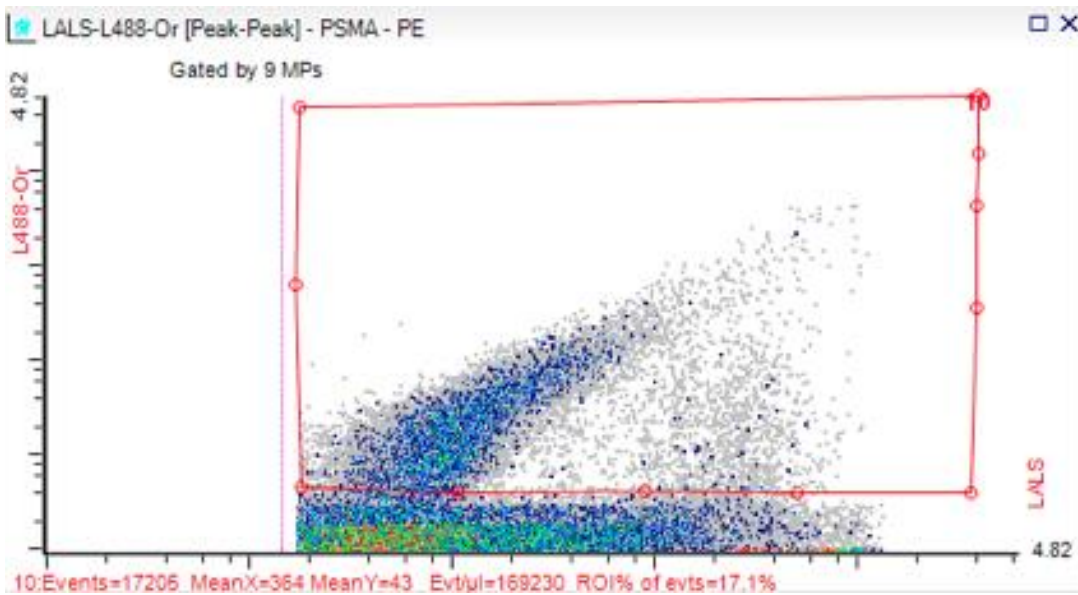


**Figure 5.** An example of histograms portraying PSMA-PE isotype (A) and PSMA-PE antibody (B). The x-axis represents sizing as long angle light scatter (LALS) and y-axis represents degree of fluorescence represented by a log scale. Each dot represents one positive event within the gate (displayed in red).

## 2.5 Data analysis and Statistics

Parameters that were recorded are as follows: total microparticles (MP) within sample, PSMA positive MP events/ $\mu\text{L}$ , STEAP1 positive MP events/ $\mu\text{L}$ , CD151 positive MP events/ $\mu\text{L}$ , GHSR1a positive MP events/ $\mu\text{L}$ , PSMA+STEAP1 positive MP events/ $\mu\text{L}$ , PSMA+CD151 positive MP events/ $\mu\text{L}$ , STEAP1+CD151 positive MP events/ $\mu\text{L}$ , PSMA+GHSR1a positive MP events/ $\mu\text{L}$ , STEAP1+GHSR1a positive MP events/ $\mu\text{L}$ , PSMA+STEAP1+CD151 positive MP events/ $\mu\text{L}$ , and PSMA+STEAP1+GHSR1a positive MP events/ $\mu\text{L}$ . An example of a triple positive MP histogram is seen in **Figure 6**. Dual positive gates for MPs are superimposed with a single positive MP gate in order to create a triple positive MP gate. For example, dual positive PSMA+STEAP1 positive MP gate will be superimposed with GHSR1a positive MP gate in order to create a triple positive PSMA+STEAP1+GHSR1a MP gate. The triple positive MP events/ $\mu\text{L}$  in the isotype sample were then subtracted from the triple positive MP events/ $\mu\text{L}$  in the antibody sample. All data were collected in an Excel spreadsheet. GraphPad Prism 7.0 was used to run statistical analysis. One-way ANOVA test was used to evaluate statistical significance across the groups. The confidence interval was set at 95% and the p-value of  $<0.05$  was considered significant.

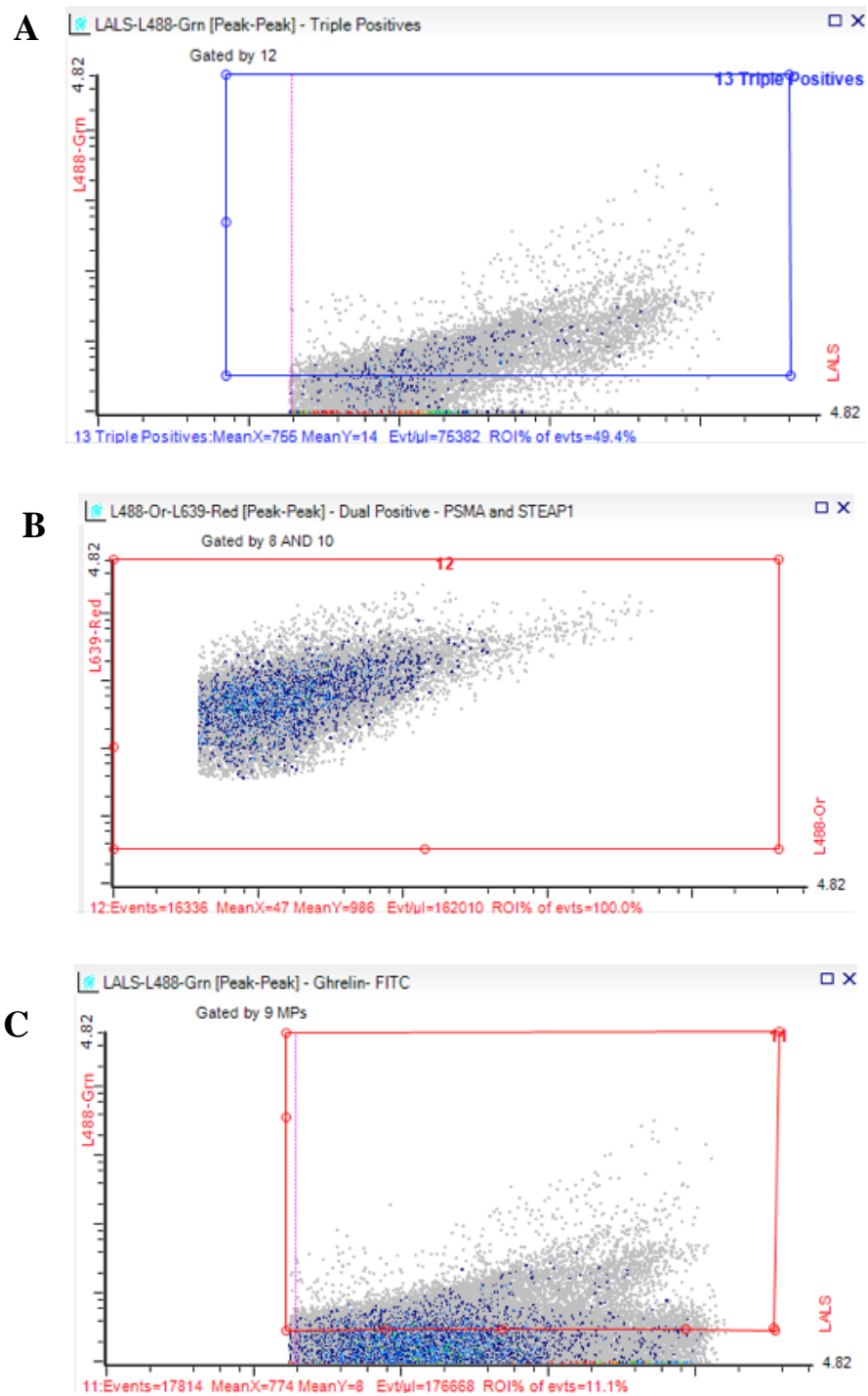


**Figure 6. Example of a triple positive histogram (A, MPs that are positive for PSMA, STEAP1 and GHSR1a). MPs within blue rectangle gate are recorded and represented as events/ $\mu$ L. The x-axis represents sizing as long angle light scatter (LALS) and y-axis represents degree of fluorescence represented by a log scale. This gate was created by superimposing dual positive MPs (B, PSMA+STEAP1) with single positive MP gate (C, GHSR1a). Each dot represents one positive event within the gate (displayed in red).**

## Chapter 3

### 3 Results

#### 3.1 Study Cohort

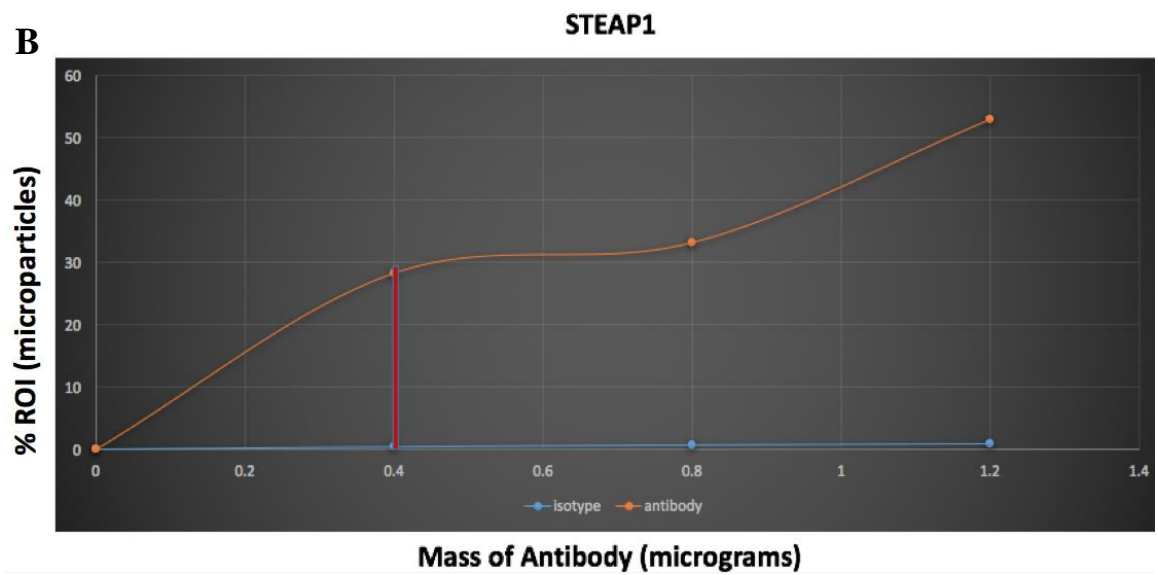
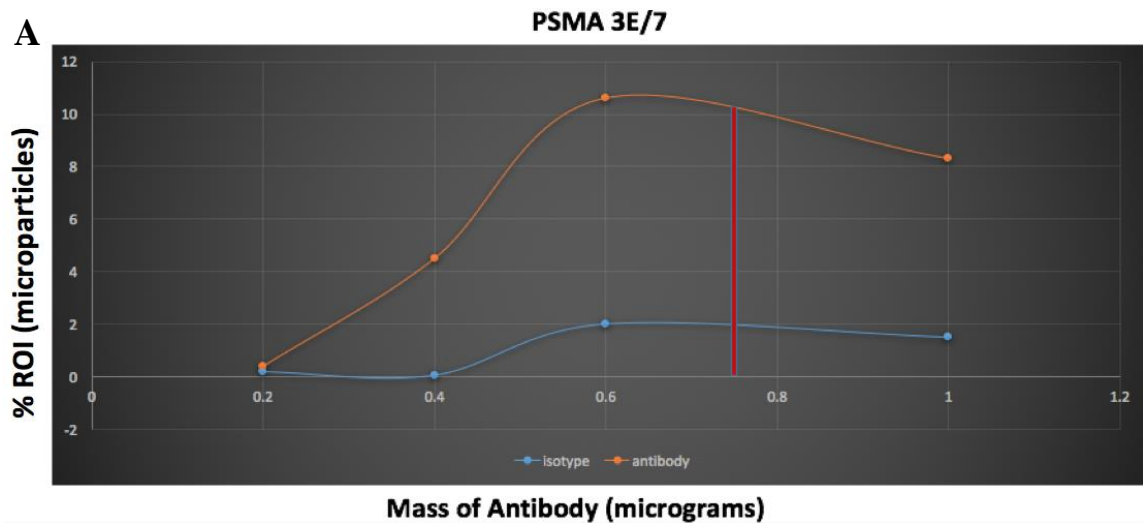
The study cohort contained plasma samples of 60 patients with prostate cancer. Patient characteristics are shown in **Table 2** (next page). The patient cohort median age is 63 years (range of 48-74 years). PSA was divided into three groups: PSA <4ng/mL contains 15 patients (25%), PSA from 4-10ng/mL contains 33 patients (55%) and PSA >10ng/mL contains 12 patients (20%). All final pathology is from examination of prostates post radical prostatectomy. There was no evidence of metastatic disease at time of surgery. There were no healthy volunteer controls or BPH patients with negative prostate biopsies that were analyzed in this study.

Median Age (range)	63 (48-74)
Clinical or Pathological Feature	Number of Patients (%)
<b>Gleason Score</b>	
6 (Grade group 1)	16 (27%)
3+4 (Grade group 2)	14 (23%)
4+3 (Grade group 3)	15 (25%)
≥8 (Grade group 4-5)	15 (25%)
<b>pT stage</b>	
pT2a	15 (25%)
pT2c	17 (28%)
pT3a	14 (23%)
pT3b	8 (13%)
<b>PSA level (ng/ml)</b>	
<4	15 (25%)
4-10	33 (55%)
>10	12 (20%)

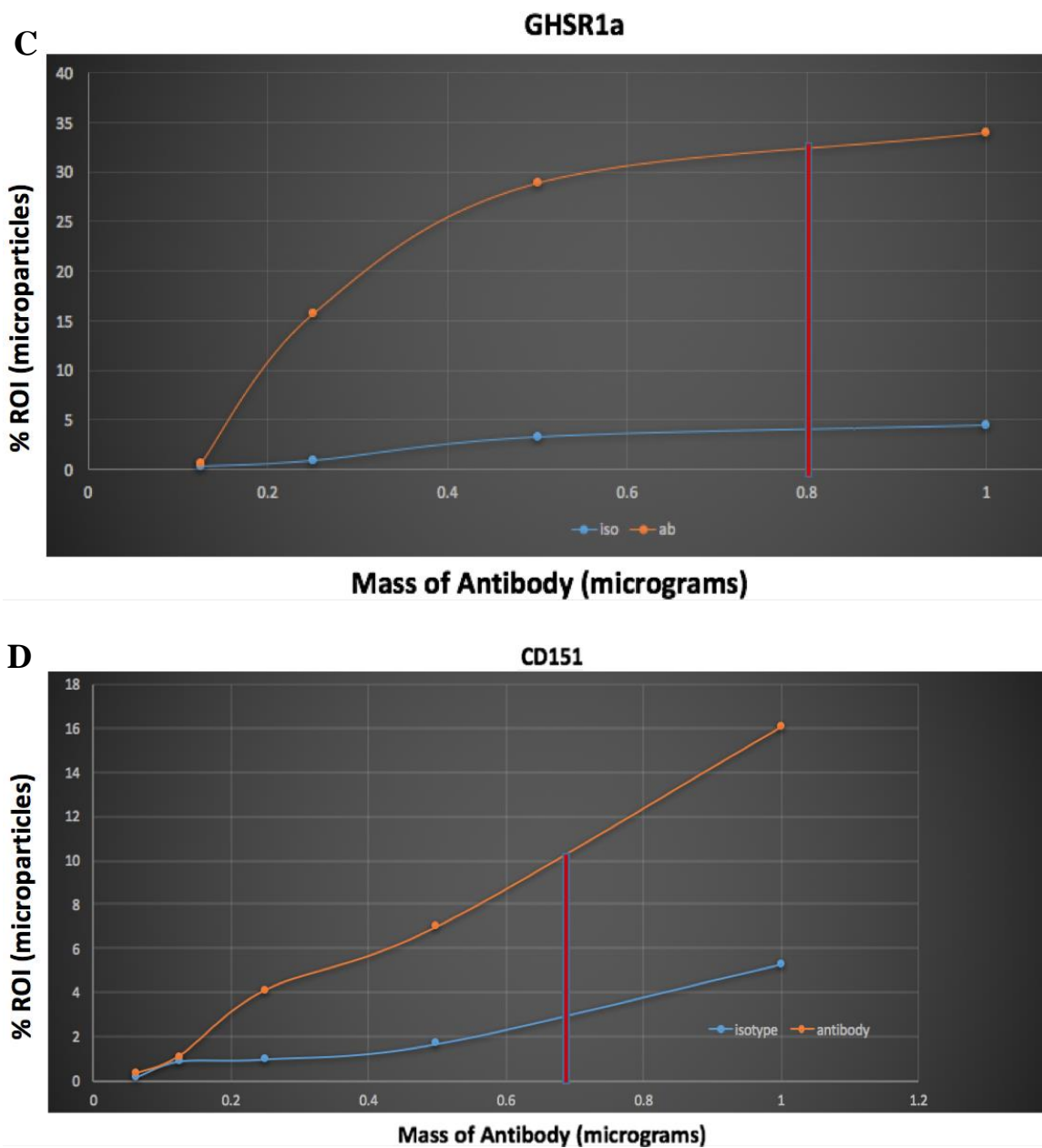
**Table 2. Clinical and pathological features of the patient cohort. Pathologic stage of six patients is unknown**

### 3.2 Optimization of Antibodies used in Detection of Prostate-derived Microparticles

Nanoscale Flow Cytometry is a rapid and sensitive technology to detect extracellular vesicles in fluids in a high-throughput manner. Optimization and standardization are required to allow a rigorous and accurate quantification of microparticles of interest. Antibody titration was performed on four metastatic prostate cancer patients for the four markers (PSMA, STEAP1, GHSR1a, CD151) in order to determine optimal concentrations. Each antibody and isotype was increased incrementally to create titration curves. An optimal mass for each antibody was defined as having a robust signal with minimal unspecific binding resulting in background noise. Detection of submicron particles in the detection limit of the flow cytometer can lead in massive coincidence (or “swarm effect”) where aggregation of small particles (<100 nm) can be counted as one true positive event resulting in count over-estimation (van der Pol et al., 2012). Caution was taken to eliminate the risk of swarm effect and avoid erroneous counts. Examples of titration curves for each antibody and respective isotype are shown in **Figures 7**.



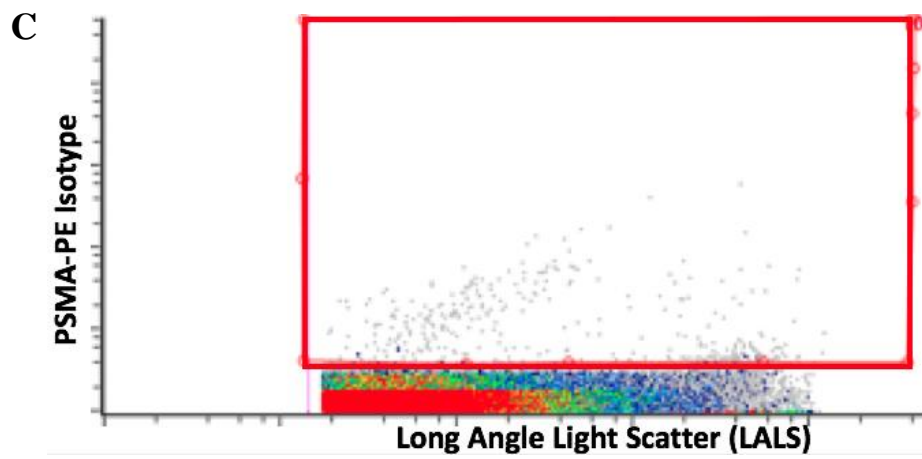
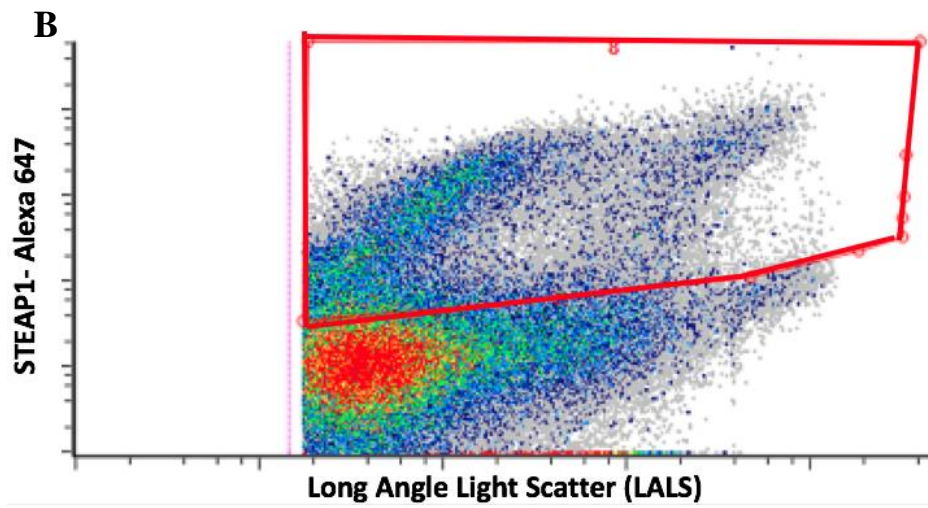
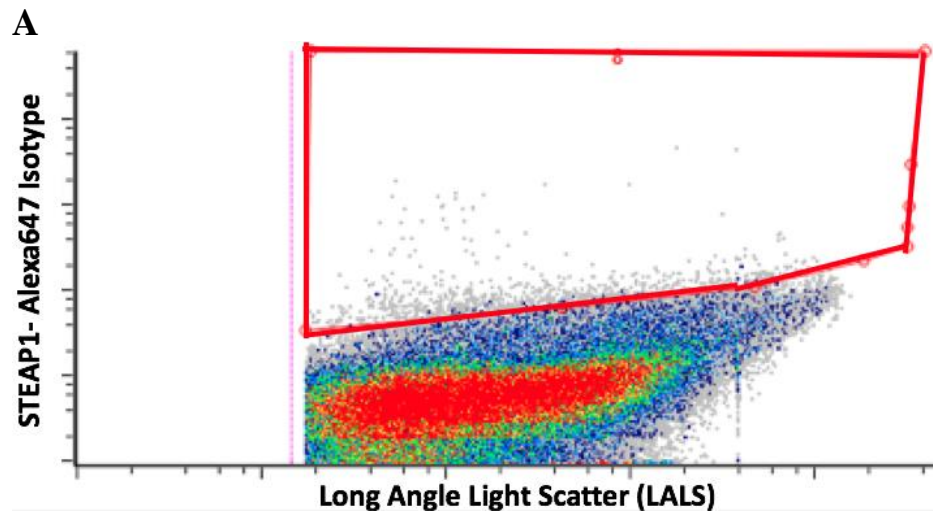


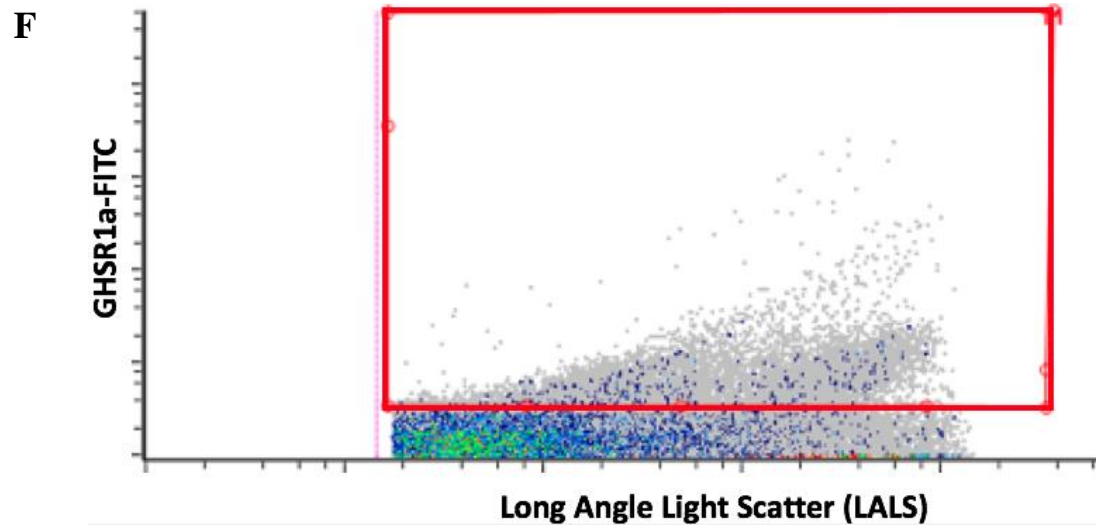
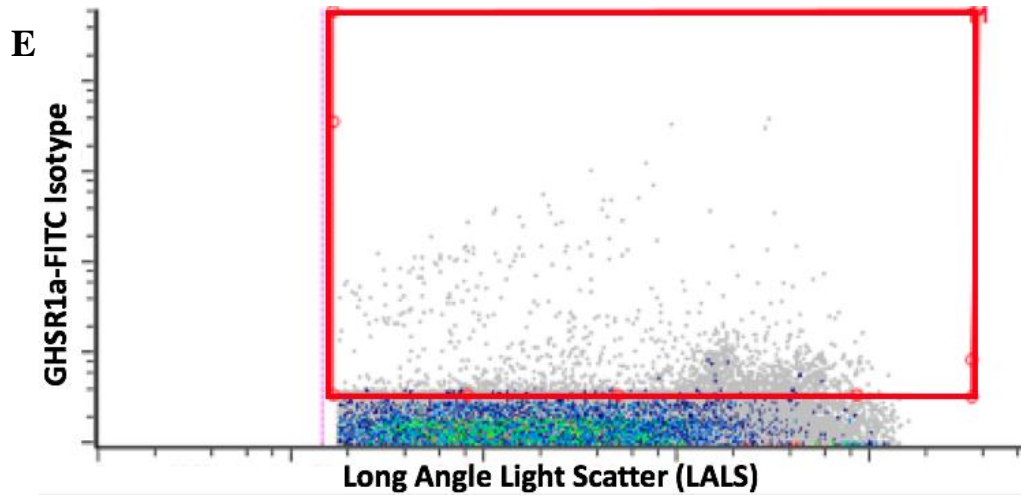
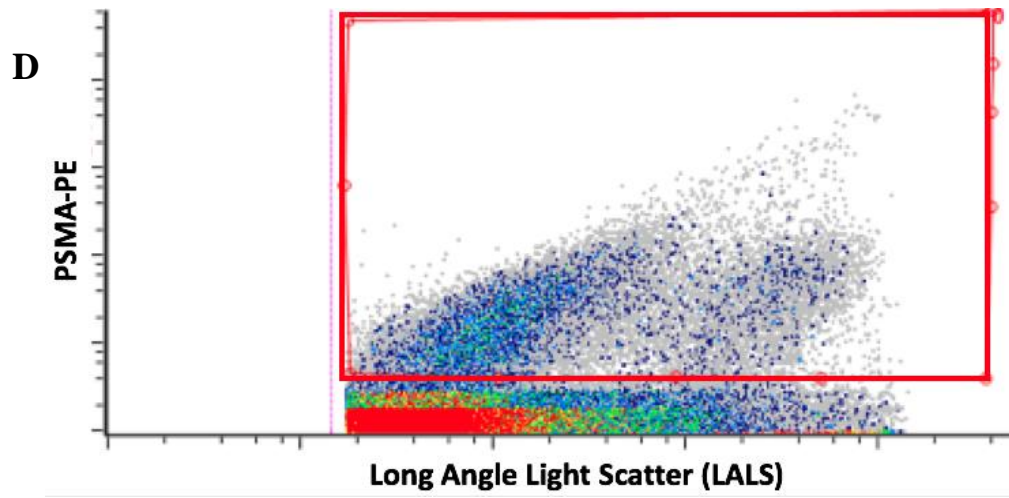


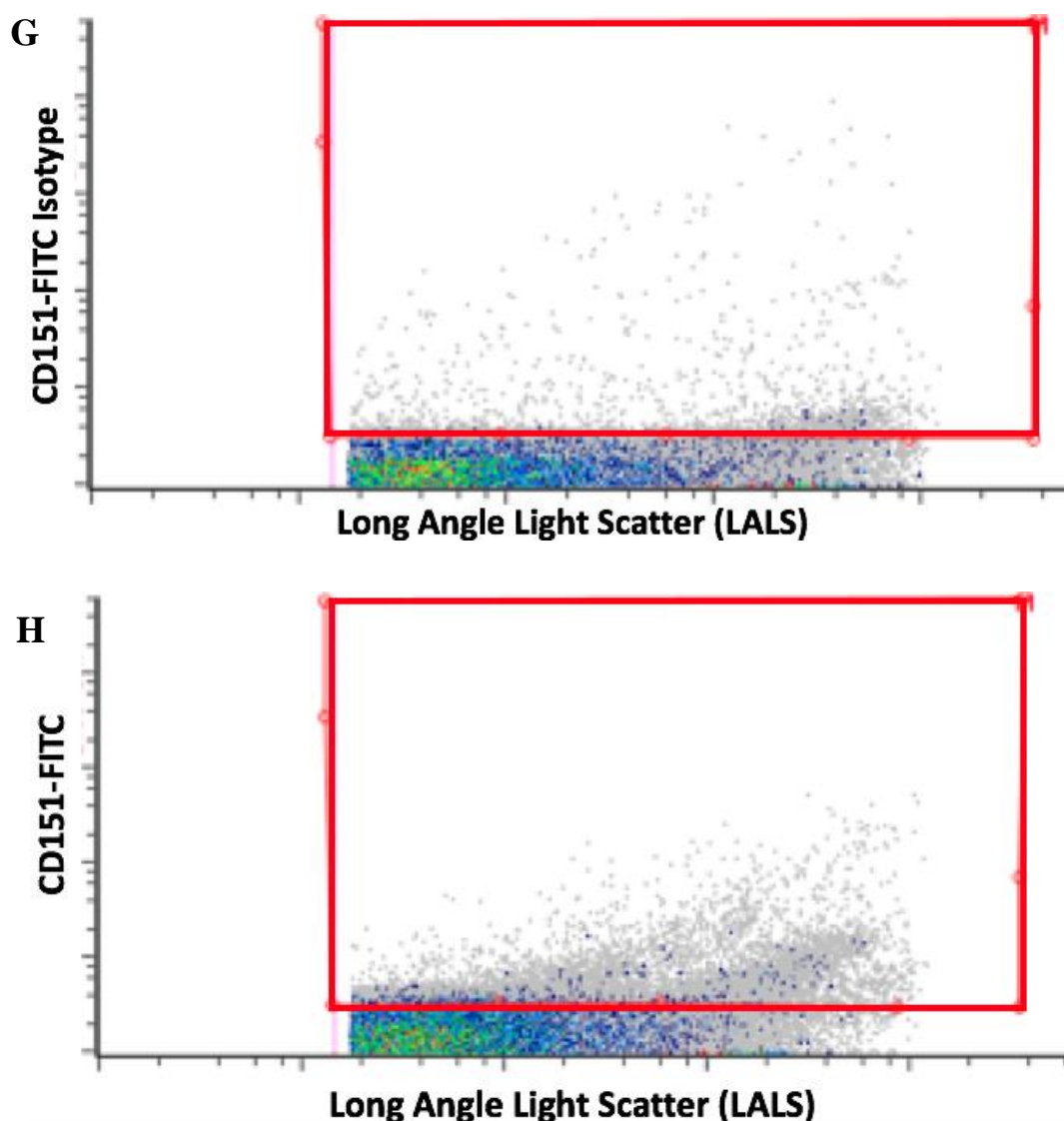
**Figure 7. Titration curve for each antibody and their respective isotype using metastatic prostate cancer patient plasma. For Prostate Specific Membrane Antigen clone 3E/7 conjugated with PE (PSMA 3E/7), 0.75  $\mu\text{g}$  was selected as optimal mass for study (A). For Six Transmembrane Antigen of Prostate-1 conjugated with Alexa Fluor 647 (STEAP1), 0.40  $\mu\text{g}$  was selected as optimal mass for study (B). For Ghrelin receptor conjugated with FITC (GHSR1a), 0.80  $\mu\text{g}$  was selected as optimal mass for study (C). For CD151 conjugated with FITC, 0.68  $\mu\text{g}$  was selected as optimal mass for study (D). X-axis indicates mass of isotype or antibody used in micrograms and y-axis indicates percentage of positive events within the region of interest (i.e. within the gate)**

### 3.3 Gating of Cytograms

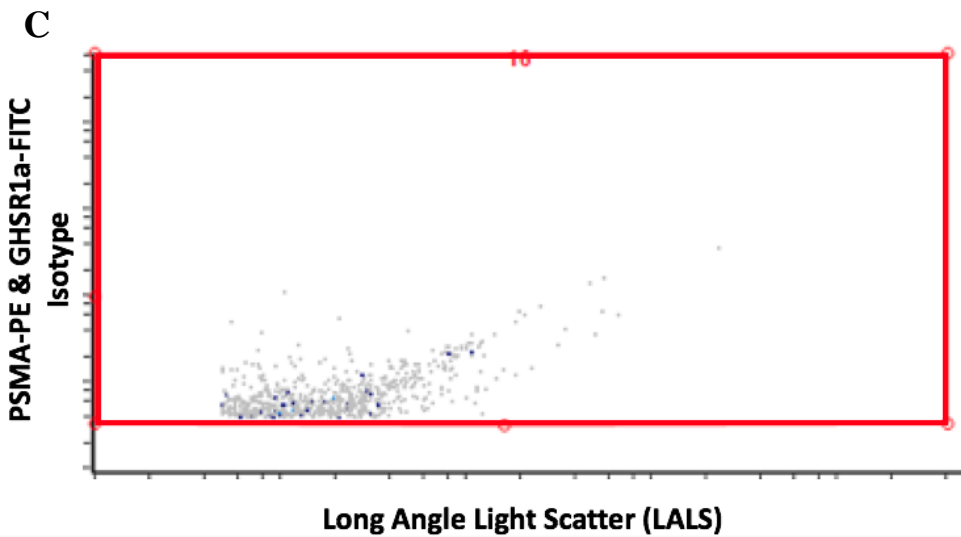
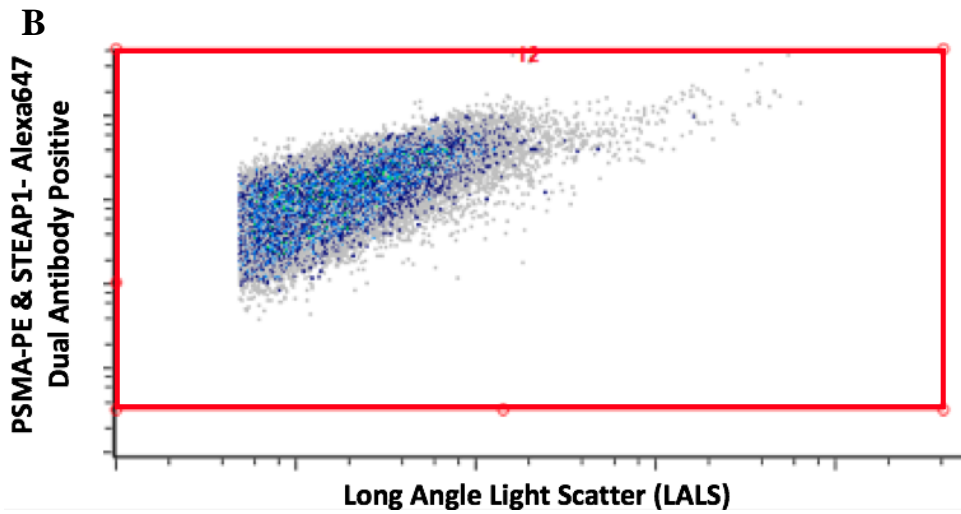
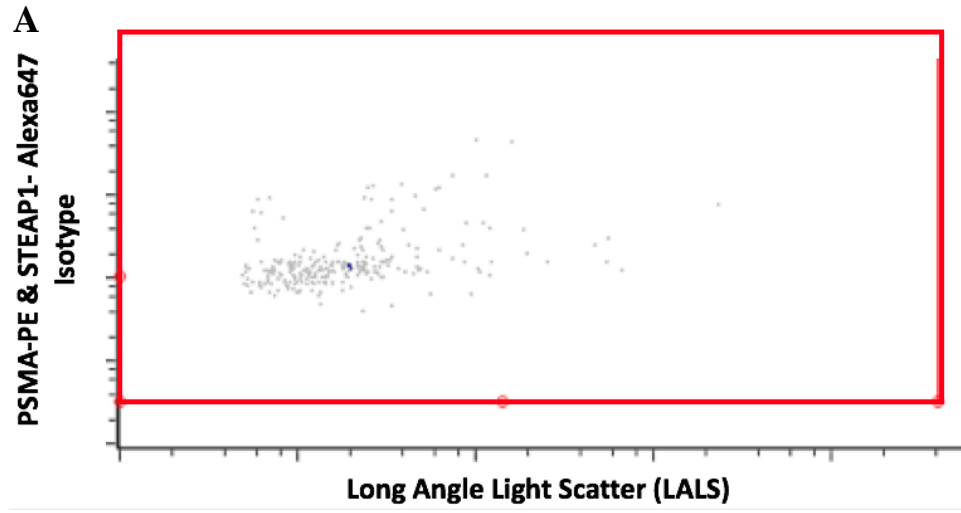
Cytograms for each single, dual and triple positive antibody combinations and isotypes are seen on **Figures 8-10**. Gates to enumerate positive events are displayed in red. The x-axis displays size using long angle light scatter (LALS) and the y-axis displays fluorescence intensity. Total events within gates are recorded as events/ $\mu$ L (not displayed).

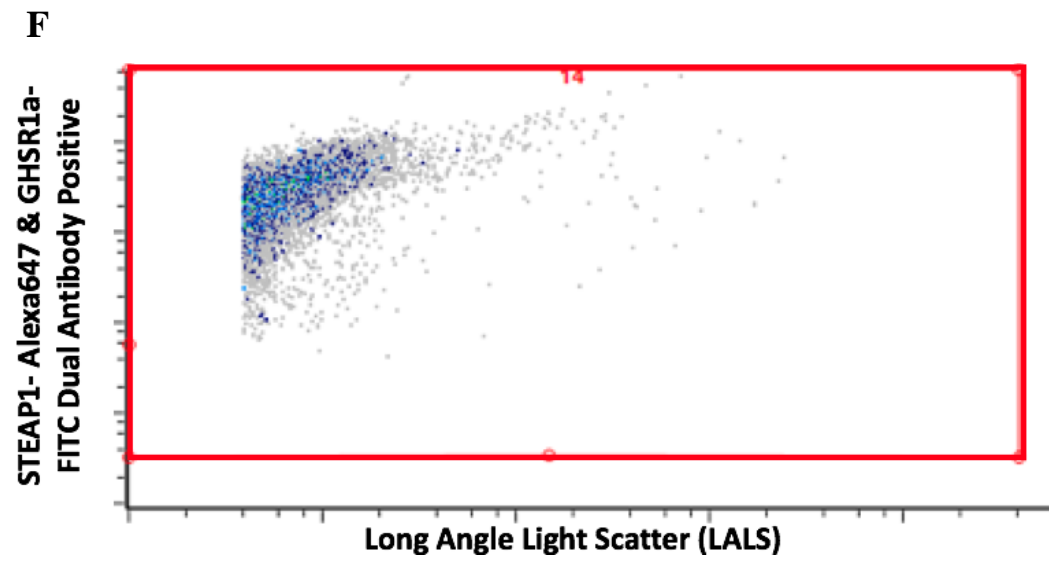
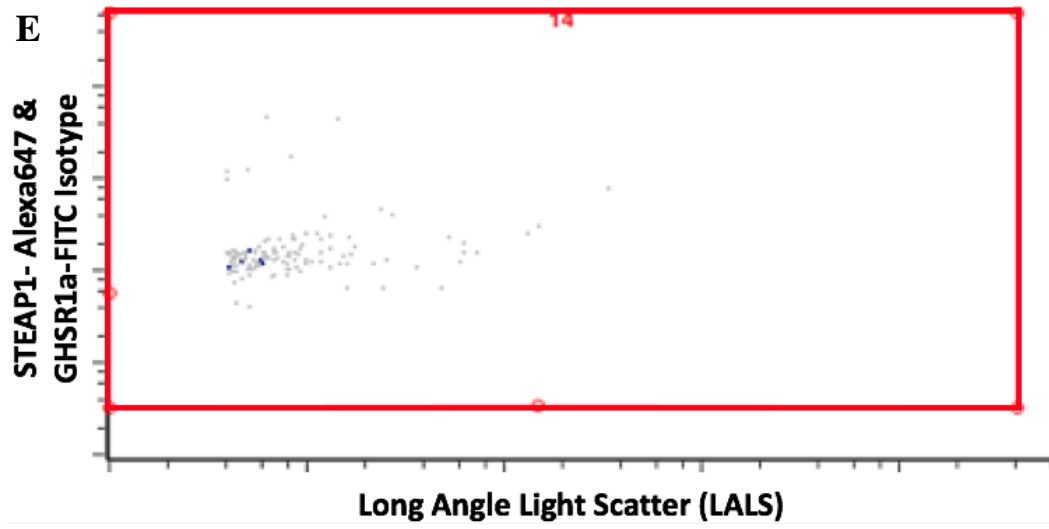
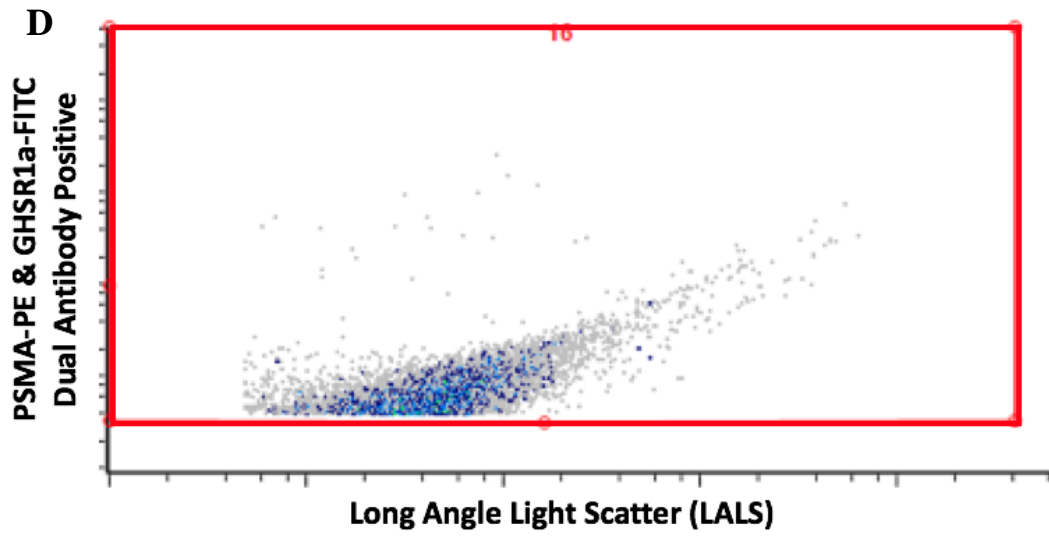


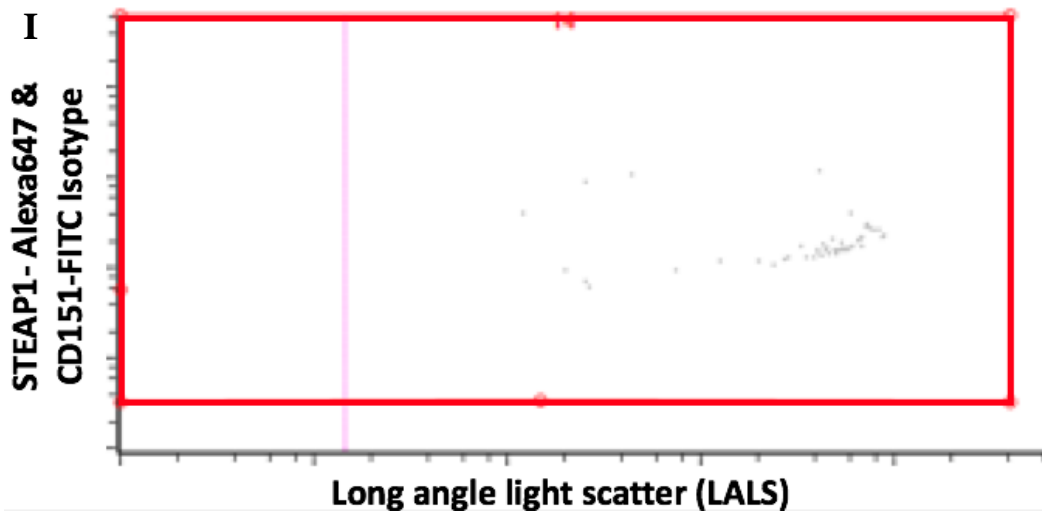
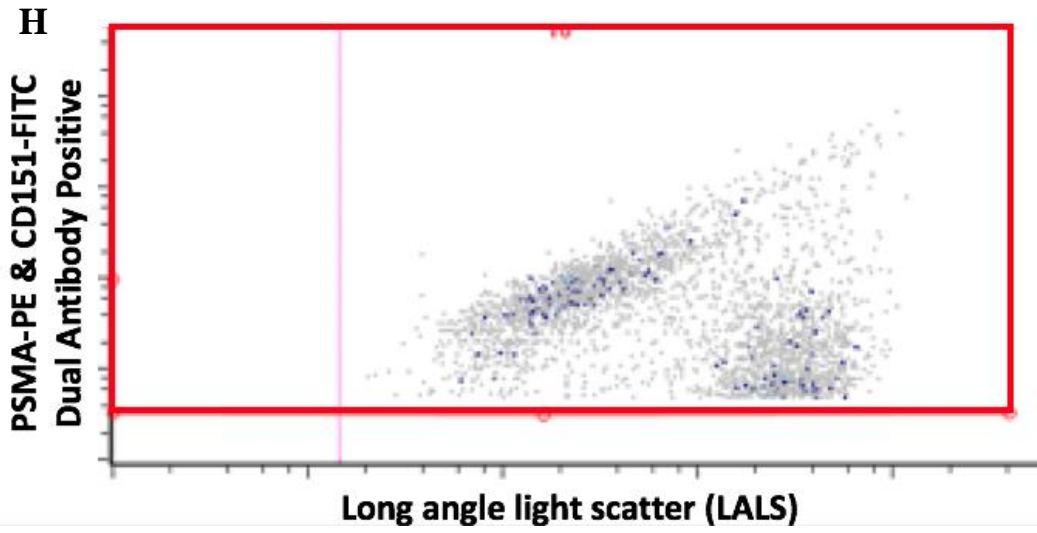
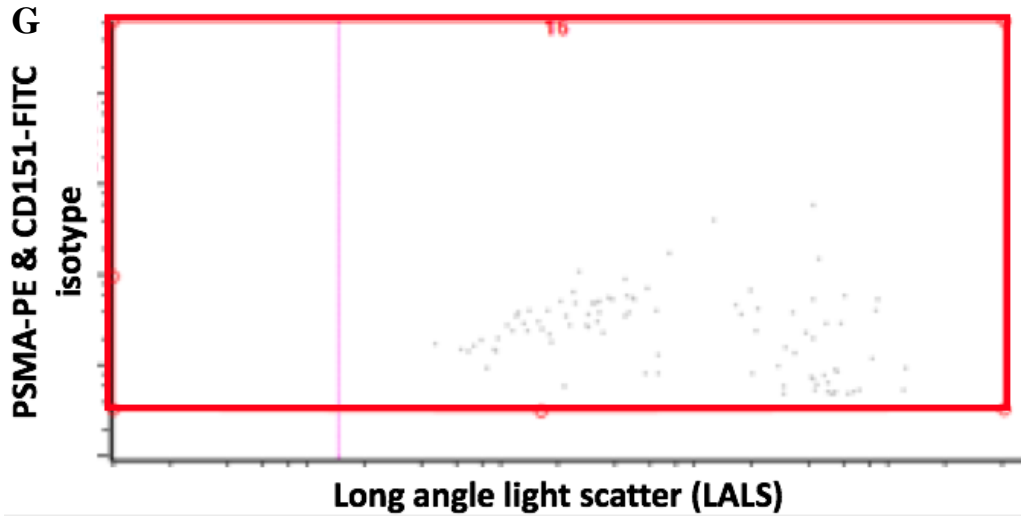




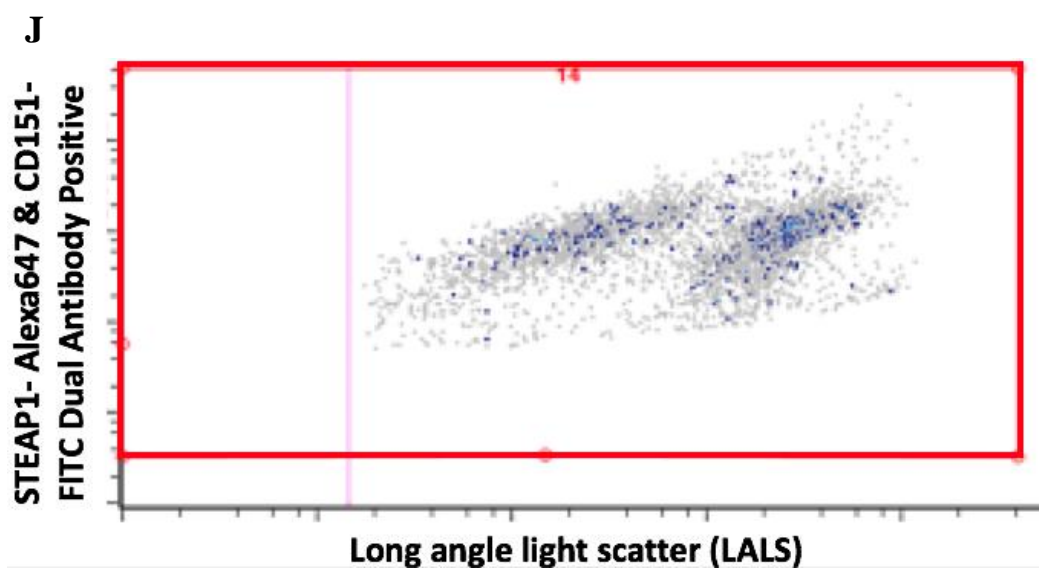
**Figure 8. Cytograms displaying single positive microparticles within their respected gates: isotype-matched controls (A) and antibodies (B) for STEAP1-Alexa647, isotype-matched controls (C) and antibodies (D) for PSMA-PE, isotype-matched controls (E) and antibodies (F) for GHSR1a-FITC, and isotype-matched controls (G) and antibodies (H) CD151-FITC. The x-axis represents sizing as long angle light scatter (LALS) and y-axis represents degree of fluorescence represented by a log scale. Each dot represents one positive event within the gate (displayed in red).**



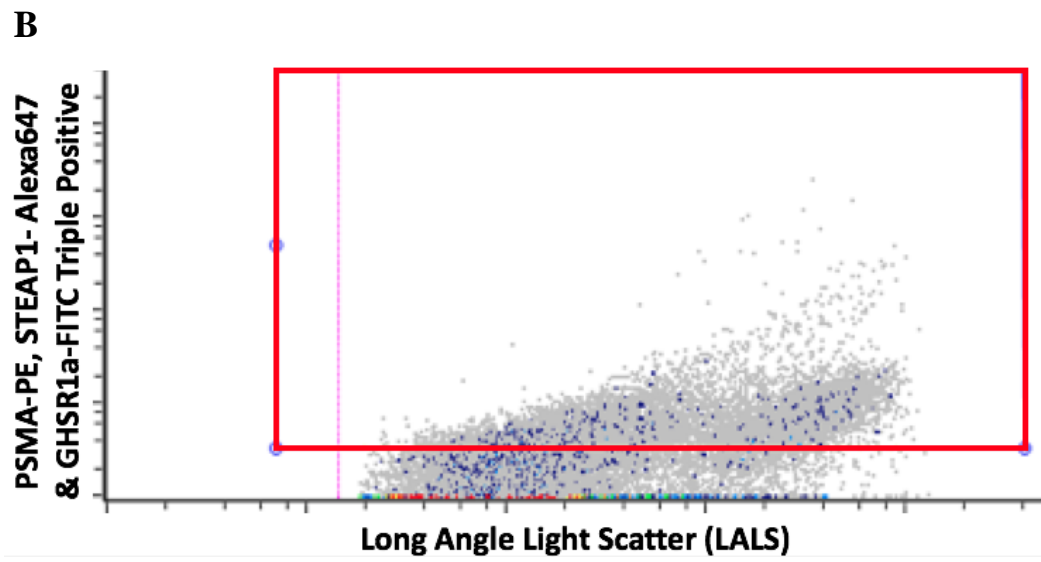
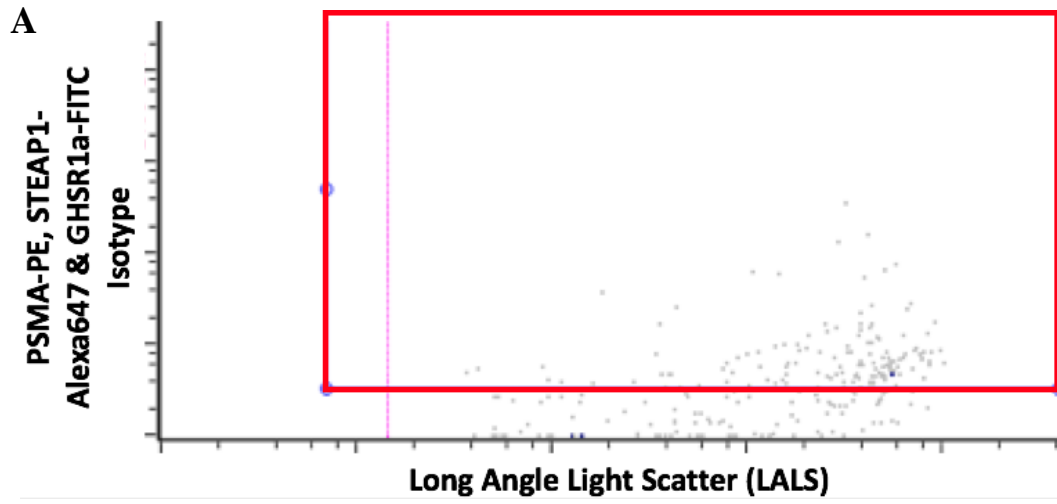








**Figure 9.** Cytograms displaying dual positive microparticles with their respected gates: isotype-matched controls (A) and antibodies (B) for PSMA-PE+STEAP1-Alexa647, isotype-matched controls (C) and antibodies (D) for PSMA-PE+GHSR1a-FITC, isotype-matched controls (E) and antibodies (F) for STEAP1-Alexa647+GHSR1a-FITC, isotype-matched controls (G) and antibodies (H) for PSMA-PE+CD151-FITC, and isotype-matched controls (I) and antibodies (J) for STEAP1-Alexa647+CD151-FITC. The x-axis represents sizing as long angle light scatter (LALS) and y-axis represents degree of fluorescence represented by a log scale. Each dot represents one positive event within the gate (displayed in red).



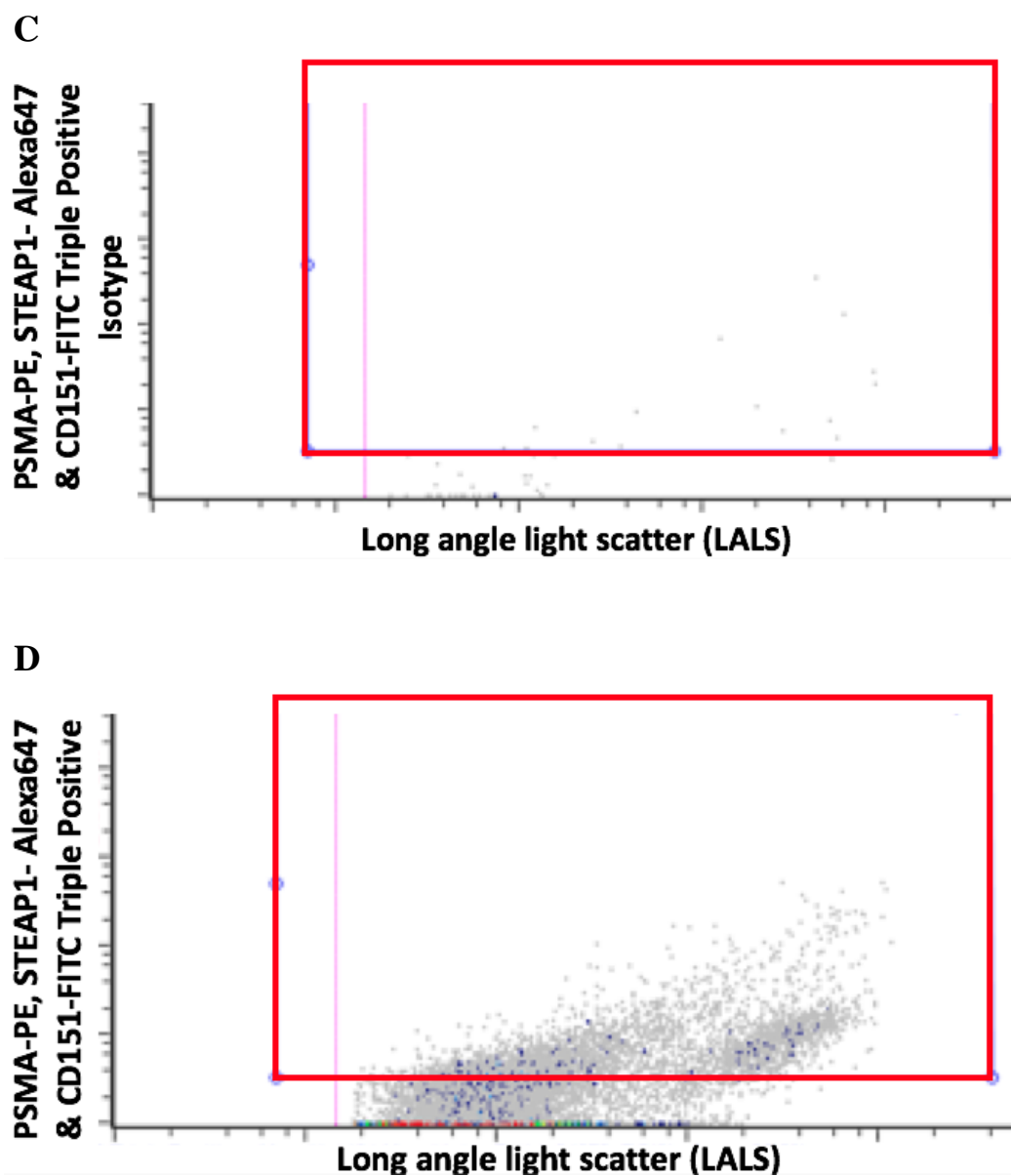


**Figure 10.** Cytograms displaying triple positive microparticles with their respected gates: isotype-matched controls (A) and antibodies (B) for PSMA-PE+STEAP1-Alexa647+GHSR1a-FITC and isotype-matched controls (C) and antibodies (D) for PSMA-PE+STEAP1-Alexa647+CD151-FITC. The x-axis represents sizing as long angle light scatter (LALS) and y-axis represents degree of fluorescence represented by a log scale. Each dot represents one positive event within the gate (displayed in red).

### 3.4 Scatterplot data

Levels of microparticles (events/ $\mu\text{L}$ ) harboring each putative biomarker (PSMA, STEAP1, GHSR1a, and CD151) were measured and analyzed (**Figure 11** and **Table 3**). PSMA expressing microparticles were detected in patient plasmas as previously described (Biggs et al., 2016). STEAP1, GHSR1a and CD151 were expressed at different levels in patient plasmas. Using one-way ANOVA with p-value of  $<0.05$  set for significance each biomarker's level of microparticles at GS6 (low-risk) were compared to GS3+4, GS4+3, and GS $\geq$ 8. Only GHSR1a showed any significant difference between GS6 and the other various Gleason scores (**Figure 11C**).

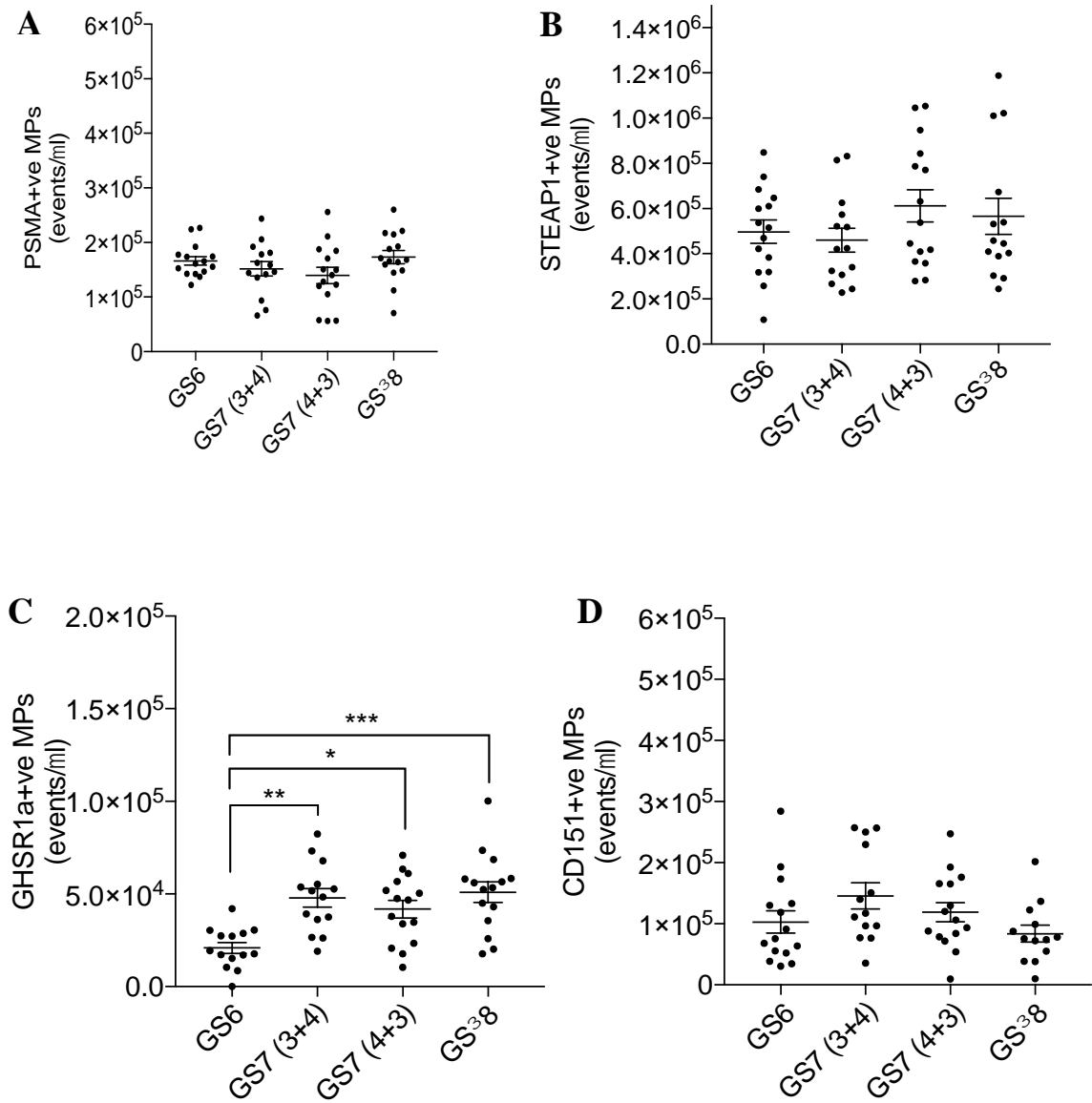
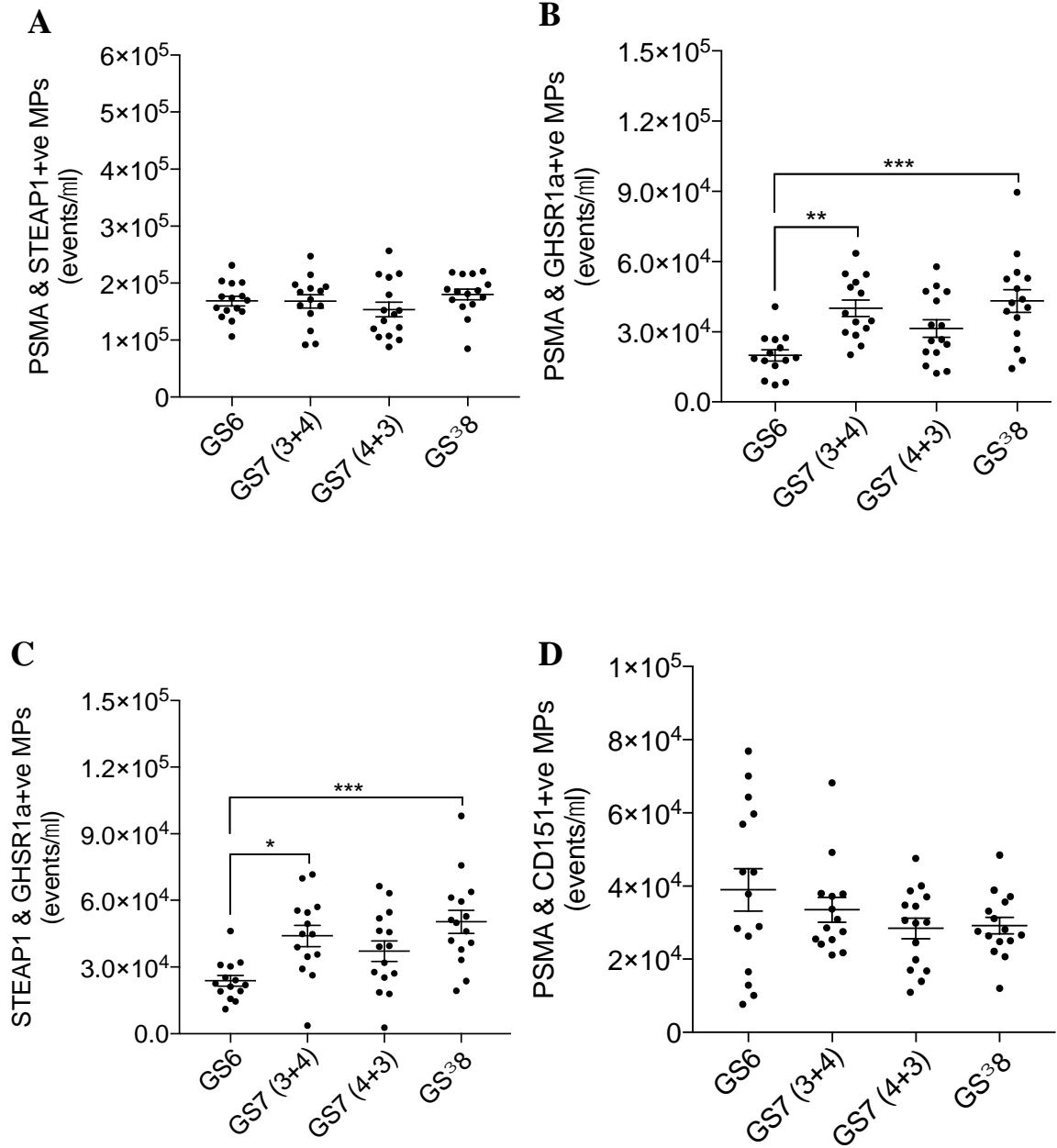


**Figure 11.** Scatterplots showing levels of PSMA (A), STEAP1 (B), GHSR1a (C), and CD151 (D) expressing MPs in patient plasmas for GS6 (n=15), GS3+4 (n=14), GS4+3 (n=15), and GS $\geq$ 8 (n=15). Bars represent the mean in events/ $\mu$ L and +/- s.e.m. (\*  $p < 0.05$ , \*\*  $p < 0.01$  in one-way ANOVA test).

<b>PSMA</b>	<b>Mean +/- s.e.m</b>	<b>Median</b>	<b>Min</b>	<b>Max</b>
<b>GS6</b>	<b>166409 +/- 7718</b>	<b>161247</b>	<b>122460</b>	<b>226557</b>
<b>GS7 (3+4)</b>	<b>151890 +/- 13173</b>	<b>152452</b>	<b>66398</b>	<b>243650</b>
<b>GS7 (4+3)</b>	<b>139878 +/- 14913</b>	<b>140430</b>	<b>56264</b>	<b>255742</b>
<b>GS<math>\geq</math>8</b>	<b>173373 +/- 11983</b>	<b>168301</b>	<b>70804</b>	<b>260445</b>
<b>STEAP1</b>	<b>Mean +/- s.e.m</b>	<b>Median</b>	<b>Min</b>	<b>Max</b>
<b>GS6</b>	<b>497378 +/- 51454</b>	<b>515925</b>	<b>108417</b>	<b>848244</b>
<b>GS7 (3+4)</b>	<b>460022 +/- 52846</b>	<b>422245</b>	<b>227612</b>	<b>832230</b>
<b>GS7 (4+3)</b>	<b>611734 +/- 71047</b>	<b>537855</b>	<b>279461</b>	<b>1053439</b>
<b>GS<math>\geq</math>8</b>	<b>565157 +/- 79882</b>	<b>451959</b>	<b>244572</b>	<b>1188707</b>
<b>GHSR1a</b>	<b>Mean +/- s.e.m</b>	<b>Median</b>	<b>Min</b>	<b>Max</b>
<b>GS6</b>	<b>20899 +/- 2918</b>	<b>18620</b>	<b>0</b>	<b>42165</b>
<b>GS7 (3+4)</b>	<b>47905 +/- 4932</b>	<b>50145</b>	<b>19092</b>	<b>82364</b>
<b>GS7 (4+3)</b>	<b>41843 +/- 4685</b>	<b>46712</b>	<b>10483</b>	<b>70918</b>
<b>GS<math>\geq</math>8</b>	<b>50984 +/- 5531</b>	<b>53412</b>	<b>17693</b>	<b>100169</b>
<b>CD151</b>	<b>Mean +/- s.e.m</b>	<b>Median</b>	<b>Min</b>	<b>Max</b>
<b>GS6</b>	<b>102972 +/- 18307</b>	<b>75838</b>	<b>30595</b>	<b>284442</b>
<b>GS7 (3+4)</b>	<b>145822 +/- 21356</b>	<b>117153</b>	<b>35604</b>	<b>257418</b>
<b>GS7 (4+3)</b>	<b>119044 +/- 15815</b>	<b>106414</b>	<b>9870</b>	<b>247495</b>
<b>GS<math>\geq</math>8</b>	<b>83971 +/- 13654</b>	<b>75915</b>	<b>10320</b>	<b>201604</b>

**Table 3. Distribution of the positive microparticles for each individual biomarker displayed as events/ $\mu$ L. GS6 (n=15), GS3+4 (n=14), GS4+3 (n=15), and GS $\geq$ 8 (n=15).**

In order to identify the presence of candidate biomarkers GHSR1a and CD151 in prostate-derived microparticles, levels of dual positive with both prostate-specific markers were measured (PSMA+STEAP1, PSMA+GHSR1a, STEAP1+GHSR1a, PSMA+CD151, and STEAP1+CD151) (**Figure 12** and **Table 4**). Dual positive microparticles at GS6 were compared to GS 3+4, GS4+3, and GS $\geq$ 8. PSMA+STEAP1 co-expressing MPs had a slight increase in MP levels in GS $\geq$ 8 when compared to GS6. However, there was no significant difference between patients expressing PSMA+STEAP1 co-expressing MPs amongst the various Gleason scores (**Figure 12A**). Interestingly, patients expressing PSMA+GHSR1a co-expressing MPs showed a significant higher mean of microparticles in GS 3+4 and GS $\geq$ 8 from GS6. GS4+3 microparticles were higher than GS6, however, this was not statistically significant (**Figure 12B**). Patients expressing STEAP1+GHSR1a co-expressing MPs showed a significantly higher mean of microparticles in GS3+4 and GS $\geq$ 8 from GS6. GS4+3 microparticles were higher, however, this was not statistically significant (**Figure 12C**). There was no statistically significant difference between PSMA+CD151 co-expressing MPs among the various GS (**Figure 12D**). Patients expressing STEAP1+CD151 co-expressing MPs showed an unexpected finding of lower level of microparticles as GS progressed. The lower mean of microparticles in GS3+4, GS4+3, and GS $\geq$ 8 were all significant to the elevated mean of microparticles within GS6 (**Figure 12E**).





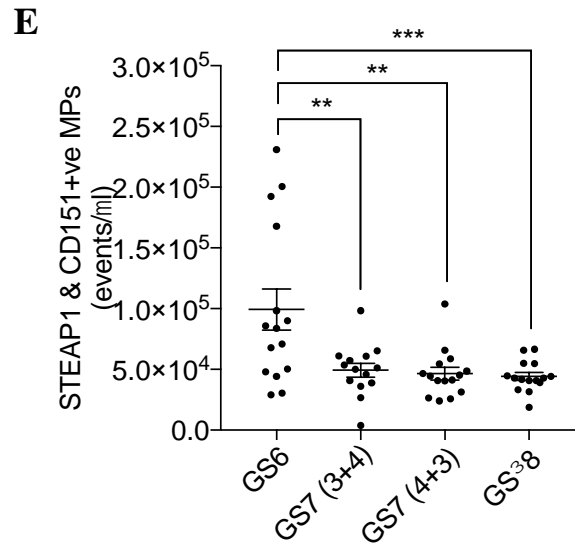


**Figure 12.** Scatterplots showing levels of PSMA+STEAP1 (A), PSMA+GHSR1a (B), STEAP1+GHSR1a (C), PSMA+CD151 (D), STEAP1+CD151 (E) co-expressing microparticles (MP) in patient plasmas for GS6 (n=15), GS3+4 (n=14), GS4+3 (n=15), and GS $\geq$ 8 (n=15). Bars represent the mean in events/ $\mu$ L and +/- s.e.m. (\* p < 0.05, \*\* p < 0.01, \*\*\* p < 0.001 in one-way ANOVA test).

<b>PSMA+STEAP1</b>	<b>Mean +/- s.e.m</b>	<b>Median</b>	<b>Min</b>	<b>Max</b>
<b>GS6</b>	168554 +/- 8212	169528	106420	231168
<b>GS7 (3+4)</b>	168067 +/- 11893	177589	91597	247058
<b>GS7 (4+3)</b>	153758 +/- 13201	145032	88309	256855
<b>GS<math>\geq</math>8</b>	180062 +/- 9287	184964	84786	220805
<b>PSMA+GHSR1a</b>	<b>Mean +/- s.e.m</b>	<b>Median</b>	<b>Min</b>	<b>Max</b>
<b>GS6</b>	19959 +/- 2393	18714	7335	40830
<b>GS7 (3+4)</b>	40047 +/- 3521	36332	20134	63502
<b>GS7 (4+3)</b>	31446 +/- 3733	26704	12367	57787
<b>GS<math>\geq</math>8</b>	43199 +/- 4921	42406	14282	89511
<b>STEAP1+GHSR1a</b>	<b>Mean +/- s.e.m</b>	<b>Median</b>	<b>Min</b>	<b>Max</b>
<b>GS6</b>	23864 +/- 2385	22260	11061	46217
<b>GS7 (3+4)</b>	44030 +/- 4816	44836	3717	71743
<b>GS7 (4+3)</b>	37223 +/- 4626	39127	2703	66482
<b>GS<math>\geq</math>8</b>	50387 +/- 5170	49994	19287	98037

<b>PSMA+ CD151</b>	<b>Mean +/- s.e.m</b>	<b>Median</b>	<b>Min</b>	<b>Max</b>
<b>GS6</b>	38944 +/- 5858	37765	7745	76897
<b>GS7 (3+4)</b>	33504 +/- 3380	29737	21094	68234
<b>GS7 (4+3)</b>	28432 +/- 2786	30129	10973	47519
<b>GS<math>\geq</math>8</b>	29199 +/- 2246	27640	12015	48452
<b>STEAP1+ CD151</b>	<b>Mean +/- s.e.m</b>	<b>Median</b>	<b>Min</b>	<b>Max</b>
<b>GS6</b>	99398 +/- 17030	83901	29008	230936
<b>GS7 (3+4)</b>	49321 +/- 5725	50789	3833	98341
<b>GS7 (4+3)</b>	46621 +/- 5143	44668	24147	10374
<b>GS<math>\geq</math>8</b>	44294 +/- 3217	42883	18923	66687

**Table 4. Distribution of microparticles that are dual positive displayed in events/ $\mu$ L. GS6 (n=15), GS3+4 (n=14), GS4+3 (n=15), and GS $\geq$ 8 (n=15).**

Finally, the number of triple-expressing microparticles (PSMA+STEAP1+GHSR1a and PSMA+STEAP1+CD151) were measured (**Figure 13** and **Table 5**). Triple-expressing microparticles at GS6 were compared to GS3+4, GS4+3, and GS $\geq$ 8. Patients expressing PSMA+STEAP1+GHSR1a triple-expressing MPs had higher levels of MP for GS3+4, GS4+3, and GS $\geq$ 8 when compared to GS6. Only GS3+4 and GS $\geq$ 8 had higher levels that were statistically significant (**Figure 13A**). Patients who expressed PSMA+STEAP1+CD151 triple-expressing MPs had a statistically significant drop in the number of MPs when comparing GS3+4, GS4+3, and GS $\geq$ 8 to GS6 (**Figure 13B**).

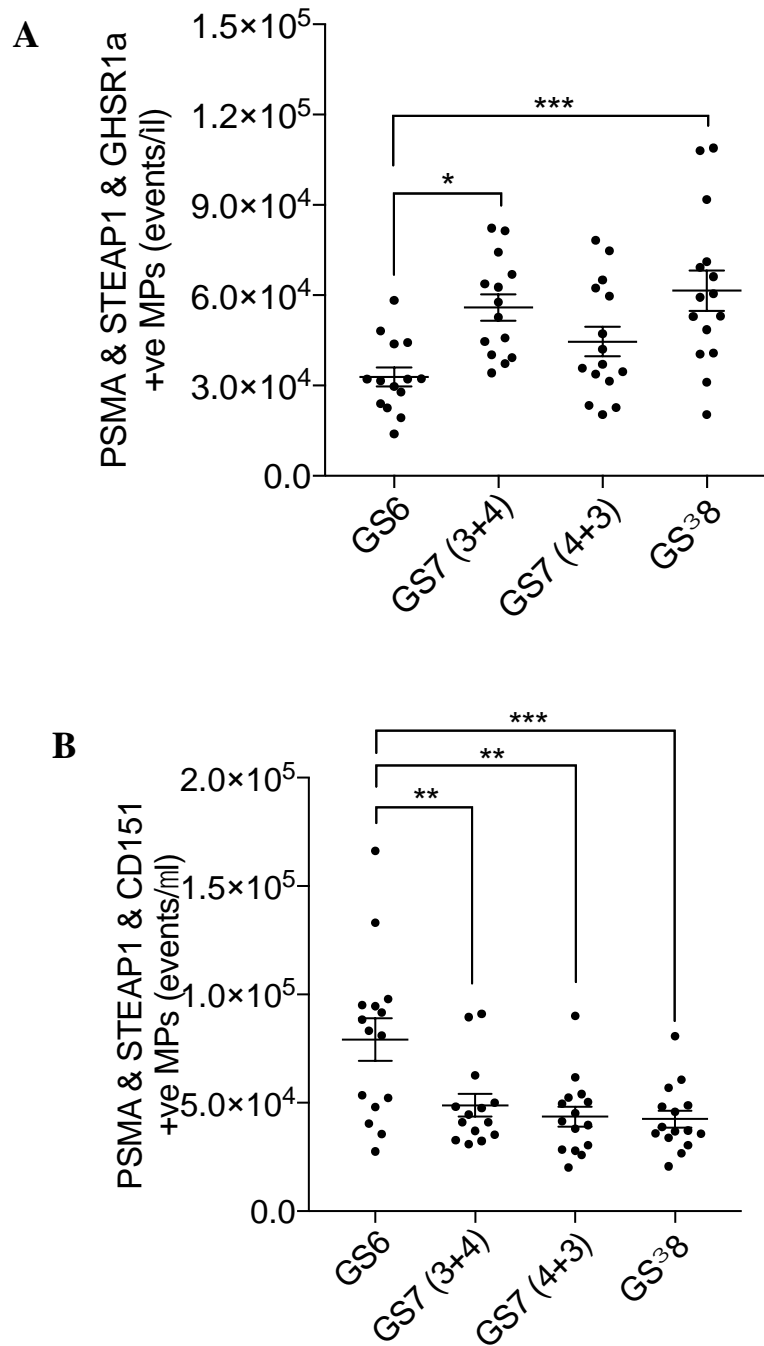


**Figure 13. Scatterplots showing levels of PSMA+STEAP1+GHSR1a (A) and PSMA+STEAP1+CD151 (B) triple-expressing MP in patient plasmas for GS6 (n=15), GS 3+4 (n=14), GS4+3 (n=15), and GS $\geq$ 8 (n=15). Bars represent the mean in events/ $\mu$ L and +/- s.e.m. (\* p < 0.05, \*\* p < 0.01, \*\*\* p < 0.001 in one-way ANOVA test).**

PSMA+ STEAP1+GHSR1a	Mean +/- s.e.m	Median	Min	Max
<b>GS6</b>	32861 +/- 3223	31851	13966	58254
<b>GS7 (3+4)</b>	55973 +/- 4384	55223	34249	82315
<b>GS7 (4+3)</b>	44583 +/- 4918	37005	20282	78374
<b>GS<math>\geq</math>8</b>	61515 +/- 6662	59346	20360	108954
PSMA+ STEAP1+ CD151	Mean +/- s.e.m	Median	Min	Max
<b>GS6</b>	79248 +/- 9763	83256	27510	166244
<b>GS7 (3+4)</b>	48890 +/- 5213	42833	30973	91001
<b>GS7 (4+3)</b>	43705 +/- 4539	41516	20232	90079
<b>GS<math>\geq</math>8</b>	42531 +/- 3899	37239	20685	80787

**Table 5. Distribution of microparticles that are triple positive displayed in events/ $\mu$ L. GS6 (n=15), GS3+4 (n=14), GS4+3 (n=15), and GS $\geq$ 8 (n=15).**

### 3.5 Assessment of Performance Characteristics

To assess the performance characteristics of each parameter, receiver operating curve (ROC) was used to calculate the area under the curve (AUC). The closer the AUC is to the value of one, the stronger the biomarker performs to distinguish between true positives from false positives. Cut-off values for each biomarker test were chosen to maximize specificity meaning avoid the detection of false positives. Combinations of parameters (dual positive and triple positive MPs) were assessed comparing GS6 to GS3+4, GS4+3, and  $GS \geq 8$ . **Figure 14-16** displays all ROC curves for the various comparisons.

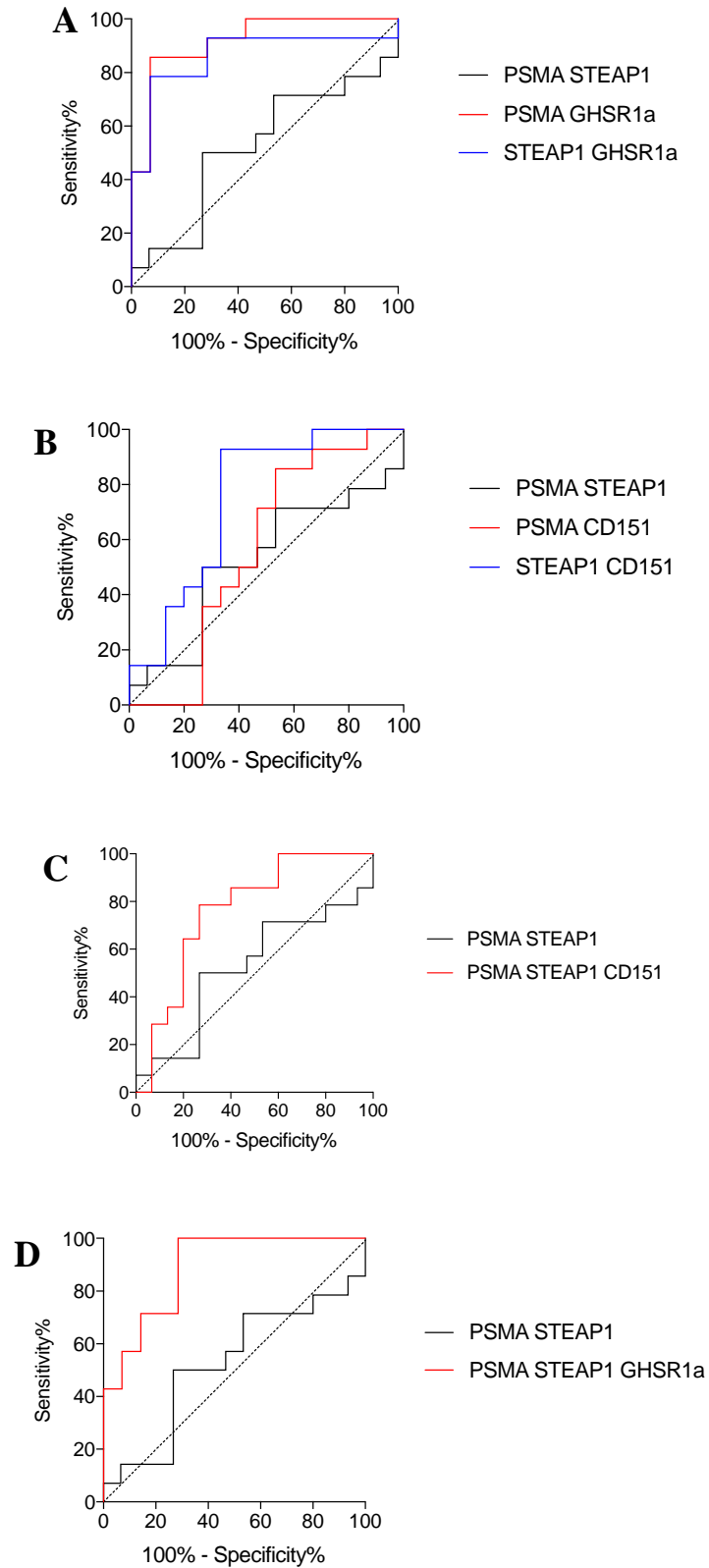


**Figure 14. ROC curves comparing GS6 to GS3+4 for various combinations of microparticles.**



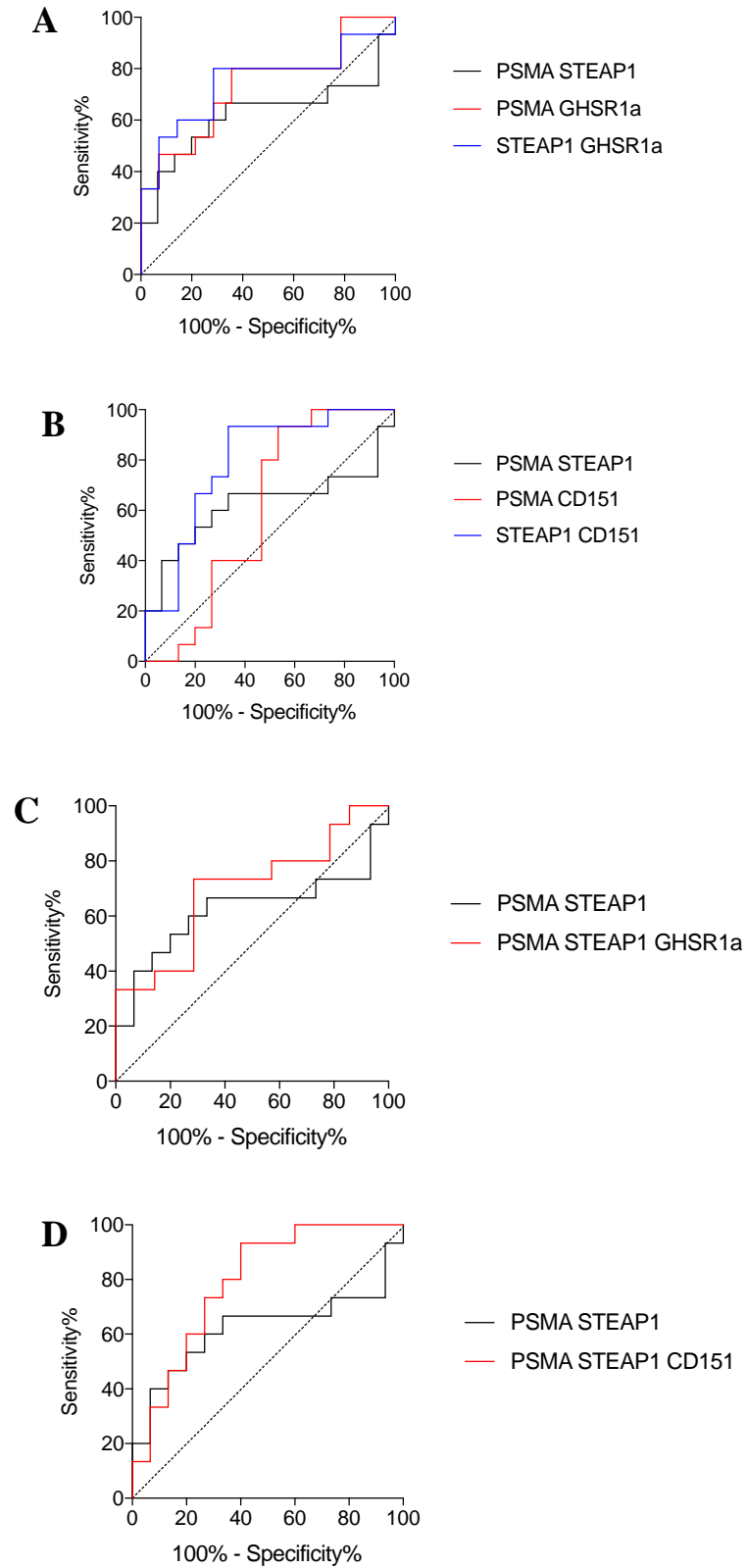


**Figure 15. ROC curves comparing GS6 to GS4+3 for various combinations of microparticles.**

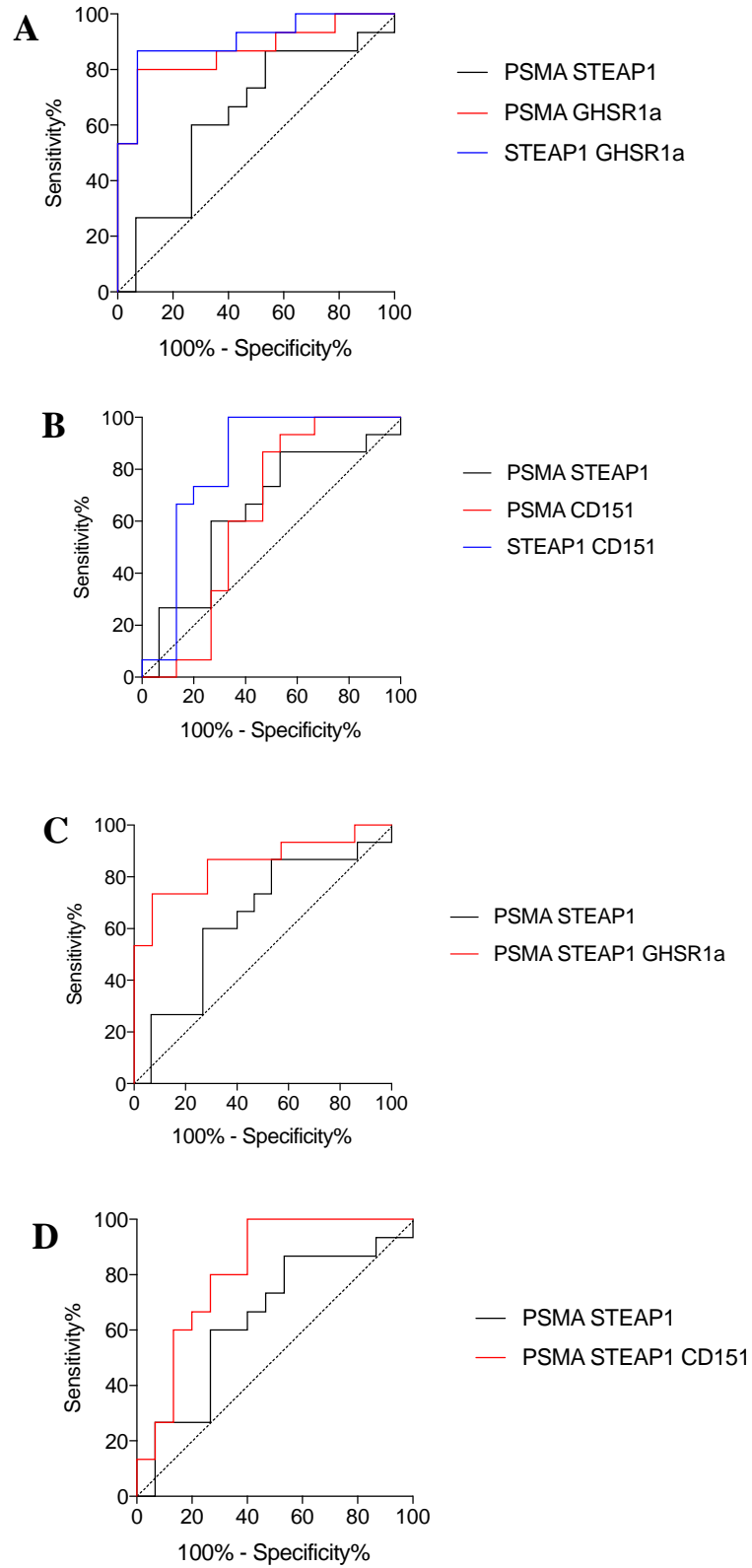


**Figure 16. ROC curve comparing GS6 to GS $\geq$ 8 for various combinations of microparticles.**

When comparing GS6 to GS3+4, PSMA+GHSR1a co-expressing MPs performed the best with an AUC 0.92. A cut-off of a level of 28002 events/ $\mu$ L provided a sensitivity and specificity of 85.71% and 92.86%, respectively. The best triple positive combination test for distinguishing GS6 from GS3+4 was PSMA+STEAP1+GHSR1a triple-expressing MPs with an AUC of 0.89. A cut-off value of 50435 events/ $\mu$ L provided a sensitivity and specificity of 57.14% and 92.86%. **Table 6** displays AUC for all biomarkers assess GS6 from GS3+4.

When comparing GS6 to GS4+3, STEAP1+CD151 co-expressing MPs and PSMA+STEAP1+CD151 triple-expressing MPs performed similar with an AUC of 0.79. A cut-off of 49418 events/ $\mu$ L provided STEAP1+CD151 co-expressing MPs a sensitivity and specificity of 73.33% and 73.33%, respectively. A cut-off of 46653 events/ $\mu$ L provided PSMA+STEAP1+CD151 triple-expressing MPs a sensitivity and specificity of 60% and 80%, respectively. **Table 7** displays AUC for all biomarkers assess GS6 from GS4+3.

When comparing GS6 to GS $\geq$ 8, STEAP1+GHSR1a co-expressing MPs performed the best with AUC 0.90. A cut-off of 32621 events/ $\mu$ L provided a sensitivity and specificity of 86.67% and 92.86%. The best performing triple positive biomarker was PSMA+STEAP1+GHSR1a triple-expressing MPs with an AUC of 0.85. A cut-off of 48364 events/ $\mu$ L provided a sensitivity and specificity of 73.33% and 92.86%. **Table 8** displays AUC for all biomarkers assess GS6 from GS $\geq$ 8.

	Parameter	AUC <sub>95%</sub> [-0.1, 0.1]	p-value	Cut-off (evts/ $\mu$ l)	Sensitivity%	95% CI	Specificity%	95% CI
GS6 vs GS7 (3+4)	PSMA <sup>+</sup> STEAP1	0.52 <sub>95%</sub> [-0.11, 0.11]	0.83	>180607	50	23.04-76.96	73.33	44.9-92.21
	PSMA <sup>+</sup> GHSR1a	0.92 <sub>95%</sub> [-0.05, 0.05]	0.002	>28002	85.71	57.19-98.22	92.86	66.13-99.82
	PSMA <sup>+</sup> CD151	0.57 <sub>95%</sub> [-0.11, 0.11]	0.54	<25910	35.71	12.76-64.86	73.33	44.9-92.21
	STEAP1 <sup>+</sup> GHSR1a	0.86 <sub>95%</sub> [-0.08, 0.08]	0.001	>33342	78.57	49.2-95.34	92.86	66.13-99.82
	STEAP1 <sup>+</sup> CD151	0.75 <sub>95%</sub> [-0.10, 0.10]	0.02	<50213	50	23.04-76.96	73.33	44.9-92.21
	PSMA <sup>+</sup> STEAP1 <sup>+</sup> GHSR1a	0.89 <sub>95%</sub> [-0.06, 0.06]	0.0005	>50435	57.14	28.86-82.34	92.86	66.13-99.82
	PSMA <sup>+</sup> STEAP1 <sup>+</sup> CD151	0.76 <sub>95%</sub> [-0.09, 0.09]	0.02	<47802	64.29	35.14-87.24	80	51.91-95.67

**Table 6. AUC results for the all combinations of microparticles comparing GS6 to GS3+4.**

	Parameter	AUC <sub>95%</sub> [-0.1, 0.1]	p-value	Cut-off (evts/ $\mu$ l)	Sensitivity%	95% CI	Specificity%	95% CI
GS6 vs GS7 (4+3)	PSMA <sup>+</sup> STEAP1	0.62 <sub>95%</sub> [-0.11, 0.11]	0.25	<147584	53.33	26.59-78.73	80	51.91-95.67
	PSMA <sup>+</sup> GHSR1a	0.73 <sub>95%</sub> [-0.09, 0.09]	0.03	>26666	53.33	26.59-78.73	78.57	49.2-95.34
	PSMA <sup>+</sup> CD151	0.60 <sub>95%</sub> [-0.11, 0.11]	0.33	<25404	40	16.34-67.71	73.33	44.9-92.21
	STEAP1 <sup>+</sup> GHSR1a	0.75 <sub>95%</sub> [-0.10, 0.10]	0.02	>35575	53.33	26.59-78.73	92.86	66.13-99.82
	STEAP1 <sup>+</sup> CD151	0.79 <sub>95%</sub> [-0.09, 0.09]	0.007	<19418	73.33	44.9-92.21	73.33	44.9-92.21
	PSMA <sup>+</sup> STEAP1 <sup>+</sup> GHSR1a	0.69 <sub>95%</sub> [-0.10, 0.10]	0.07	>53196	33.33	11.82-61.62	92.86	66.13-99.82
	PSMA <sup>+</sup> STEAP1 <sup>+</sup> CD151	0.79 <sub>95%</sub> [-0.08, 0.08]	0.07	<16653	60	32.29-83.66	80	51.91-95.67

**Table 7. AUC results for the all combinations of microparticles comparing GS6 to GS4+3.**

	Parameter	AUC <sub>95%</sub> [-0.1, 0.1]	p-value	Cut-off (evts/ $\mu$ l)	Sensitivity%	95% CI	Specificity%	95% CI
GS6 vs GS $\geq$ 8	PSMA <sup>+</sup> STEAP1	0.64 <sub>95%</sub> [-0.10, 0.10]	0.19	>179189	60	32.29-83.66	73.33	44.9-92.21
	PSMA <sup>+</sup> GHSR1a	0.87 <sub>95%</sub> [-0.07, 0.07]	0.0008	>28331	80	51.91-95.67	92.86	66.13-99.82
	PSMA <sup>+</sup> CD151	0.63 <sub>95%</sub> [-0.11, 0.11]	0.24	<25675	33.33	11.82-61.62	73.33	44.9-92.21
	STEAP1 <sup>+</sup> GHSR1a	0.90 <sub>95%</sub> [-0.06, 0.06]	0.0002	>32621	86.67	59.54-8.34	92.86	66.13-99.82
	STEAP1 <sup>+</sup> CD151	0.82 <sub>95%</sub> [-0.09, 0.09]	0.003	<14379	66.67	38.38-88.18	86.67	59.54-98.34
	PSMA <sup>+</sup> STEAP1 <sup>+</sup> GHSR1a	0.85 <sub>95%</sub> [-0.07, 0.07]	0.001	>18364	73.33	44.9-92.21	92.86	66.13-99.82
	PSMA <sup>+</sup> STEAP1 <sup>+</sup> CD151	0.82 <sub>95%</sub> [-0.08, 0.08]	0.003	<16967	66.67	38.38-88.18	80	51.91-95.67

**Table 8. AUC results for the all combinations of microparticles comparing GS6 to GS $\geq$ 8.**

## Chapter 4

### 4 Discussion

#### 4.1 General Discussion

Prostate cancer remains the most commonly diagnosed cancer in Canadian men and a world leader in cancer related deaths (Canadian Cancer Society, 2017; Globocan, 2012). Introduction of PSA in the 1980s (Rao et al., 2008) has revolutionized the screening of prostate cancer as it has reduced the number of men presenting with advanced disease (Howlader et al., 2017, Newcomer et al., 1997). However, widespread use of PSA screening and the long natural history of prostate cancer has led to a stage migration of clinically localized disease (T1c) (O'Donnell et al., 2008). With the ubiquitous use of PSA and ease of obtaining a prostate biopsy, we risk exposing patients to over-diagnosis and overtreatment. The ERSPC trial and the PLCO trial challenged the use of PSA as a screening tool for prostate cancer (de Koning et al., 2002; Auvinen et al., 1996). Based primarily on these studies, the U.S. Preventative Task Force and Canadian Preventive Task Force recommended against the use of PSA screening in men of all ages (U.S. Task Force, 2012; Canadian Task Force, 2014). PSA lacks sensitivity and specificity in cancer detection and thus it is not a robust cancer biomarker.

Men with elevated PSA values often undergo TRUS biopsy to detect the presence of cancer. However, a standard 10-12 core biopsy has a positive yield of about 49% (Lawrentschuk et al., 2009). Thus, many men who undergo biopsy will have a negative result or may be diagnosed with low volume, low grade disease as seen in the ERSPC trial (Auvinen et al., 1996). The procedure exposes men to many side effects including a 4% risk of life threatening sepsis resulting in increased hospitalizations over the last 10 years (Nam et al., 2010).

An ideal prostate cancer biomarker should be able to identify a patient population that would have clinically significant prostate cancer and reduce the number of unnecessary biopsies in healthy men. To address the challenge of developing a superior prostate

cancer biomarker assay, I quantified prostate cancer tumor cell fragments known as prostate cancer microparticles (PCMPs) through a specialized instrument known as a nanoscale flow cytometer in a high-throughput and multi-parametric format. Unlike conventional flow cytometer machines, this instrument can analyze cell fragments as small as 100 nm in diameter. Dr. Leong's Translational Prostate Cancer Research Laboratory (St. Joseph's Hospital, Lawson Health Research Institute, London, ON) is focused on developing a "liquid biopsy" for high-risk prostate cancer using PSMA as a biomarker. The laboratory was able to identify a significant increase in the expression of PSMA expressing extracellular vesicles or microparticles in patient plasmas for those who had GS $\geq$ 8 prostate cancer (Biggs et al., 2016). In my study, I looked to improve on this "liquid biopsy" by adding additional biomarkers to analyze PCMPs that are expressing STEAP1, GHRSA and CD151.

Since a microparticle is an outward budding of the cell membrane, it carries with it the cell surface antigens present on the parent cell (Huang-Doran et al., 2017). In order to identify PCMPs from patient plasma, PSMA and STEAP1 surface markers were used to specifically identify PCMPs in patient plasmas using monoclonal antibodies for PSMA and STEAP1. PSMA and STEAP1 are considered prostate specific markers as they are highly expressed in the prostate gland in comparison to other tissues within the body (Human Protein Atlas, 2017). I looked to improve the ability of differentiating GS6 from GS3+4, GS4+3 and GS $\geq$ 8 by examining levels of PCMPs co-expressing PSMA and STEAP1 and one cancer specific marker, GHRSA or CD151. (Ang et al., 2004; Lu et al., 2012).

## 4.2 Potential Role of PCMP Assay in the Diagnosis of Prostate Cancer

PSA is an organ-specific serine protease that is widely accepted as a prostate cancer tumor marker, however, it is not cancer specific as numerous causes can alter PSA serum levels (Warade, 2014; Klein and Lowe, 1997). This enzyme is released into the blood by glandular epithelial cells of the prostate regardless of disease processes. PCMPs are unique in the way that they contain surface proteins found on epithelial prostate cell

membranes, providing a biochemical profile of the tissue. PCMPs are different from other biomarkers as they may reflect changes seen on epithelial prostate cells as Gleason grade progresses. Therefore, our PCMP biomarker assay can be used as an adjunct to PSA screening to help determine which men would benefit from a prostate biopsy. This “liquid biopsy” assay can be used to detect the expression of PCMPs in patient plasma samples. Our results have shown that we can accurately differentiate GS6 from GS3+4, 4+3 and  $GS \geq 8$  when we compare the level of expression of serum PCMPs. This assay would provide clinicians valuable information for risk stratification prior to obtaining tissue biopsy and would be very useful in a situation where PSA serum levels are no longer helpful. For example, if a patient with a suspicious PSA is being investigated for prostate cancer, a tissue biopsy is required in order to make the diagnosis. However, the PSA assay lacks the ability to risk stratify which patients may have intermediate or high-risk prostate cancer from low risk prostate cancer (GS 3+3). It is conceivable that the PCMP assay could then be used to detect if there are suspicious levels of PCMPs in a non-invasive plasma test prior to needle biopsy. Patients who have PCMP levels in ranges indicative of intermediate (GS3+4 or GS 4+3) or high-risk ( $GS \geq 8$ ) prostate cancer should then be recommended to undergo the TRUS biopsy. If the performance test characteristics of this “liquid biopsy” are excellent and accurate, then implementation prior to needle biopsy may allow clinicians to avoid TRUS biopsy in men who have low risk prostate cancer (GS 3+3), thus reducing patient anxiety related to the diagnosis of cancer as well as the complications related to the TRUS biopsy which are substantial. The benefit of this research is that the “liquid biopsy” is ultimately compared to the results of the Gleason Score assigned to final pathology of whole gland specimens from radical prostatectomy. The gold standard in this case would be final pathology and not PSA, which is not reflective of the biology of the tumor.

### 4.3 Measurement of Microparticles

This is the first study to enumerate MPs that co-express PSMA and STEAP1 with a cancer-specific marker, GHSR1a or CD151, in human plasma to develop a “liquid biopsy” for risk stratification of prostate cancer prior to surgery. Each biomarker (PSMA, STEAP1, GHSR1a, CD151) was assessed individually to determine their level of

expression in groups of prostate cancer patient plasmas representing different Gleason scores. To increase the probability of measuring MPs from the prostate, we elected to enumerate two surface proteins that are highly expressed on epithelial prostate tissue (PSMA and STEAP1). It should be noted that there are no healthy control volunteer plasma samples or plasma samples of patients who have BPH and negative prostate biopsies. Therefore, this pilot study is not powered to draw conclusions on PCMPs as a screening tool for prostate cancer and is more relevant to being used in the context of decision making for prescribing a needle biopsy or not after a PSA test result.

The only single biomarker that had a statistically significant difference of MP levels between GS6 and GS3+4 ( $p < 0.01$ ), GS4+3 ( $p < 0.05$ ), or  $GS \geq 8$  ( $p < 0.001$ ) was GHRS1a. As previously mentioned, GHRS1a is a receptor that is expressed on a wide variety of tissues involved in the gastrointestinal tract as well as skin, lung, prostate, pituitary and other peripheral tissues (Gnanapavan et al., 2002). Therefore, it is not a reliable marker on its own for detecting PCMPs. However, it is not surprising to see an increase in the expression of GHRS1a expressing MPs as the GS progressed in comparison to GS6. Previous research used a modified fluorescein-ghrelin probe which indirectly showed elevated expression of the GHRS1a (ghrelin receptor) in prostate cancer cell lines (LNCAP and PC3) and prostate cancer specimens from radical prostatectomy (Lu et al., 2012). Since the sample size in the study is small, it would be interesting to see if the elevated GHRS1a expressing MPs pattern continues to be elevated as the sample size is increased. Tissue microarrays (TMA) could be used to validate the findings of higher GHRS1a expression as Gleason score increases. The level of MPs expressing GHRS1a should be reflected in the degree of staining on the TMA. The results could be further validated through the use of The Cancer Genome Atlas (TCGA). TCGA is a repository that contains gene expression level of various proteins in more than 300 cases of prostate cancer along with clinical data for each patient. Degree of GHRS1a gene expression should be comparable to the level of MPs expressing the putative surface antigen. Both TMA and TCGA investigations could be expanded to validate the MP level of PSMA, STEAP1 and CD151.



It was surprising to see that there were no significant differences seen in the PSMA expressing MPs. Dr. Leong's lab previously showed that PSMA expressing MPs were significantly elevated in  $GS \geq 8$  (Biggs et al., 2016). However, a small increase in the level of PSMA expressing MPs in Gleason score 8 was observed. Any differences that Dr. Leong's lab had previously identified could be masked by the small cohort in this study as they used 256 patients with localized prostate cancer. STEAP1 expressing MPs also revealed no significant difference amongst the various GS's even though STEAP1 expressing MPs had the most recorded events from all single biomarkers. When looking at the region of interest (ROI) percentage (data not shown), MPs expressing STEAP1 monoclonal antibody accounted for 40-60% of total MPs within plasmas. This was seen in multiple patient plasma samples such as: patient 3, 5, 10, 14, 26, 27, 35, 45, 47, and 53. In fact, patient 44 had 80% of MPs positive for STEAP1. The remaining 49 patients had ~25% of MPs positive for STEAP1. Considering that MPs are released by a wide variety of cells (Brett et al., 2015), it is hard to image that such a high number of MPs are released from the prostate or that these MPs are truly all STEAP1 positive. This may suggest the STEAP1 monoclonal antibody used in this pilot study was binding less specifically than PSMA which often had an ROI that ranges from 2-15%. An exception was seen in plasmas: 5, 10, 20, 25, 30, 44 and 65 of whom had a ROI that ranged from 15-25% for PSMA. Only patient 26 and 27 had a higher ROI of 36%. This study was limited by the fact that multiple STEAP1 monoclonal antibodies were tested, however, only STEAP1 monoclonal antibody from Novus Biologicals worked on the flow cytometer. Using a STEAP1 monoclonal antibody that is custom designed to be more specific to the extracellular component of the STEAP1 antigen could potentially improve the performance characteristics of the antibody. A new STEAP1 antibody can be validated with immunohistochemistry and flow cytometry before using it in future studies. Furthermore, additional STEAP1 antibodies that are commercially available can be tested to determine if any other monoclonal antibodies on the market have better specificity.

Next, several permutations of dual positive MPs were assessed to determine if any combination could differentiate between the various GSs. When using two prostate specific markers, PSMA+STEAP1, these co-expressing MPs did not show any significant

differences amongst the various GS's. This is not surprising as both individually performed poorly in differentiating between GS's. PSMA+GHSR1a co-expressing MPs and STEAP1+GHSR1a co-expressing MPs both showed significant differences between GS6 and GS3+4 ( $p < 0.01$ ) or  $GS \geq 8$  ( $p < 0.001$ ). Of these two dual markers, STEAP1+GHSR1a co-expressing MPs should be interpreted with caution since the levels of STEAP1 expressing MPs were inexplicably elevated and likely did not bind with high specificity as previously described. The nonspecific binding of the STEAP1 antibody resulted in almost all of the single GHSR1a MP population recorded as events that were dual positive for both STEAP1 and GHSR1a by the flow cytometer. Therefore, due to the lack of specificity of STEAP1 antibody, the dual positive MP population would be less reflective of MPs truly positive for STEAP1 and GHSR1a only and would be reflective of a subpopulation of GHSR1a only. The performance of dual and triple positive MPs were assessed using the receiver operating characteristic (ROC) curve which will be discussed later on in the discussion.

The results of STEAP1+CD151 co-expressing MPs and PSMA+CD151 co-expressing MPs were a surprising finding. Ang et al. 2004, quantified the level of expression of CD151 in various prostate cancer specimens with immunohistochemistry. Their study found that CD151 was strongly expressed in poorly differentiated cancers (Ang et al., 2004). It was unexpected to see the abundance of both STEAP1+CD151 co-expressing MPs and PSMA+CD151 co-expressing MPs decrease as the GS increased. Only STEAP1+CD151 co-expressing MPs showed significant decline in the level of MPs when GS6 was compared to GS3+4, GS4+3, or  $GS \geq 8$ . One potential explanation could be that the MPs that expressed PSMA or STEAP1 on their surface were of a different size than the MPs expressing CD151 on their surface. Therefore, less MPs would be expressing both STEAP1 and CD151 or PSMA and CD151 demonstrating a lower level of dual MP expression. Atomic force microscopy has previously been used to detect MP size (Leong et al., 2011) and could be used to confirm that there exists varying sizes of CD151 expressing MPs when compared to STEAP1 expressing MPs and PSMA expressing MPs. Another potential theory for the decline in CD151 single could be that this tetraspanin internalizes in the MP as GS progresses. Therefore, the fluorescent CD151 antibody would not bind to the surface of MPs and the flow cytometer would not

read the MPs being positive for CD151. To test this theory, immunohistochemistry of prostatic cancer tissue of different GSs could be performed and visualized under confocal microscopy. This instrument can detect if the fluorescence of the CD151 antibody is seen on the cell membrane or internalized within the cell.

Triple positive MPs expressing PSMA, STEAP1 and CD151 significantly declined when comparing GS6 to GS3+4 ( $p < 0.01$ ), GS4+3 ( $p < 0.01$ ), or  $GS \geq 8$  ( $p < 0.001$ ). Two potential theories were previously mentioned in the past paragraph. Triple positive MPs expressing PSMA, STEAP1 and GHSR1a only showed a significant rise when comparing GS6 with GS3+4 or  $GS \geq 8$ . The increased expression of PSMA, STEAP1 and GHSR1a triple positive MPs in GS4+3 were not significant when compared to GS6. This inconsistent trend could be explained by the initial handling of the plasma when it was collected from the patients. If the collection of plasma during centrifugation was not optimal or the plasma wasn't initially stored under ideal temperatures, there could be degradation in the number of MPs within the plasma which would produce fewer triple positive events.

#### 4.4 Calculated Area Under the Curve (AUC) for Biomarkers.

In order to assess the performance characteristics for each parameter, receiver operating curves (ROC) were used to calculate the area under the curve (AUC) for test specificity and sensitivity. The closer the AUC is to a value of one, the stronger the biomarker performs at distinguishing true positives from false positives (1-specificity). ROC curves assessing the performance of biomarkers comparing GS6 vs GS3+4, GS6 vs 4+3 and GS6 vs  $GS \geq 8$  were used to assess various combinations of dual and triple positive MPs. GS6 was chosen as our comparison group as evidence supports active surveillance in this cohort and active treatment for those who have higher Gleason scores (Klotz et al., 2014). For each biomarker, cut off values of MPs calculated as events/ $\mu$ L were chosen to maximize specificity in order reduce number of false positives. The confidence intervals for each biomarker are also portrayed. Overall, the confidence intervals for each biomarker are quite wide and increasing the sample size may tighten these values assuming a normal distribution of these final results.

PSMA+GHSR1a co-expressing MPs was the best performing biomarker for GS6 vs GS3+4 with an AUC of 0.92 at a cut off of >28,002 events/ $\mu$ L. This provides a sensitivity of 85.71% and a specificity of 92.86%. The second-best biomarker was PSMA+STEAP1+GHSR1a triple expressing MPs with an AUC of 0.89 at a cut off value of >50,435 events/ $\mu$ L. This provides a sensitivity of 57.14% and a specificity of 92.86%. The worst performing biomarker was PSMA+STEAP1 co-expressing MPs with an AUC 0.52. PSMA+STEAP1+CD151 triple expressing MPs had an AUC of 0.76.

PSMA+STEAP1+CD151 triple expressing MPs was the best performing biomarker for GS6 vs GS4+3 with an AUC of 0.79 at a cut off of <46,653 events/ $\mu$ L. The sensitivity and specificity at this cut off value are 60.0% and 80.0%, respectively. STEAP1+CD151 co-expressing MPs performed similarly with an AUC of 0.79 at a cut off of <49418 events/ $\mu$ L. Sensitivity and specificity at this value was 73.3%. The addition of a third biomarker allowed the cut off value to drop and specificity to increase at the expense of sensitivity. With a small sample size, it is difficult to confirm if in fact STEAP1+CD151 co-expressing MPs performs similar to PSMA+STEAP1+CD151 triple expressing MPs. PSMA+STEAP1 co-expressing MPs was amongst one of the worst performing biomarkers with an AUC of 0.62. PSMA+STEAP1+GHSR1a triple expressing MPs exhibited an AUC of 0.69.

The best performing biomarker at GS6 vs GS $\geq$ 8 was STEAP1+GHSR1a co-expressing MPs with an AUC of 0.90 at a cut off of >32,621 events/ $\mu$ L. This provided a sensitivity and specificity of 86.67% and 92.86%, respectively. PSMA+GHSR1a co-expressing MPs came second with an AUC of 0.87 at a cut off of >28,331 events/ $\mu$ L. This provided a sensitivity and specificity of 80% and 92.86% respectively. The triple expressing MPs, PSMA+STEAP1+GHSR1a and PSMA+STEAP1+CD151, had AUC's of 0.85 and 0.82, respectively. PSMA+CD151 co-expressing MPs performed poorly with an AUC of 0.64.

Overall, the object of the pilot study was to assess whether adding an additional cancer specific marker, GHSR1a or CD151, to PSMA and STEAP1 would improve biomarker performance. In fact, both PSMA+STEAP1+GHSR1a and PSMA+STEAP1+CD151 performed better than PSMA+STEAP1 MPs at all three GS comparisons (GS3+4,

GS4+3, and GS $\geq$ 8). PSMA+STEAP1+GHSR1a performed best at GS3+4 (AUC 0.89) and GS $\geq$ 8 (AUC 0.85). PSMA+STEAP1+CD151 performed best at GS4+3 (AUC 0.79).

In this pilot study, we were able to determine the performance of the various permutations of biomarker combinations to give us an idea of which combination to use in a much larger training set of patient plasmas representing all risk phenotypes of prostate cancer. Both dual positive and triple positive biomarkers for enumeration of PCMPs have been identified. A larger cohort will be needed to further assess their performance to determine which combination has the most robust performance at an optimal cut off value for sensitivity and specificity.

## 4.5 Limitations

There are some key limitations to this study that should be addressed. As discussed earlier, a STEAP1 antibody that is more specific for the extracellular component of STEAP1 surface antigen could provide more reliable results. Risk of human pipetting error could add unpredictable variability when incubating plasma samples. We attempted to reduce this variability by using a cocktail of an antibody at a set concentration before incubating all samples. Furthermore, the cohort size is quite small to draw any significant conclusions except for elimination of some biomarker combinations that would appear to fail in a much larger analysis of patient plasmas. Our pilot study contained 60 patients with 15 patients in each Gleason score group. The cohort size is hypothesis generating but more patients will be required in order to make a more definitive conclusion. Another limitation in the study is a lack of a healthy volunteer group. Having a healthy group would strengthen the results by giving insight of a potential baseline of MPs. It would be interesting to see if there is a threshold of MPs that could suggest a diagnosis of cancer in comparison to healthy patients. An ideal healthy volunteer group would consist of both healthy men and women that are age matched to the other prostate cancer patient plasmas. A cohort of women would be useful in assessing the level of MPs that co-express PSMA and STEAP1 as these should be higher in men due to the presence of the prostate gland. A BPH group would also help strengthen the study. As the prostate becomes enlarged, the MP level could potentially increase as does the PSA level in most

patients. Overall, this study doesn't address if MPs can be used as a screening test as there is no healthy volunteer or BPH cohort. It does shed evidence that MPs can be used to potentially detect progression of Gleason score as our results highlighted that different GS's have different levels of MP expression.

This study did not look address a number of factors that could influence MP expression. There are a number of medications that are known to exert their effects on the prostate. For example, 5-alpha reductase inhibitors prevent hormonal interaction within the prostate. Since these classes of medications can reduce prostate size, they may impact MP levels. This study also did not assess how the volume of prostate cancer in surgical samples or pathologic staging could influence MP level. Due to the low volume of patients, these objectives would be difficult to address. Furthermore, our cohort data lacked epidemiologic data regarding race and age which are known risk factors for prostate cancer. Finally, no post-radical prostatectomy patient plasma was analyzed. Therefore, no comment can be made regarding treatment response after surgery and the decline of MP levels, as previously shown by Briggs et al, 2016.

## Chapter 5

### 5 Conclusion

#### 5.1 Conclusion

Apogee A-50Micro nanoscale flow cytometer was capable of identifying MPs that were positive for the surface markers: PSMA, STEAP1, GHSR1a, and CD151, in a high throughput and multi-parametric manner. When dual and triple positive MPs were enumerated, a significant difference between the expression of GS6 to GS3+4, GS4+3 and GS $\geq$ 8 was measurable. PSMA+GHSR1a, STEAP1+GHSR1a, and PSMA+STEAP1+GHSR1a expressing MPs saw a significant increase in expression between GS6 vs GS3+4 and GS $\geq$ 8. STEAP1+CD151 and PSMA+STEAP1+CD151 expressing MPs showed a significant decrease in expression of MPs between GS6 vs GS3+4, GS4+3 and GS $\geq$ 8.

When it came to assessing biomarker performance, PSMA+STEAP1+GHSR1a and PSMA+STEAP1+CD151 triple-expressing MPs, outperformed PSMA+STEAP1co-expressing MPs in all comparison groups of Gleason score. Further exploration with larger patient numbers may help identify which biomarker can best discriminate patients amongst the various Gleason scores.

## 5.2 Future Directions

The next step is to increase the cohort size of the study and reassess the performance of the biomarkers that performance the best. Currently, the procurement of more patient plasma samples from the biobanks is underway. The plan is also to add a healthy volunteer cohort and a BPH cohort to further strengthen the study, which is arguably the greatest limitation of this study aside from the cohort size. The samples will be analyzed, using the same standardized protocol outlined in this study, while maintaining experimental blinding. Antibodies mass produced from reliable manufactures using the same lot number will used to run experiments to reduce variability within their performance. To further reduce the risk pipetting variability, we will use a cocktail of antibodies that are thoroughly mixed at a set concentration before starting our antibody-plasma incubation. Tissue microarrays will be used as a visual confirmation to validate the MP level of expression seen for each biomarker: PSMA, STEAP1, CD151 and GHSR1 as Gleason score progresses.



## Bibliography

- Adams, E.F., Huang, B., Buchfelder, M., Howard, A., Smith, R.G., Feighner, S.D., Van der Ploeg, L.H., Bowers, C.Y., & Fahlbusch, (1998). R. Presence of growth hormone secretagogue receptor mRNA in human pituitary tumours and rat GH<sub>3</sub> cells. *Journal of Clinical Endocrinology and Metabolism* 83, 638–642.
- Al-Nedawi K., Meehan B., & Rak J. (2009) Microvesicles: messengers and mediators of tumor progression. *Cell Cycle* 8, 2014–2018.
- American Cancer Society. (2016). Prostate cancer staging. Retrieved January, 2017, from <https://www.cancer.org/cancer/prostate-cancer/detection-diagnosis-staging/staging.html>.
- Amin Al Olama, A., Dadaev, T., Hazelett, D. J., Li, Q., Leongamornlert, D., Saunders, E. J., . . . Kote-Jarai, Z. (2015). Multiple novel prostate cancer susceptibility signals identified by fine-mapping of known risk loci among Europeans. *Hum Mol Genet*, 24(19), 5589-5602. doi:10.1093/hmg/ddv203
- Andriole, G. L., Crawford, E. D., Grubb, R. L., 3rd, Buys, S. S., Chia, D., Church, T. R., . . . Team, P. P. (2012). Prostate cancer screening in the randomized Prostate, Lung, Colorectal, and Ovarian Cancer Screening Trial: mortality results after 13 years of follow-up. *J Natl Cancer Inst*, 104(2), 125-132.
- Ang, J., Fang, B. L., Ashman, L. K., & Frauman, A. G. (2010). The migration and invasion of human prostate cancer cell lines involves CD151 expression. *Oncol Rep*, 24(6), 1593-1597.
- Ang, J., Lijovic, M., Ashman, L. K., Kan, K., & Frauman, A. G. (2004). CD151 protein expression predicts the clinical outcome of low-grade primary prostate cancer better than histologic grading: a new prognostic indicator? *Cancer Epidemiol Biomarkers Prev*, 13(11 Pt 1), 1717-1721.
- Apogee Flow systems. (2017). Micro Flow Cytometer. Retrieved in February, 2017, from <http://www.apogee-flow.com/micro-flow-cytometer.php>.
- Aubry, W., Lieberthal, R., Willis, A., Bagley, G., Willis, S. M., 3rd, & Layton, A. (2013). Budget impact model: epigenetic assay can help avoid unnecessary repeated prostate biopsies and reduce healthcare spending. *Am Health Drug Benefits*, 6(1), 15-24.
- Aumüller, G. (1979). Prostate Gland and Seminal Vesicles. Berlin-Heidelberg: Springer-Verlag.
- Auvinen, A., Rietbergen, J. B., Denis, L. J., Schroder, F. H., & Prorok, P. C. (1996). Prospective evaluation plan for randomised trials of prostate cancer screening. The International Prostate Cancer Screening Trial Evaluation Group. *J Med Screen*, 3(2), 97-104.

Baillargeon, J., Pollock, B. H., Kristal, A. R., Bradshaw, P., Hernandez, J., Basler, J., . . . Thompson, I. (2005). The association of body mass index and prostate-specific antigen in a population-based study. *Cancer*, *103*(5), 1092-1095.

Barry, M.J., (2009). Screening for prostate cancer: the controversy that refuses to die. *N Engl J Med*. *360*, 1351-1354.

Barteneva, N. S., Fasler-Kan, E., Bernimoulin, M., Stern, J. N., Ponomarev, E. D., Duckett, L., & Vorobjev, I. A. (2013). Circulating microparticles: square the circle. *BMC Cell Biol*, *14*, 23.

Bazinet, M., Meshref, A. W., Trudel, C., Aronson, S., Peloquin, F., Nachabe, M., . . . Elhilali, M. M. (1994). Prospective evaluation of prostate-specific antigen density and systematic biopsies for early detection of prostatic carcinoma. *Urology*, *43*(1), 44-51; discussion 51-42.

Biggs, C. N., Siddiqui, K. M., Al-Zahrani, A. A., Pardhan, S., Brett, S. I., Guo, Q. Q., . . . Leong, H. S. (2016). Prostate extracellular vesicles in patient plasma as a liquid biopsy platform for prostate cancer using nanoscale flow cytometry. *Oncotarget*, *7*(8), 8839-8849.

Bismar, T. A., Lewis, J. S., Jr., Vollmer, R. T., & Humphrey, P. A. (2003). Multiple measures of carcinoma extent versus perineural invasion in prostate needle biopsy tissue in prediction of pathologic stage in a screening population. *Am J Surg Pathol*, *27*(4), 432-440.

Bjurlin, M. A., Carter, H. B., Schellhammer, P., Cookson, M. S., Gomella, L. G., Troyer, D., . . . Taneja, S. S. (2013). Optimization of initial prostate biopsy in clinical practice: sampling, labeling and specimen processing. *J Urol*, *189*(6), 2039-2046.

Bostwick, D. G., Pacelli, A., Blute, M., Roche, P., & Murphy, G. P. (1998). Prostate specific membrane antigen expression in prostatic intraepithelial neoplasia and adenocarcinoma: a study of 184 cases. *Cancer*, *82*(11), 2256-2261.

Bouye, S., Potiron, E., Puech, P., Leroy, X., Lemaitre, L., & Villers, A. (2009). Transition zone and anterior stromal prostate cancers: zone of origin and intraprostatic patterns of spread at histopathology. *Prostate*, *69*(1), 105-113.

Bradley, L. A., Palomaki, G. E., Gutman, S., Samson, D., & Aronson, N. (2013). Comparative effectiveness review: prostate cancer antigen 3 testing for the diagnosis and management of prostate cancer. *J Urol*, *190*(2), 389-398.

Brawer, M. K. (1999). Prostate-specific antigen: current status. *CA Cancer J Clin*, *49*(5), 264-281.

Brawer, M. K., Aramburu, E. A., Chen, G. L., Preston, S. D., & Ellis, W. J. (1993). The inability of prostate specific antigen index to enhance the predictive value of prostate specific antigen in the diagnosis of prostatic carcinoma. *J Urol*, *150*(2 Pt 1), 369-373.

- Brett, S. I., Kim, Y., Biggs, C. N., Chin, J. L., & Leong, H. S. (2015). Extracellular vesicles such as prostate cancer cell fragments as a fluid biopsy for prostate cancer. *Prostate Cancer Prostatic Dis*, 18(3), 213-220.
- Brody, I., Ronquist, G., & Gottfries, A. (1983). Ultrastructural localization of the prostasome - an organelle in human seminal plasma. *Ups J Med Sci*, 88(2), 63-80.
- Bul, M., Zhu, X., Valdagni, R., Pickles, T., Kakehi, Y., Rannikko, A., . . . Roobol, M. J. (2013). Active surveillance for low-risk prostate cancer worldwide: the PRIAS study. *Eur Urol*, 63(4), 597-603.
- Bussemakers, M. J., van Bokhoven, A., Verhaegh, G. W., Smit, F. P., Karthaus, H. F., Schalken, J. A., . . . Isaacs, W. B. (1999). DD3: a new prostate-specific gene, highly overexpressed in prostate cancer. *Cancer Res*, 59(23), 5975-5979.
- Canadian Cancer Society's Advisory Committee on Cancer Statistics. *Canadian Cancer Statistics 2017*. Toronto, ON: Canadian Cancer Society; 2017. Available at: [cancer.ca/Canadian-Cancer-Statistics-2017-EN.pdf](http://cancer.ca/Canadian-Cancer-Statistics-2017-EN.pdf) (September 3, 2017).
- Canadian Task Force on Preventive Health, C., Bell, N., Connor Gorber, S., Shane, A., Joffres, M., Singh, H., . . . Tonelli, M. (2014). Recommendations on screening for prostate cancer with the prostate-specific antigen test. *CMAJ*, 186(16), 1225-1234.
- Carter, H. B., Morrell, C. H., Pearson, J. D., Brant, L. J., Plato, C. C., Metter, E. J., . . . Walsh, P. C. (1992). Estimation of prostatic growth using serial prostate-specific antigen measurements in men with and without prostate disease. *Cancer Res*, 52(12), 3323-3328.
- Carvalho, G. F., Smith, D. S., Mager, D. E., Ramos, C., & Catalona, W. J. (1999). Digital rectal examination for detecting prostate cancer at prostate specific antigen levels of 4 ng./ml. or less. *J Urol*, 161(3), 835-839.
- Catalona, W. J., Hudson, M. A., Scardino, P. T., Richie, J. P., Ahmann, F. R., Flanigan, R. C., . . . et al. (1994). Selection of optimal prostate specific antigen cutoffs for early detection of prostate cancer: receiver operating characteristic curves. *J Urol*, 152(6 Pt 1), 2037-2042.
- Challita-Eid, P. M., Morrison, K., Etesami, S., An, Z., Morrison, K. J., Perez-Villar, J. J., . . . Jakobovits, A. (2007). Monoclonal antibodies to six-transmembrane epithelial antigen of the prostate-1 inhibit intercellular communication in vitro and growth of human tumor xenografts in vivo. *Cancer Res*, 67(12), 5798-5805.
- Chang, S. S. (2004). Overview of prostate-specific membrane antigen. *Rev Urol*, 6 Suppl 10, S13-18.
- Chaput, N., Taieb, J., Scharz, N. E., Andre, F., Angevin, E., & Zitvogel, L. (2004). Exosome-based immunotherapy. *Cancer Immunol Immunother*, 53(3), 234-239.

- Chargaff, E., West, R. (1946). The biological significance of the thromboplastic protein of blood. *J Biol Chem*, 166(1), 189-197.
- Chopin, L. K., Seim, I., Walpole, C. M., & Herington, A. C. (2012). The ghrelin axis--does it have an appetite for cancer progression? *Endocr Rev*, 33(6), 849-891.
- Cohen, R.J., Shannon, B.A., Phillips, M., Moorin, R.E., Wheeler, T.M., & Garrett, K.L. (2008). Central zone carcinoma of the prostate gland: a distinct tumor type with poor prognostic features. *The Journal of Urology* 179, 1762-7.
- Collin, S. M., Martin, R. M., Metcalfe, C., Gunnell, D., Albertsen, P. C., Neal, D., . . . Donovan, J. (2008). Prostate-cancer mortality in the USA and UK in 1975-2004: an ecological study. *Lancet Oncol*, 9(5), 445-452.
- Cooperberg, MR., Grossfeld, GD., Lubeck, DP., & Carroll, PR. (2003). National practice patterns and time trends in androgen ablation for localized prostate cancer. *JNCI* 95, 981-9.
- Cooperberg, M. R., Lubeck, D. P., Meng, M. V., Mehta, S. S., & Carroll, P. R. (2004). The changing face of low-risk prostate cancer: trends in clinical presentation and primary management. *J Clin Oncol*, 22(11), 2141-2149.
- Crawford N. (1971). The presence of contractile proteins in platelet microparticles isolated from human and animal platelet-free plasma. *Br J Haematol* 21, 53-69.
- Dashevsky, O., Varon, D., & Brill, A. (2009). Platelet-derived microparticles promote invasiveness of prostate cancer cells via upregulation of MMP-2 production. *Int J Cancer*, 124(8), 1773-1777.
- de Keyzer, Y., Lenne, F. & Bertagna, X. (1997). Widespread transcription of the growth hormone releasing peptide gene in neuroendocrine human tumours. *European Journal of Endocrinology* 137, 715-718.
- de Kok, J. B., Verhaegh, G. W., Roelofs, R. W., Hessels, D., Kiemeney, L. A., Aalders, T. W., . . . Schalken, J. A. (2002). DD3(PCA3), a very sensitive and specific marker to detect prostate tumors. *Cancer Res*, 62(9), 2695-2698.
- de Koning, H. J., Auvinen, A., Berenguer Sanchez, A., Calais da Silva, F., Ciatto, S., Denis, L., . . . International Prostate Cancer Screening Trials Evaluation, G. (2002). Large-scale randomized prostate cancer screening trials: program performances in the European Randomized Screening for Prostate Cancer trial and the Prostate, Lung, Colorectal and Ovary cancer trial. *Int J Cancer*, 97(2), 237-244.
- Detchokul, S., Newell, B., Williams, E.D., & Frauman, A.G. (2014). CD151 is associated with prostate cancer cell invasion and lymphangiogenesis in vivo. *Oncology Reports*, 31, 241-247.

Doran, M. G., Watson, P. A., Cheal, S. M., Spratt, D. E., Wongvipat, J., Steckler, J. M., . . . Lewis, J. S. (2014). Annotating STEAP1 regulation in prostate cancer with 89Zr immuno-PET. *J Nucl Med*, *55*(12), 2045-2049.

Drake, R. R., & Kislinger, T. (2014). The proteomics of prostate cancer exosomes. *Expert Rev Proteomics*, *11*(2), 167-177.

Duijvesz, D., Luiders, T., Bangma, C. H., & Jenster, G. (2011). Exosomes as biomarker treasure chests for prostate cancer. *Eur Urol*, *59*(5), 823-831.

Epstein, J.I., Allsbrook, W.C., Amin, M.B., Egevad, L.L., & ISUP Grading Committee. (2005). The 2005 International Society of Urological Pathology (ISUP) Consensus Conference on Gleason Grading of Prostatic Carcinoma. *Am J Surg Pathol*, *29*, 1228-42.

Esposito, K., Chiodini, P., Capuano, A., Bellastella, G., Maiorino, M. I., Parretta, E., . . . Giugliano, D. (2013). Effect of metabolic syndrome and its components on prostate cancer risk: meta-analysis. *J Endocrinol Invest*, *36*(2), 132-139.

Etzioni, R., Tsodikov, A., Mariotto, A., Szabo, A., Falcon, S., Wegelin, J., . . . Feuer, E. (2008). Quantifying the role of PSA screening in the US prostate cancer mortality decline. *Cancer Causes Control*, *19*(2), 175-181.

European Association of Urology. (2016). EAU Guidelines on Prostate Cancer 2016. Retrieved on January, 2017, from <https://uroweb.org/guideline/prostate-cancer/?type=archive>.

Felletto, E., Bang, A., Cole-Clark, D., Chalasani, V., Rasiah, K., & Smith, D. P. (2015). An examination of prostate cancer trends in Australia, England, Canada and USA: Is the Australian death rate too high? *World J Urol*, *33*(11), 1677-1687.

Filter, E., Gabril, M., Gomez, J., Wang, P., Chin, J., Izawa, J., & Moussa, M. (2017). Incidental prostate adenocarcinoma in cystoprostatectomy specimens: partial versus complete prostate sampling. *Int J Surg Pathol*, *25*(5), 414-420.

Fitter, S., Tetaz, T., Berndt, M., & Ashman, L. (1995). Molecular cloning of cDNA encoding a novel platelet-endothelial cell tetra-span antigen, PETA-3. *Blood*, *86*(4), 1348-1355.

Geary, S. M., Cambareri, A. C., Sincock, P. M., Fitter, S., & Ashman, L. K. (2001). Differential tissue expression of epitopes of the tetraspanin CD151 recognised by monoclonal antibodies. *Tissue Antigens*, *58*(3), 141-153.

Ghani, K. R., Grigor, K., Tulloch, D. N., Bollina, P. R., & McNeill, S. A. (2005). Trends in reporting Gleason score 1991 to 2001: changes in the pathologist's practice. *Eur Urol*, *47*(2), 196-201.

Gleason, D. F. (1966). Classification of prostatic carcinomas. *Cancer Chemother Rep*, *50*(3), 125-128.

- Gleason, D. F., & Mellinger, G. T. (1974). Prediction of prognosis for prostatic adenocarcinoma by combined histological grading and clinical staging. *J Urol*, *111*(1), 58-64.
- Globocan 2012: Estimated Cancer Incidence, Mortality, and Prevalance Worldwide in 2012. (2015). Retrieved January, 2017, from [http://globocan.iarc.fr/Pages/fact\\_sheets\\_cancer.aspx](http://globocan.iarc.fr/Pages/fact_sheets_cancer.aspx)
- Gnanapavan, S., Kola, B., Bustin, S. A., Morris, D. G., McGee, P., Fairclough, P., . . . Korbonits, M. (2002). The tissue distribution of the mRNA of ghrelin and subtypes of its receptor, GHS-R, in humans. *J Clin Endocrinol Metab*, *87*(6), 2988.
- Gomes, I. M., Maia, C. J., & Santos, C. R. (2012). STEAP proteins: from structure to applications in cancer therapy. *Mol Cancer Res*, *10*(5), 573-587.
- Groskopf, J., Aubin, S. M., Deras, I. L., Blase, A., Bodrug, S., Clark, C., . . . Rittenhouse, H. (2006). APTIMA PCA3 molecular urine test: development of a method to aid in the diagnosis of prostate cancer. *Clin Chem*, *52*(6), 1089-1095.
- Hara, R., Jo, Y., Fujii, T., Kondo, N., Yokoyama, T., Miyaji, Y., & Nagai, A. (2008). Optimal approach for prostate cancer detection as initial biopsy: prospective randomized study comparing transperineal versus transrectal systematic 12-core biopsy. *Urology*, *71*(2), 191-195.
- Hargett, L. A., & Bauer, N. N. (2013). On the origin of microparticles: From "platelet dust" to mediators of intercellular communication. *Pulm Circ*, *3*(2), 329-340.
- Hasegawa, H., Watanabe, H., Nomura, T., Utsunomiya, Y., Yanagisawa, K., & Fujita, S. (1997). Molecular cloning and expression of mouse homologue of SFA-1/PETA-3 (CD151), a member of the transmembrane 4 superfamily. *Biochim Biophys Acta*, *1353*(2), 125-130.
- Heijnen, H. F., Schiel, A. E., Fijnheer, R., Geuze, H. J., & Sixma, J. J. (1999). Activated platelets release two types of membrane vesicles: microvesicles by surface shedding and exosomes derived from exocytosis of multivesicular bodies and alpha-granules. *Blood*, *94*(11), 3791-3799.
- Hinkle, G. H., Burgers, J. K., Neal, C. E., Texter, J. H., Kahn, D., Williams, R. D., . . . Badalament, R. A. (1998). Multicenter radioimmunosciintigraphic evaluation of patients with prostate carcinoma using indium-111 capromab pendetide. *Cancer*, *83*(4), 739-747.
- Hovels, A. M., Heesakkers, R. A., Adang, E. M., Jager, G. J., Strum, S., Hoogeveen, Y. L., . . . Barentsz, J. O. (2008). The diagnostic accuracy of CT and MRI in the staging of pelvic lymph nodes in patients with prostate cancer: a meta-analysis. *Clin Radiol*, *63*(4), 387-395.

- Howard, A. D., Feighner, S. D., Cully, D. F., Arena, J. P., Liberator, P. A., Rosenblum, C. I., . . . Van der Ploeg, L. H. (1996). A receptor in pituitary and hypothalamus that functions in growth hormone release. *Science*, *273*(5277), 974-977.
- Howlader N, Noone AM, Krapcho M, Miller D, Bishop K, Kosary CL, Yu M, Ruhl J, Tatalovich Z, Mariotto A, Lewis DR, Chen HS, Feuer EJ, Cronin KA (eds). (2017). SEER Cancer Statistics Review, 1975-2014, National Cancer Institute. Bethesda, MD, [https://seer.cancer.gov/csr/1975\\_2014/](https://seer.cancer.gov/csr/1975_2014/), based on November 2016 SEER data submission
- Huang-Doran, I., Zhang, C., Vidal-Puig, A. (2017). Extracellular Vesicles: Novel Mediators of Cell Communication in Metabolic Disease. *Trends in Endocrinology & Metabolism* *28*, 3-16.
- Hubert, R. S., Vivanco, I., Chen, E., Rastegar, S., Leong, K., Mitchell, S. C., . . . Afar, D. E. (1999). STEAP: a prostate-specific cell-surface antigen highly expressed in human prostate tumors. *Proc Natl Acad Sci U S A*, *96*(25), 14523-14528.
- Israeli, R. S., Powell, C. T., Fair, W. R., & Heston, W. D. (1993). Molecular cloning of a complementary DNA encoding a prostate-specific membrane antigen. *Cancer Res*, *53*(2), 227-230.
- Jeffery, P. L., Herington, A. C., & Chopin, L. K. (2002). Expression and action of the growth hormone releasing peptide ghrelin and its receptor in prostate cancer cell lines. *J Endocrinol*, *172*(3), R7-11.
- Joelle, E., & Jeanny, B. (2013). The changing landscape in the treatment of metastatic castration-resistant prostate cancer. *Ther Adv Med Oncol*, *5*(1), 25-40.
- John, E. M., Stern, M. C., Sinha, R., & Koo, J. (2011). Meat consumption, cooking practices, meat mutagens, and risk of prostate cancer. *Nutr Cancer*, *63*(4), 525-537.
- Kaelberer, J. B., O'Donnell, M. A., Mitchell, D. L., Snow, A. N., Mott, S. L., Buatti, J. M., . . . Watkins, J. M. (2016). Incidental prostate cancer diagnosed at radical cystoprostatectomy for bladder cancer: disease-specific outcomes and survival. *Prostate Int*, *4*(3), 107-112.
- Key, T.J. (2014). Nutrition, hormones and prostate cancer risk: results from the European prospective investigation into cancer and nutrition. *Recent Results Cancer Res* *202*, 39.
- Klein, L. T., & Lowe, F. C. (1997). The effects of prostatic manipulation on prostate-specific antigen levels. *Urol Clin North Am*, *24*(2), 293-297.
- Klotz, L., Vesprini, D., Sethukavalan, P., Jethava, V., Zhang, L., Jain, S., . . . Loblaw, A. (2015). Long-term follow-up of a large active surveillance cohort of patients with prostate cancer. *J Clin Oncol*, *33*(3), 272-277.

- Kojima, M., Hosoda, H., Date, Y., Nakazato, M., Matsuo, H., & Kangawa, K. (1999). Ghrelin is a growth-hormone-releasing acylated peptide from stomach. *Nature*, *402*(6762), 656-660.
- Kufe DW, Pollock RE, Weichselbaum RR, et al., editors. *Holland-Frei Cancer Medicine*, 6<sup>th</sup> Edition. Hamilton (ON): BC Decker, 2003.
- Kulasingam, V., & Diamandis, E. P. (2008). Strategies for discovering novel cancer biomarkers through utilization of emerging technologies. *Nat Clin Pract Oncol*, *5*(10), 588-599.
- Kupelian PA., Buchsbaum JC., Elshaikh MA., Reddy CA., & Klein EA. (2003). Improvement in relapse-free survival throughout the PSA era in patients with localized prostate cancer treated with definitive radiotherapy: Year of treatment an independent predictor of outcome. *Int J Radiat Oncol Biol Phys* *57*, 629–34.
- Langsteiger, W., Haim, S., Knauer, M., Waldenberger, P., Emmanuel, K., Loidl, W., . . . Beheshti, M. (2012). Imaging of bone metastases in prostate cancer: an update. *Q J Nucl Med Mol Imaging*, *56*(5), 447-458.
- Lawrentschuk, N., Toi, A., Lockwood, G. A., Evans, A., Finelli, A., O'Malley, M., . . . Fleshner, N. E. (2009). Operator is an independent predictor of detecting prostate cancer at transrectal ultrasound guided prostate biopsy. *J Urol*, *182*(6), 2659-2663.
- Lazzeri, M., Haese, A., de la Taille, A., Palou Redorta, J., McNicholas, T., Lughezzani, G., . . . Guazzoni, G. (2013). Serum isoform [-2]proPSA derivatives significantly improve prediction of prostate cancer at initial biopsy in a total PSA range of 2-10 ng/ml: a multicentric European study. *Eur Urol*, *63*(6), 986-994.
- Le, B. V., Griffin, C. R., Loeb, S., Carvalhal, G. F., Kan, D., Baumann, N. A., & Catalona, W. J. (2010). [-2]Proenzyme prostate specific antigen is more accurate than total and free prostate specific antigen in differentiating prostate cancer from benign disease in a prospective prostate cancer screening study. *J Urol*, *183*(4), 1355-1359.
- Leong, H. S., Podor, T. J., Manocha, B., & Lewis, J. D. (2011). Validation of flow cytometric detection of platelet microparticles and liposomes by atomic force microscopy. *J Thromb Haemost*, *9*(12), 2466-2476.
- Liu, H., Rajasekaran, A. K., Moy, P., Xia, Y., Kim, S., Navarro, V., . . . Bander, N. H. (1998). Constitutive and antibody-induced internalization of prostate-specific membrane antigen. *Cancer Res*, *58*(18), 4055-4060.
- Longo, N., Yanez-Mo, M., Mittelbrunn, M., Rosa, G., Muñoz, M. L., Sanchez-Madrid, F., Sanchez-Mateos, P. (2001). Regulatory role of tetraspanin CD9 in tumor-endothelial cell interaction during transendothelial invasion of melanoma cells. *Blood* *98*, 3717-3726.



- Lu, C., McFarland, M. S., Nesbitt, R. L., Williams, A. K., Chan, S., Gomez-Lemus, J., . . . Lewis, J. D. (2012). Ghrelin receptor as a novel imaging target for prostatic neoplasms. *Prostate*, 72(8), 825-833.
- Mathivanan, S., Ji, H., & Simpson, R. J. (2010). Exosomes: extracellular organelles important in intercellular communication. *J Proteomics*, 73(10), 1907-1920.
- McNeal, J. E. (1969). Origin and development of carcinoma in the prostate. *Cancer* 23, 24-34.
- McNeal, J.E., (1981). The zonal anatomy of the prostate. *Prostate* 2, 35-49.
- Mhaweck-Fauceglia, P., Zhang, S., Terracciano, L., Sauter, G., Chadhuri, A., Herrmann, F. R., & Penetrante, R. (2007). Prostate-specific membrane antigen (PSMA) protein expression in normal and neoplastic tissues and its sensitivity and specificity in prostate adenocarcinoma: an immunohistochemical study using mutiple tumour tissue microarray technique. *Histopathology*, 50(4), 472-483.
- Miller, D.C., Hafez, K.S., Stewart, A., Montie, J.E., & Wei, J.T. (2003). Prostate carcinoma presentation, diagnosis, and staging: an update from the National Cancer Data Base. *Cancer* 98, 1169-78.
- Muir, C.S., Nectoux, J., & Staszewski, J. (1991). The epidemiology of prostatic cancer. Geographical distribution and time-trends. *Acta Oncol* 30, 133-40.
- Musunuru, H., Yamamoto, T., Klotz, L., Ghanem, G., Mamedov, A., & Loblaw, A. (2016). Active surveillance for intermediate risk prostate cancer: survival outcomes in the Sunnybrook experience. *J Urol* 196(6), 1651-1658.
- Nam, R. K., Saskin, R., Lee, Y., Liu, Y., Law, C., Klotz, L. H., . . . Narod, S. A. (2010). Increasing hospital admission rates for urological complications after transrectal ultrasound guided prostate biopsy. *J Urol*, 183(3), 963-968.
- National Cancer Institute. (2015). SEER Stat fact sheets: Prostate cancer. Retrieved May, 2016, from <http://seer.cancer.gov/statfacts/html/prost.html>.
- Newcomer, L. M., Stanford, J. L., Blumenstein, B. A., & Brawer, M. K. (1997). Temporal trends in rates of prostate cancer: declining incidence of advanced stage disease, 1974 to 1994. *J Urol*, 158(4), 1427-1430.
- Nilsson, J., Skog, J., Nordstrand, A., Baranov, V., Mincheva-Nilsson, L., Breakefield, X. O., & Widmark, A. (2009). Prostate cancer-derived urine exosomes: a novel approach to biomarkers for prostate cancer. *Br J Cancer*, 100(10), 1603-1607.

- Oesterling, J. E., Jacobsen, S. J., Chute, C. G., Guess, H. A., Girman, C. J., Panser, L. A., & Lieber, M. M. (1993). Serum prostate-specific antigen in a community-based population of healthy men. Establishment of age-specific reference ranges. *JAMA*, *270*(7), 860-864.
- Otto, B., Barbieri, C., Lee, R., Te, A. E., Kaplan, S. A., Robinson, B., & Chughtai, B. (2014). Incidental prostate cancer in transurethral resection of the prostate specimens in the modern era. *Adv Urol*, *2014*, 627290.
- Petronis, J. D., Regan, F., & Lin, K. (1998). Indium-111 capromab pendetide (ProstaScint) imaging to detect recurrent and metastatic prostate cancer. *Clin Nucl Med*, *23*(10), 672-677.
- Pinto, J. T., Suffoletto, B. P., Berzin, T. M., Qiao, C. H., Lin, S., Tong, W. P., . . . Heston, W. D. (1996). Prostate-specific membrane antigen: a novel folate hydrolase in human prostatic carcinoma cells. *Clin Cancer Res*, *2*(9), 1445-1451.
- Podor, T. J., Singh, D., Chindemi, P., Foulon, D. M., McKelvie, R., Weitz, J. I., . . . Davies, R. (2002). Vimentin exposed on activated platelets and platelet microparticles localizes vitronectin and plasminogen activator inhibitor complexes on their surface. *J Biol Chem*, *277*(9), 7529-7539.
- Prostate cancer information from the foundation of the prostate gland. Prostate Cancer Treatment Guide. (2010). Retrieved January, 2017, from <http://www.prostate-cancer.com/prostate-cancer-treatment-overview/overview-prostate-anatomy.html>
- Prostate cancer statistics. Canadian Cancer Society. (2017). Retrieved January, 2017, from <http://www.cancer.ca/en/cancer-information/cancer-type/prostate/statistics/?region=sk>
- Rajasekaran, S. A., Anilkumar, G., Oshima, E., Bowie, J. U., Liu, H., Heston, W., . . . Rajasekaran, A. K. (2003). A novel cytoplasmic tail MXXXL motif mediates the internalization of prostate-specific membrane antigen. *Mol Biol Cell*, *14*(12), 4835-4845.
- Rao, A.R., Motiwala, H.G., & Karim, O.M. (2008). The discovery of prostate-specific antigen. *BJU Int*. *101*, 5-10.
- Rodeberg, D. A., Nuss, R. A., Elsawa, S. F., & Celis, E. (2005). Recognition of six-transmembrane epithelial antigen of the prostate-expressing tumor cells by peptide antigen-induced cytotoxic T lymphocytes. *Clin Cancer Res*, *11*(12), 4545-4552.
- Roehrborn, C.G., Pickens, G.J., & Carmody, T. 3rd. (1996). Variability of repeated serum prostate-specific antigen (PSA) measurements within less than 90 days in a well-defined patient population. *Urology* *47*, 59-66.

- Ronquist, G., & Hedstrom, M. (1977). Restoration of detergent-inactivated adenosine triphosphatase activity of human prostatic fluid with concanavalin A. *Biochim Biophys Acta*, 483(2), 483-486.
- Ronquist, G. K., Larsson, A., Stavreus-Evers, A., & Ronquist, G. (2012). Prostatosomes are heterogeneous regarding size and appearance but affiliated to one DNA-containing exosome family. *Prostate*, 72(16), 1736-1745.
- Saini, S. (2016). PSA and beyond: alternative prostate cancer biomarkers. *Cell Oncol (Dordr)*, 39(2), 97-106.
- Sandvig, K., & Llorente, A. (2012). Proteomic analysis of microvesicles released by the human prostate cancer cell line PC-3. *Mol Cell Proteomics*, 11(7), M111 012914.
- Schroder, F. H., Hugosson, J., Roobol, M. J., Tammela, T. L., Ciatto, S., Nelen, V., . . . Investigators, E. (2009). Screening and prostate-cancer mortality in a randomized European study. *N Engl J Med*, 360(13), 1320-1328.
- Schroder, F. H., Hugosson, J., Roobol, M. J., Tammela, T. L., Zappa, M., Nelen, V., . . . Investigators, E. (2014). The European Randomized Study of Screening for Prostate Cancer- Prostate Cancer Mortality at 13 Years of Follow-up. *Lancet*, 384(9959), 2027-2035.
- Schroder, F. H., van der Maas, P., Beemsterboer, P., Kruger, A. B., Hoedemaeker, R., Rietbergen, J., & Kranse, R. (1998). Evaluation of the digital rectal examination as a screening test for prostate cancer. Rotterdam section of the European Randomized Study of Screening for Prostate Cancer. *J Natl Cancer Inst*, 90(23), 1817-1823.
- Semjonow, A., Brandt, B., Oberpenning, F., Roth, S., & Hertle, L. (1996). Discordance of assay methods creates pitfalls for the interpretation of prostate-specific antigen values. *Prostate Suppl*, 7, 3-16.
- Siegel, R.L., Miller, K.D., & Jemal, A. (2016). Cancer statistics, 2016. *CA Cancer J Clin* 66, 7-30.
- Sokoll, L. J., Ellis, W., Lange, P., Noteboom, J., Elliott, D. J., Deras, I. L., . . . Vessella, R. L. (2008). A multicenter evaluation of the PCA3 molecular urine test: pre-analytical effects, analytical performance, and diagnostic accuracy. *Clin Chim Acta*, 389(1-2), 1-6.
- Stoianovici, D. (2012). Technology advances for prostate biopsy and needle therapies. *J Urol*, 188(4), 1074-1075.
- Taira, A., Merrick, G., Wallner, K., & Dattoli, M. (2007). Reviving the acid phosphatase test for prostate cancer. *Oncology (Williston Park)*, 21(8), 1003-1010.

- Tarazona, R., Delgado, E., Guarnizo, M. C., Roncero, R. G., Morgado, S., Sanchez-Correa, B., . . . Casado, J. G. (2011). Human prostasomes express CD48 and interfere with NK cell function. *Immunobiology*, 216(1-2), 41-46.
- Tavoosidana, G., Ronquist, G., Darmanis, S., Yan, J., Carlsson, L., Wu, D., . . . Kamali-Moghaddam, M. (2011). Multiple recognition assay reveals prostasomes as promising plasma biomarkers for prostate cancer. *Proc Natl Acad Sci U S A*, 108(21), 8809-8814.
- Testa, J. E., Brooks, P. C., Lin, J. M., & Quigley, J. P. (1999). Eukaryotic expression cloning with an antimetastatic monoclonal antibody identifies a tetraspanin (PETA-3/CD151) as an effector of human tumor cell migration and metastasis. *Cancer Res*, 59(15), 3812-3820.
- The Human Protein Atlas. Retrieved May, 2017, from <http://www.proteinatlas.org>.
- They, C., Zitvogel, L., & Amigorena, S. (2002). Exosomes: composition, biogenesis and function. *Nat Rev Immunol*, 2(8), 569-579.
- Thompson, I. M., Pauler, D. K., Goodman, P. J., Tangen, C. M., Lucia, M. S., Parnes, H. L., . . . Coltman, C. A., Jr. (2004). Prevalence of prostate cancer among men with a prostate-specific antigen level  $\leq 4.0$  ng per milliliter. *N Engl J Med*, 350(22), 2239-2246.
- Tosoian, J. J., Loeb, S., Feng, Z., Isharwal, S., Landis, P., Elliot, D. J., . . . Sokoll, L. J. (2012). Association of [-2]proPSA with biopsy reclassification during active surveillance for prostate cancer. *J Urol*, 188(4), 1131-1136.
- Troyer, J. K., Beckett, M. L., & Wright, G. L., Jr. (1997). Location of prostate-specific membrane antigen in the LNCaP prostate carcinoma cell line. *Prostate*, 30(4), 232-242.
- U.S. Preventive Services Task Force (2012). *Prostate Cancer: Screening*. Retrieved January, 2017, from <https://www.uspreventiveservicestaskforce.org/Page/Document/UpdateSummaryFinal/prostate-cancer-screening>.
- U.S. Preventive Services Task Force (2017). Draft Recommendation Statement, *Prostate Cancer: Screening*. Retrieved July 2017, from <https://www.uspreventiveservicestaskforce.org/Page/Document/draft-recommendation-statement/prostate-cancer-screening1>
- Valenti, M. T., Dalle Carbonare, L., Donatelli, L., Bertoldo, F., Giovanazzi, B., Caliarì, F., & Lo Cascio, V. (2009). STEAP mRNA detection in serum of patients with solid tumours. *Cancer Lett*, 273(1), 122-126.
- van der Pol, E., Coumans, F. A., Grootemaat, A. E., Gardiner, C., Sargent, I. L., Harrison, P., . . . Nieuwland, R. (2014). Particle size distribution of exosomes and microvesicles

determined by transmission electron microscopy, flow cytometry, nanoparticle tracking analysis, and resistive pulse sensing. *J Thromb Haemost*, 12(7), 1182-1192.

van der Pol, E., van Gemert, M. J., Sturk, A., Nieuwland, R., & van Leeuwen, T. G. (2012). Single vs. swarm detection of microparticles and exosomes by flow cytometry. *J Thromb Haemost*, 10(5), 919-930.

van der Pol, E., Hoekstra, A. G., Sturk, A., Otto, C., van Leeuwen, T. G., & Nieuwland, R. (2010). Optical and non-optical methods for detection and characterization of microparticles and exosomes. *J Thromb Haemost*, 8(12), 2596-2607.

Varon, D., Hayon, Y., Dashevsky, O., & Shai, E. (2012). Involvement of platelet derived microparticles in tumor metastasis and tissue regeneration. *Thromb Res*, 130 Suppl 1, S98-99.

Walz, J., Graefen, M., Chun, F. K., Erbersdobler, A., Haese, A., Steuber, T., . . . Karakiewicz, P. I. (2006). High incidence of prostate cancer detected by saturation biopsy after previous negative biopsy series. *Eur Urol*, 50(3), 498-505.

Warade., J. (2014). Review of variability in PSA measurement. *International J. of Healthcare and Biomedical Research* 03, 36-42.

Wein. A.J., Kavoussi, L.R., Novick, A.C., Partin, A.W., & Peters, C.A., eds. Campbell-Walsh Urology, 11th Edition. Philadelphia: Saunders, 2016. pages 500, 506, 2573, 2574, 2567.

Wolf, J. S., Jr., Bennett, C. J., Dmochowski, R. R., Hollenbeck, B. K., Pearle, M. S., Schaeffer, A. J., & Pace, K.T., (2012). Urologic Surgery Antimicrobial Prophylaxis. *Best Practice Statements*. Updated 2011.

Wolf P. (1967). The nature and significance of platelet products in human plasma. *Br J Haematol*, 13, 269-88.

Wolf, A. M., Wender, R. C., Etzioni, R. B., Thompson, I. M., D'Amico, A. V., Volk, R. J., . . . American Cancer Society Prostate Cancer Advisory, C. (2010). American Cancer Society guideline for the early detection of prostate cancer: update 2010. *CA Cancer J Clin*, 60(2), 70-98.

Wu, K., Hu, F. B., Willett, W. C., & Giovannucci, E. (2006). Dietary patterns and risk of prostate cancer in U.S. men. *Cancer Epidemiol Biomarkers Prev*, 15(1), 167-171.

Xu, Y., Nakane, N., & Maurer-Spurej, E. (2011). Novel test for microparticles in platelet-rich plasma and platelet concentrates using dynamic light scattering. *Transfusion*, 51(2), 363-370.

Yamamoto, T., Musunuru, B., Vesprini, D., Zhang, L., Ghanem, G., Loblaw, A., Klotz, L. (2016). Metastatic Prostate Cancer in Men Initially Treated with Active Surveillance. *J*

*Urol*, 195(5),1409-1414.

Yamamoto, T., Tamura, Y., Kobayashi, J., Kamiguchi, K., Hirohashi, Y., Miyazaki, A., . . . Sato, N. (2013). Six-transmembrane epithelial antigen of the prostate-1 plays a role for in vivo tumor growth via intercellular communication. *Exp Cell Res*, 319(17), 2617-2626.

Yeh, A. H., Jeffery, P. L., Duncan, R. P., Herington, A. C., & Chopin, L. K. (2005). Ghrelin and a novel preproghrelin isoform are highly expressed in prostate cancer and ghrelin activates mitogen-activated protein kinase in prostate cancer. *Clin Cancer Res*, 11(23), 8295-8303.

Yuana, Y., Sturk, A., Nieuwland, R. (2013). Extracellular vesicles in physiological and pathological conditions. *Blood Reviews* 27, 31-39.


Zeegers, M.P., Jellema, A., & Ostrer. (2003). H. Empiric risk of prostate carcinoma for relatives of patients with prostate carcinoma: a meta-analysis. *Cancer* 97, 1894–903.

Zwicker, J. I. (2010). Impedance-based flow cytometry for the measurement of microparticles. *Semin Thromb Hemost*, 36(8), 819-823.

## Appendices

**Appendix 1.** Figure 1, used with permission (Copyright Clearance License #4138431458631). Figure 2, 3 and 4 did not require needing permission for use.

**Appendix 2. REB approval letter.**



**Western  
Research**

**Western University Health Science Research Ethics Board  
HSREB Annual Continuing Ethics Approval Notice**

Research Ethics

**Date:** December 08, 2016  
**Principal Investigator:** Dr. Hon Leong  
**Department & Institution:** Schulich School of Medicine and Dentistry/Oncology, London Health Sciences Centre

**Review Type:** Expedited  
**HSREB File Number:** 103156  
**Study Title:** Retrospective analysis of patient plasmas to assess the diagnostic power of prostate cell microparticles.

**HSREB Renewal Due Date & HSREB Expiry Date:**  
 Renewal Due -2017/10/31  
 Expiry Date -2017/11/14

**LAPSE IN APPROVAL:** -2016/11/14-2016/12/08

The Western University Health Science Research Ethics Board (HSREB) has reviewed the Continuing Ethics Review (CER) Form and is re-issuing approval for the above noted study.

The Western University HSREB operates in compliance with the Tri-Council Policy Statement Ethical Conduct for Research Involving Humans (TCPS2), the International Conference on Harmonization of Technical Requirements for Registration of Pharmaceuticals for Human Use Guideline for Good Clinical Practice (ICH E6 R1), the Ontario Freedom of Information and Protection of Privacy Act (FIPPA, 1990), the Ontario Personal Health Information Protection Act (PHIPA, 2004), Part 4 of the Natural Health Product Regulations, Health Canada Medical Device Regulations and Part C, Division 5, of the Food and Drug Regulations of Health Canada.

Members of the HSREB who are named as Investigators in research studies do not participate in discussions related to, nor vote on such studies when they are presented to the REB.

The HSREB is registered with the U.S. Department of Health & Human Services under the IRB registration number IRB 00000940.

Ethics Officer, on behalf of Dr. Joseph Gilbert, HSREB Chair

Ethics Officer: Erika Basile  Katelyn Harris \_\_\_ Nicole Kaniki \_\_\_ Grace Kelly \_\_\_ Vikki Tran \_\_\_ Karen Gopaul \_\_\_

Western University, Research, Support Services Bldg., Rm. 5150  
 London, ON, Canada N6G 1G9 t. 519.661.3036 f. 519.850.2466 www.uwo.ca/research/ethics

## Curriculum Vitae

**Name:** Harmenjit Brar

**Post-secondary Education and Degrees:** University of Manitoba  
Winnipeg, Manitoba, Canada  
2007-2011 B.Sc. Microbiology

University of Manitoba  
Winnipeg, Manitoba, Canada  
2011-2015 Doctor of Medicine M.D.

The University of Western Ontario  
London, Ontario, Canada  
2016-Present MSc of Surgery Candidate

The University of Western Ontario  
London, Ontario, Canada  
2015-Present Urology Residency

**Honours and Awards:** University of Manitoba Entrance Scholarship (Worth \$1200)  
2007

Canadian Millennium Scholarship (Worth \$4500)  
2009-2010

University of Manitoba Dean's Honor Roll List  
2007-2011



<b>Research</b>	PI; <u>Harmenjit Brar</u> , Co-Investigators; Stephen Pautler, FRCSC,
<b>Grants:</b>	Hon Sing Leong, PhD, Nicholas Power, FRCSC. Liquid Biopsies for improved prostate cancer risk stratification and patient monitoring. Canadian Urologic Oncology Group (CUOG) 2016 Janssen Award. Grant: \$10 000.
<b>Related Work</b>	Presenter
<b>Experience</b>	The University of Western Ontario Annual JK Wyatt Urology Residents Research Day 2016 Antibiotic prophylaxis use in children with vesicoureteral reflux: Resident Debate
	Presenter
	The University of Western Ontario Annual JK Wyatt Urology Residents Research Day 2017 Microparticles as a “liquid biopsy” for the risk stratification of prostate cancer.
	Poster Presentation
	The University of Western Ontario Robert Zhong Department of Surgery Research Day 2017 Microparticles as a “liquid biopsy” for the risk stratification of prostate cancer.